Title
The Role of Progranulin in CNS Injury and Disease

Author
Martens, Lauren Herl

Publication Date
2012

Peer reviewed|Thesis/dissertation

The Role of Progranulin in CNS Injury and Disease

by

Lauren Herl Martens

DISSERTATION

Submitted in partial satisfaction of the requirements for the degree of

DOCTOR OF PHILOSOPHY

in

Biomedical Sciences

in the

GRADUATE DIVISION

of the

UNIVERSITY OF CALIFORNIA, SAN FRANCISCO

Acknowledgements

Publications and Contributions

The data in chapter 2 is published as a Brief Report in the *Journal of Clinical Investigation* (epub October 8, 2012) entitled, "Progranulin deficiency promotes neuroinflammation and neuron loss following toxin-induced injury" by Lauren Herl Martens, Jiasheng Zhang, Sami J. Barmada, Ping Zhou, Sherry Kamiya, Binggui Sun, Sang-Won Min, Li Gan, Steven Finkbeiner, Eric J. Huang, and Robert V. Farese, Jr. The authors contributing to chapter 2 would like to thank L. Mitic and T. Nguyen for helpful discussions, L.Elia for murine PGRN ELISA assistance, Y. Zhou for lentiviral preparation, M.G. Tansey for Etanercept, G. Diaz-Ramirez for mouse husbandry. This work was supported by grants from the NIH [P50 AG023501 (RVF, Jr.), GMO 100909 (RVF, Jr.), F31 AG034793 (LHM), P01 AG022074 (SF), K26 OD010927 (EJH), K08 NS072233 (SJB)], VA Merit Award BX001108 (EJH), the Consortium for Frontotemporal Dementia Research (RVF Jr), the ALS Association (SF), and the Gladstone Institutes.

The data in chapter 3 was acquired in close collaboration with Dr. Erik Roberson's laboratory at the University of Alabama, Birminghm. It has been submitted for publication to *Journal of Neuroscience* entitled, "Frontotemporal Dementia-related Deficits Induced by Progranulin Haploinsufficiency Do Not Require Gliosis" by Anthony J. Filiano*, Lauren Herl Martens*, Allen Young, Brian A. Warmus, Ping Zhou, Grisell Diaz-Ramierez, Jian Jao, Zhijun Zhang, Eric J. Huang, Fen-Biao Gao, Robert V. Farese, Jr., and Erik D. Roberson. *- authors contributed equally to this work. The authors

contributing to chapter 3 would like to thank James Black, Dheepa Sekar, and Miriam Roberson for colony maintenance and tissue processing, Zhiyong Li for help with fear conditioning, and Alicia Hall for help with the water maze. We thank Laura Mitic for comments on an earlier draft of the manuscript. This work was supported by the Cellular & Synaptic Physiology and Cellular & Molecular Neuropathology Cores of the Alabama Neuroscience Blueprint Core at UAB, with particular thanks to Jing Wang, Felecia Hester, and David Sweatt. The work was supported by the Consortium for Frontotemporal Dementia Research (to EDR, EJH, FBG, and RVF) and by the National Institutes of Health (NS054811 and NS075487 to EDR, AG023501 to RVF, AG034793 to LHM, and NS057098 to the Alabama Neuroscience Blueprint Core).

The data in chapter 4 is ongoing work in collaboration with Eric J. Huang at UCSF. The microarray data for the aging progranulin deficient mice was performed by Giovanni Coppola while in Daniel H. Geschwind's laboratory at University of California, Los Angeles. Members of the Huang laboratory, Sherry Kamiya and Hansen Lui, performed the quantification of the gliosis, neuronal death, and vasculature in the aged PGRN-deficient mice.

The data in chapter 5 includes unpublished experiments that currently do not fit into a particular manuscript. I would like to thank Sami J. Barmada, Thi T. Nguyen, Giovanni Coppola, and Ping Zhou for their contributions to these experiments.

I would like to thank all of the scientists who contributed to the following manuscripts for productive collaborations and positive scientific interactions:

A collaboration with Dr. Fen-Biao Gao's laboratory while at UCSF in *Plos One* [2010 May 10;5(5)] entitled, "MicroRNA-29b regulates the expression level of human

progranulin, a secreted glycoprotein implicated in frontotemporal dementia" by Jian Jao, Lauren D. Herl, Robert V. Farese, Jr., and Fen-Biao Gao.

A collaboration with Dr. Aimee Kao's laboratory at UCSF in *Proceedings of the National Academy of Sciences* [2011 March 15;108(11)] entitled, "A neurodegenerative disease mutation that accelerates the clearance of apoptotic cells" by Aimee W. Kao, Robin J. Eisenhut, Lauren Herl Martens, Ayumi Nakamura, Anne Huang, Josh A. Bagley, Ping Zhou, Alberto de Luis, Lucas J. Neukomm, Juan Cabello, Robert V. Farese, Jr., and Cynthia Kenyon.

A collaboration with Dr. Dan Geschwind's laboratory at UCLA in *Neuron* [2011 September 22;71(6)] entitled, "Functional Genomic Analyses Identify Pathways Dysregulated by Progranulin Deficiency, Implicating Wnt Signaling" by Ezra Y. Rosen, Eric M. Wexler, Revital Versano, Giovanni Coppola, Fuying Gao, Kellen D. Winden, Michael C. Oldham, Lauren Herl Martens, Ping Zhou, Robert V. Farese, Jr., and Daniel H. Geschwind.

Personal Acknowledgements

I'm indebted to many individuals who have contributed mentorship, ideas, support, and friendship to my scientific endeavors over the past six years. I could not have possibly completed my Ph.D. successfully without their collective efforts.

First and foremost, I would like to thank my mentor Dr. Robert V. Farese, Jr. I not only took a risk in joining Bob's laboratory to pursue a project outside of his area of expertise, but he took a risk by placing the responsibility of a huge, new project in my hands. It was an amazing experience to be such an integral part of the formation of the

Consortium for Frontotemporal Dementia Research (CFR). Bob gave me lots of freedom to direct the project and explore my own questions. He supported my efforts through all their successes and failures. He encouraged me to seek out the expertise of others, which gave me the opportunity to interact with many amazing scientists. He always supported my ideas, offered constructive criticism and positive feedback, and taught me how to ask good, scientific questions that allowed me to develop into the scientist that I am today. I have gained so much from working with Bob and will utilize these skills during my future scientific career.

Dr. Eric Huang not only served on my thesis committee, but also was a co-mentor to me. He took great interest in my projects and not only suggested, but made sure that experiments were completed in order to thoroughly answer the hypotheses we developed. He was always available to look at raw data, and excited to discuss next steps and future experiments. He treated me like a colleague rather than a student. I am grateful for all of the time he invested in my scientific development.

I would also like to thank the other members of my thesis committee, Drs Steven Finkbeiner and Marta Margeta. Steve challenged me at every thesis committee meeting and scientific encounter with great questions that allowed me to look beyond my data, deeper into the scientific understanding of the answers we were uncovering. He always suggested great experiments that would help cement our findings. Marta was the glia expert on my committee. She offered great suggestions and knowledge at all of our encounters. She also provided great career advice and it was great to be mentored by a successful female scientist.

All of the members of the Farese laboratory, past and present, have contributed to my work and daily life for the past five years through both scientific and non-scientific interactions. I owe Carrie Grueter my entire *in vivo* mouse expertise. She was always willing to show me procedures, plan *in vivo* experiments, and provide overall moral support with a smile. Caroline Mrejen helped me to critically look at my data, challenged me to always perform the best experiments, and offered future career advice. She was a sounding board for anything and taught me how to "laugh it off" on even the worst days. Charlie Harris always challenged me with difficult questions and earning his respect as a scientist was one of my biggest personal goals. Thi Nguyen joined the lab towards the end of my tenure and provided endless hours of scientific discussion, experiment planning, and life advice. She always reaffirmed that I was on the right track scientifically. Sarah Coughlin was my progranulin buddy and desk mate for almost two years. It was amazing to work with such a motivated and enthusiastic young scientist with so many aspirations.

Beyond the Farese lab, I had an entire network of great scientific collaborators due to my involvement with the CFR. Jiasheng Zhang and Sherry Kamiya in the Huang lab were amazing collaborators who taught me all about mouse pathology. They dropped everything they were working on when I needed help with experiments. They were so giving with their time and patience that I strive to be as great a collaborator to others as they were to me. Sami Barmada in the Finkbeiner lab provided the expertise on key experiments for my thesis work. He was enthusiastic about every potential experiment that I brought to him and worked tirelessly to provide thorough analysis of all of the data he contributed to my work. Bruce Miller, Bill Seeley, and Joachim Herz thought critically

about my data and provided helpful feedback to improve my research. They always showed interest, support, and excitement when I presented my data. They made me feel as though I was truly working towards uncovering scientific knowledge that would benefit patients in the future. Li Gan and members of her laboratory (Sakura Minami, Michael Ward, Binggui Sun, Sang-Won Min, and Yungui Zhou) were extremely generous with real-time sharing of data, reagents, and microglial expertise, and scientific discussions. Finally, Laura Mitic was one of my biggest cheerleaders and taught me to believe in myself as a scientist. She was a scientific and life mentor more than she'll ever know.

Graduate school is an emotional roller coaster that is difficult for non-scientists to grasp, as 99% of experiments fail and dealing with that failure is difficult. I was blessed to be surrounded by a group of classmates that were always up for providing a pep talk or listening to frustration over a glass of wine. They also reaffirmed to me that scientists have hobbies away from the bench, as I was exposed to many new non-scientific adventures and hobbies by spending time with them. I would especially like to thank Mark White and his wife Emily for providing Ryan and I with a California family.

I am indebted to my parents, Gary and Carol Herl, for a lifetime of support that was so strong from 3000 miles away over the past six years. They have always encouraged me to follow my dreams no matter what it takes. They supported me though many highs and lows of my graduate career. They reminded me to never give up and why I had decided to pursue a Ph.D. Most of all, they celebrated my accomplishments with me as if they were right by my side.

My husband, Ryan Martens, deserves the credit for the maintenance of my sanity for the past six years. He convinced me that UCSF was the best graduate program for my future when I was apprehensive about moving away from my friends and family. He kept my life balanced with the pursuit of new hobbies and relaxing vacations. He never let me give up and always tried to grasp what I was doing on a daily basis in order to fully understand and support me. Our relationship grew expontially over the past six years and I wouldn't trade our time in San Francisco for anything.

Every scientific encounter that I have had at UCSF, from classes to collaborations, has been beneficial and a positive experience. I have built a great network of collegues and friends during my tenure here. I'm excited to see what the future holds for everyone!

Abstract

Loss-of-function mutations in progranulin (*GRN*) that result in haploinsufficiency of the progranulin protein (PGRN) have been causally linked to frontotemporal dementia (FTD). PGRN levels are tightly regulated, as high levels cause cancer and low levels cause FTD. PGRN is a secreted glycoprotein implicated in cell survival, proliferation, and inflammation. In the central nervous system (CNS), PGRN is expressed by neurons and microglia, but its cellular functions remain unclear. We generated a murine model of PGRN-deficiency in order to begin to elucidate the CNS function of PGRN, and to model aspects of human FTD. We explored the cell type contributions of PGRN deficiency to CNS injury using the acute toxin model of 1-methyl-4-(2'methylphenyl)-1,2,3,6-tetrahydrophine (MPTP), which is known to cause both neuroinflammation and neuron death. We determined that PGRN deficiency leads to uncontrolled neuroinflammation that is detrimental to neuron survival. Therefore, microglial PGRN is critical for regulating neuroinflammation following acute brain injury. The PGRN deficient mice were aged in order to determine whether they model FTD behaviorally and/or pathologically. The homozygous PGRN deficient mice developed behavioral changes that may be linked to their age-dependent CNS inflammatory phenotype. These data suggest the importance of microglial PGRN in normal aging. Interestingly, the heterozygous and homozygous PGRN deficient mice have similar early behavioral changes, but the heterozygous mice lack any gross neuroinflammatory pathology. These early behavioral phenotypes in PGRN-deficient animals are linked to alterations in

neuronal activity, suggesting that PGRN is important for neuronal function. It is likely that PGRN deficiency causes early neuron dysfunction that triggers gliosis. The gliosis then proceeds uncontrolled due to the lack of microglial PGRN that exacerbates the neuronal phenotype, thereby causing a vicious positive feedback loop that is detrimental to neuronal function and survival. Our data suggests that PGRN is important for both neuronal and microglial function in normal aging. Further characterization of these aging phenotypes in cell-type specific models of PGRN deficiency are critical for exploring this hypothesis. Overall, the development of therapeutic strategies to regulate PGRN levels in both neurons and microglia has implications for both neurodegeneration and CNS injury.

Table of Contents

Acknowledgements……iii

Abstract……x

Table of Contents……...xii

List of Tables……xv

List of Figures…….....xvi

Chapter 1: Introduction to Progranulin Biology……..1

Progranulin Deficiency and Neurological Disorders……1

Progranulin: Structure and Expression……4

Progranulin: Receptors……7

Progranulin: A Putative Growth Factor……...8

Progranulin: An Inflammatory Molecule……...10

Murine Models of Progranulin Deficiency0……12

Goal of Our Studies……14

Chapter 2: Progranulin Deficiency Promotes Neuroinflammation and Neuron Loss Following Toxin-Induced Injury……15

Abstract……..16

Introduction……17

Results & Discussion……19

Methods……..28

Chapter 3: Dissociation Between Frontotemporal Dementia–like Deficits and Neuroinflammation in Progranulin Haploinsufficient Mice……..30

Abstract……..31

Introduction……32

Materials & Methods..……...35

Results……45

Discussion……..60

Chapter 4: Age-dependent Neuroinflammation, Vascular Alterations, and Obsessive Compulsive Disorder-like Behaviors in a Mouse Model of Progranulin Deficiency…....66

Summary……67

Introduction……68

Results……70

Discussion & Future Directions……80

Methods……..83

Chapter 5: Insights into Progranulin Biology……86

Progranulin regulates the microglial inflammatory response……....87

Microglia conditioned media affects $Grn^{+/+}$ and $Grn^{-/-}$ neuron survival differently……...91

Recombinant progranulin is not sufficient to rescue the Progranulin-deficient exaggerated myeloid pro-inflammatory response……..95

What disease are we modeling with $Grn^{-/-}$ mice?.....100

$Grn^{+/-}$ mice do not have Frontotemporal Dementia-like pathology……....106

Cell-specific PGRN-deficient mice……108

Summary……..113

References……114

Appendix I: Supplemental Material for Chapter 2……..126

Supplemental Methods…….127

Supplemental Results……...133

Supplemental Figures……...135

Appendix II: Supplemental Material for Chapter 3…….144

Library Publishing Agreement…….149

List of Tables

Table 5.1 *Grn*$^{-/-}$ microglial conditioned media causes an increased risk of death of wild-type neurons over time……...89

Table 5.2 Signficant lysosomal GO categories in aging *Grn*$^{-/-}$ mice ..……...103

Table A1.1. Progranulin-deficiency affects cortical neuron survival *in vitro*…….135

List of Figures

Figure 1.1 Primary structure of progranulin…..……..6

Figure 2.1 Increased neuron death and microglial activation caused by progranulin deficiency in a model of CNS injury…….20

Figure 2.2 Microglial PGRN deficiency increases the death of cultured neurons…….22

Figure 2.3. Progranulin-deficient microglia exhibit a hyperactivated inflammatory response……..24

Figure 3.1 Progranulin haploinsufficiency causes social deficits……..46

Figure 3.2 Progranulin haploinsufficiency impairs fear conditioning……...49

Figure 3.3 Progranulin deficiency does not affect postnatal developmental or motor/exploratory behavior……...51

Figure 3.4 Progranulin-deficient mice have normal hippocampal function and spine density……53

Figure 3.5 Absence of neuroinflammation in *Grn*$^{+/-}$ mice with FTD-related behavioral abnormalities……..54

Figure 3.6 Absence of lipofuscinosis in *Grn*$^{+/-}$ mice…….57

Figure 3.7 Decreased neuronal activation in the amygdala of *Grn*$^{+/-}$ mice……...59

Figure 4.1 OCD-like behaviors in PGRN-deficient mice……..71

Figure 4.2 Region-specific gliosis in PGRN-deficient mice ……..……..73

Figure 4.3 Loss of progranulin leads to an abnormal vascular phenotype……76

Figure 4.4 WGCNA analysis of aging PGRN-deficient mice……...78

Figure 5.1 *Grn*$^{-/-}$ microglial conditioned media accumulates cytotoxic factors over time that contribute to increased death of wild-type neurons……88

Figure 5.2 Microglial conditioned media has differential effects on wild-type and progranulin-deficient neurons……92

Figure 5.3 Cortical neurons secrete very little progranulin *in vitro*…….93

Figure 5.4 Recombinant PGRN is not sufficient to rescue the increased pro-inflammatory response of *Grn*$^{-/-}$ bone marrow-derived macrophages…….97

Figure 5.5 Lipofuscin accumulates in neurons of *Grn*$^{-/-}$ mice……105

Figure 5.6. Generation of progranulin deficient mouse lines using various promoters to drive Cre recombinase expression……...109

Figure 5.7. The cell-specific progranulin deficient mice do not have altered plasma PGRN levels…….....110

Figure A1.1 Generation of progranulin-deficient mice……...136

Figure A1.2 Progranulin expression in the CNS…….137

Figure A1.3 Death of all neuronal populations in the SNpc following MPTP treatment……..139

Figure A1.4 Efficiency and phenotype of *Cd11b-Cre* mice following MPTP treatment……..140

Figure A1.5 Murine PGRN lentiviral infection restores PGRN expression in microglia……..142

Figure A1.6 Depletion of TNFα using Etanercept is not sufficient to rescue cytotoxic neuronal death *in vitro*…….143

Figure A2.1 Progranulin levels are reduced by approximately 50% in *Grn*$^{+/-}$ mice…...145

Figure A2.2 Progranulin deficient mice do not have age-related anxiety……..146

Figure A2.3 Progranulin deficiency does not alter hippocampal spine density in a separate *Grn* mouse model……...147

Figure A2.4 Map indicating areas for c-fos quantification……148

CHAPTER 1

Introduction to Progranulin Biology

Progranulin Deficiency and Neurological Disorders

Frontotemporal dementia (FTD) has increasingly been recognized as a common neurodegenerative disease as successful research efforts have allowed it to be distinguished from Alzheimer's disease and psychiatric disorders (Ratnavalli et al., 2002, Rabinovici and Miller, 2010). Currently, it is the second most common neurodegenerative disease and the most common neurodegenerative disease in patients under the age of 65 (Ratnavalli et al., 2002). Diagnosis has been difficult due to the heterogeneity of both the clinical symptoms and pathology. Patients are characterized by personality, behavior, and/or language abnormalities associated with atrophy of the frontal and temporal lobes (Roberson, 2006). The majority of cases are of unknown or sporadic origin, but approximately 30-50% of cases have a family history with dominantly inherited genetic mutations that cause the disease. Mutations in *MAPT*, which encodes the tau protein (Hutton et al., 1998), progranulin (*GRN*) (Baker et al., 2006, Cruts et al., 2006), and a hexanucleotide repeat found in a non-coding region of the *C9ORF72* gene (DeJesus-Hernandez et al., 2011, Renton et al., 2011) account for the majority of genetically inherited cases of FTD. Rarer FTD causing mutations are found in the valosin-containing protein (*VCP*) (Watts et al., 2004) and the gene encoding for charged multivesicular body protein 2b (*CHMP2B*) (Skibinski et al., 2005).

Mutiatons in *GRN* were not causatively linked to FTD until 2006, as patients were mistaken to have *MAPT* mutations (*GRN* is located only a few megabases away on chromosome 17). Approximately 69 *GRN* mutations that span the entire gene have been identified in 231 families worldwide and include nonsense, missense, frameshift, splice-site, and signal peptide mutations, kozak sequence disruptions, and deletion of the coding

region (Cruts and Van Broeckhoven, 2008, Eriksen and Mackenzie, 2008) [www.molgen.ua.ac.be/FTDMutations]. *GRN* mutations are inherited in an autosomal dominant manner with incomplete penetrance (Gass et al., 2006, Rademakers et al., 2007). Most mutations result in a premature termination codon in one allele, thereby causing the mutant mRNA to be targeted for nonsense-mediated decay, creating a functionally null allele (Baker et al., 2006, Cruts et al., 2006, Cruts and Van Broeckhoven, 2008, Eriksen and Mackenzie, 2008). The other mutations are predicted to produce nonfunctional or unstable protein (Mukherjee et al., 2008, Shankaran et al., 2008). Serum progranulin (PGRN) levels are reduced by 70-80% in mutation carriers and patients compared to controls (Finch et al., 2009). Thus, PGRN deficient FTD is caused by progranulin haploinsufficiency or loss of function rather than a toxic gain of function, as is the case for many other neurodegenerative disorders (Cruts and Van Broeckhoven, 2008, Eriksen and Mackenzie, 2008).

The pathology associated with progranulin deficient FTD includes dystrophic neurites, inflammation, neuronal and microglial ubiquitin-positive inclusions, and neuron loss that is most severe in the frontal and temporal lobes. Pathology can also be found in the striatum, thalamus, substantia nigra, and hippocampus (Cruts and Van Broeckhoven, 2008, Eriksen and Mackenzie, 2008). The intracellular inclusions do not contain progranulin but hyperphosphorylated, ubiquitinated, and proteolytically cleaved Tar DNA binding protein-43 (TDP-43), a highly conserved, ubiquitously expressed nuclear protein (Neumann et al., 2006). TDP-43 is believed to function as a transcriptional repressor and inhibitor of exon splicing (Neumann et al., 2006). TDP-43 is also a RNA binding protein that binds many mRNAs, including *GRN* (Sephton et al., 2010,

Polymenidou et al., 2011). Loss of normal, nuclear TDP-43 localization is typical in cells with aggregates. Evidence suggests a pathogenic role for the mislocalization of TDP-43 to the cytoplasm, thereby causing loss of nuclear TDP-43 function (Barmada et al., 2010). Interestingly, progranulin deficiency FTD is not the only neurodegenerative disease with TDP-43-positive inclusions; TDP-43 proteinopathies also include Alzheimer's disease, amyotrophic lateral sclerosis, and chronic brain injury (Cohen et al., 2011).

Recently, two patients homozygous for *GRN* mutations were reported with undetectable levels of circulating PGRN. While progranulin haploinsufficiency leads to FTD, these patients develop adult onset neuronal ceriod lipofuscinosis (NCL) in their early 20s with progressive vision loss, retinal dystrophy, ataxia, and seizures (Smith et al., 2012). NCLs are a group of genetic disorders that result in lysosomal dysfunction and the accelerated accumulation of the aging pigment known as lipofuscin (Kohlschutter and Schulz, 2009). Autofluorescent lipofuscin results from the aggregation of oxidized and cross-linked proteins and lipids, which can be toxic to cells by enhancing oxidative damage that leads to mitochondrial and lysosomal dysfunction (Kohlschutter and Schulz, 2009). It is unknown whether these patients will also exhibit pathology similar to FTD in the frontal and temporal lobes with age.

Progranulin: Structure & Expression

Progranulin is a 593aa, 70-90 kDa, cysteine-rich, heavily glycosylated, secreted protein known to be involved in many cellular processes (He and Bateman, 1999, He and Bateman, 2003). It is also referred to as granulin-epithelin precursor (GEP), proepithelin, PC cell-derived growth factor (PCDGF), acrogranin, and epithelial transforming growth

factor (TGFe) depending on the field in which it is being studied (He and Bateman, 2003). *GRN* is comprised of 12 coding exons and is translated into a holoprotein containing 7.5 cysteine-rich motifs. *GRN* is known to undergo alternative splicing with exon skipping at the C-terminus, but the biology of the full-length versus shortened *GRN* transcripts are unknown (Plowman et al., 1992). The PGRN protein has an ordered structure, consisting of stacked β-hairpins with disulfide bridges, that has the most homology with EGF (He and Bateman, 2003). The 7.5 cysteine-rich motifs can be proteolytically processed by various proteases, including matrix metalloproteinases 12 and 14 (Butler et al., 2008, Suh et al., 2012), neutrophil elastase (Zhu et al., 2002), proteinase 3 (Kessenbrock et al., 2008), and a disintegrin and metalloproteinase with thrombospondin motifs-7 (ADAMTS-7) (Bai et al., 2009) to generate 6-25 kDa granulin (GRN) peptides (Figure 1.1). GRNs were purified prior to the discovery of the holoprotein (He and Bateman, 2003). Binding of PGRN to secretory leukocyte protease inhibitor (SLPI) or HDL has been shown to block cleavage of the full-length protein (Zhu et al., 2002, Okura et al., 2010). PGRN and GRNs are believed to have differential functions in inflammation (Zhu et al., 2002, Tolkatchev et al., 2008) although known functions for all of the GRNs have not been clearly defined.

Progranulin is widely expressed in the periphery by epithlial, myeloid, and immune cells. In the CNS, PGRN is expressed by most neuronal populations and microglia (Ryan et al., 2009). PGRN can be detected at high levels in the blood and at significantly lower levels in the cerebrospinal fluid (Finch et al., 2009). It is evident by its expression pattern that PGRN plays important roles in multiple physiological processes and disease, including cancer, autoimmunity, and neurodegeneration.

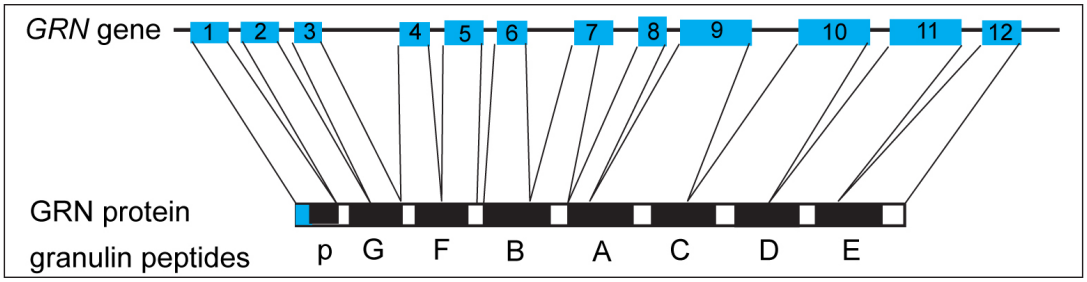

Figure 1.2. Primary structure of progranulin.

GRN has 12 exons that when spliced together encode the 593-amino acid PGRN protein. The PGRN protein can be cleaved by various proteases to produce seven different granulin (GRN) peptides.

Progranulin was identified as a secreted protein with growth factor-like qualities due to its function in cell cycle progression and cell motility (He and Bateman, 2003). Progranulin stimulates proliferation of fibroblasts that lack the insulin-like growth factor 1 (IGF1) receptor when grown in medium lacking serum (Xu et al., 1998). This finding suggests that progranulin activates signaling cascades related to those activated by IGF1, such as PI-3K/Akt and extracellularly-mediated kinase cascades (He and Bateman, 1999, Zanocco-Marani et al., 1999). It also has roles in tumor growth and metastasis, as its expression is elevated in various epithelial cancers (He and Bateman, 1999). PGRN derived from myeloid cells plays regulatory roles in inflammation and wound healing (He et al., 2003, Ong et al., 2006).

Progranulin: Receptors

When *GRN* mutations were first causally linked to FTD, PGRN receptors were unknown. Since then, Hu *et al.* determined that the C-terminus of PGRN binds to sortilin on neurons, with the last granulin, GRN E, being sufficient for binding (Hu et al., 2010). Sortilin is a multi-ligand receptor and therefore has many functions including binding the neuropeptide neurotensin, serving as a co-receptor for proneurotrophin on neurons (Lee et al., 2001), as well as playing a role in hepatic VLDL secretion (Musunuru et al., 2010). Sortilin regulates PGRN levels, as receptor-ligand binding results in the endocytosis of the protein into lysosomes (Hu et al., 2010). The function of PGRN in the lysosome is still unknown, but it is interesting that both human and murine progranulin deficiency cause lipofuscinosis, which is an indication of lysosomal dysfunction (Ahmed et al., 2010, Smith et al., 2012). Circulating PGRN levels are increased in sortilin-deficient mice, and deletion of sortilin in the $Grn^{+/-}$ mice restores circulating PGRN to wild-type

levels (Hu et al., 2010). Interestingly, PGRN can still bind to *Sort1*$^{-/-}$ neurons (Hu et al., 2010), indicating that sortilin is not the only neuronal PGRN receptor. It is also likely that other neuronal receptors exist for the various GRNs.

Progranulin is believed to bind to the tumor necrosis factor receptors (TNFRs), thereby blocking TNFα binding and its downstream signaling cascades (Tang et al., 2011). TNFR1 is expressed by most cell types and TNFα binding activates the apoptotic and pro-inflammatory cytokine signaling cascades. TNFR2 is primarily expressed on myeloid and endothelial cells and TNFα binding promotes proliferation and survival of these cells (Cabal-Hierro and Lazo, 2012). However, it is likely that other myeloid PGRN and GRN receptors remain to be discovered.

Progranulin: A Putative Growth Factor

Progranulin is overexpressed in many tumors (Liau et al., 2000, Ong and Bateman, 2003, Serrero, 2003, Matsumura et al., 2006, Cuevas-Antonio et al., 2010), where it acts similarly to a growth factor by stimulating proliferation, survival, and invasion (He and Bateman, 1999, He et al., 2002, Tangkeangsirisin and Serrero, 2004, Monami et al., 2006). Progranulin overexpression creates aggressive cancers and is currently being therapeutically targeted, as *in vivo* anti-progranulin treatment reduces tumorigenicity (Zhang and Serrero, 1998, Lu and Serrero, 2000). The mechanism of PGRN-induced growth factor signaling is unclear in cancer, although PGRN is known to activate the typical cell signaling proliferation pathways such as ERK, PI3K, and Akt pathways (He et al., 2002, Tangkeangsirisin and Serrero, 2004, Monami et al., 2006, Feng et al., 2010). In addition, PGRN promotes the proliferation of endothelial cells to aid in angiogenesis, which aids in metastasis (He et al., 2003).

Progranulin has been shown to possess neurotrophic properties as the addition of recombinant PGRN rescues excitatory, oxidative, and MPTP toxin-induced death of wild-type neurons (Xu et al., 2011), and promotes neurite outgrowth (Van Damme et al., 2008, Gao et al., 2010, Gass et al., 2012). Many groups have demonstrated that neuronal PGRN knockdown or deficiency is detrimental to neuronal survival. These neurons have decreased dendritic length and spine density (Kleinberger et al., 2010, Xu et al., 2011). Neurons lacking PGRN have reduced neurite outgrowth and branching, dendrite length, spine density, and survival *in vitro* (Van Damme et al., 2008, Gao et al., 2010, Gass et al., 2012). Some of these phenotypes can be rescued by expression of recombinant PGRN (Gass et al., 2012). GRNs can also promote neurite outgrowth, and either GRN E or C can rescue the progranulin-deficient neurite outgrowth deficits (Gass et al., 2012). Sortilin deficient neurons still respond to PGRN for increased neurite outgrowth (Gass et al., 2012), indicating that another PGRN receptor or different GRN receptors mediate this neurotrophic function.

Recently, pluripotent stem cells (iPSCs) generated from a patient carrying the *GRN S116X* mutation have been differentiated into mature, postmitotic neurons (Almeida et al., 2012). These heterozygous neurons had a 50% reduction in mRNA, intracellular, and secreted protein levels of PGRN. *GRN S116X* neurons were more susceptible that sporadic FTD neurons to the PI3K inhibitor-, wortmannin, and staurosporine-induced stress. These stressors also caused more TDP-43 mislocalization compared to the sporadic FTD neurons. The phenotype could be rescued by the expression of PGRN (Almeida et al., 2012), indicating that PGRN is required for neuron survival, especially following specific types of cellular stress.

Progranulin: An Inflammatory Molecule

Progranulin plays a role in innate, acute, and chronic inflammation in both the CNS and periphery. Overall, PGRN is believed to be anti-inflammatory, but its exact inflammatory function may be context dependent. The cleavage of the full-length protein into the various GRNs are believed to antagonize the full-length protein's anti-inflammatory function (He and Bateman, 2003). Cleavage and/or the PGRN/GRN receptors may also be context- and cell-type dependent.

In innate immunity, progranulin is important in macrophage antigen presentation through binding to the toll-like receptor (TLR) 9 (Park et al., 2011), thereby playing a role in the recognition of microbial DNA (McIsaac et al., 2012). *Grn*$^{-/-}$ macrophages bound microbial DNA less efficiently than wild-type macrophages, and this could be rescued by addition of recombinant PGRN (Park et al., 2011). *Grn*$^{-/-}$ mice infected with *Listeria monocytogenes* do not effectively recruit macrophages to clear the infection (Yin et al., 2009). These data indicate that PGRN is critical for eliciting a proper innate immune response against micro-organisms.

During acute inflammation, progranulin expression is upregulated in various cell types. For example, during the wound healing process, PGRN promotes the proliferation of fibroblasts and endothelial cells to aid in angiogenesis (He et al., 2003). Its expression is upregulated in unison with the pro-inflammatory response, where it is believed to help recruit inflammatory cells to prevent and/or clear infection (Zhu et al., 2002). The addition of recombinant PGRN has been shown to enhance wound healing (Zhu et al., 2002). In the peripheral nervous system, PGRN is upregulated following spinal cord injury in both motor neurons and activated microglia (Lim et al., 2011, Yasui et al.,

2011). *Grn*$^{-/-}$ mice show impaired motor function recovery following spinal cord trauma (Lim et al., 2011), with microglial PGRN expression regulated in a time-dependent manner during the inflammatory process (Naphade et al., 2010).

The persistence of pathogens, uncontrolled immune reactions, and dysregulated pro-inflammatory cytokine production lead to the development of chronic inflammation associated with various diseases. PGRN-deficient mice have a reduced anti-inflammatory response in a model of asthma due to decreased levels of the cytokines interlukin (IL)-4, IL-5, and IL-13 (Guo et al., 2012). The addition of recombinant PGRN to neurons *in vitro* also leads to the secretion of the anti-inflammatory cytokines IL-4 and IL-5 (Pickford et al., 2011). Chronic inflammation may also persist in PGRN deficiency, as PGRN is believed to be a chemoattractant for both macrophages (Yin et al., 2009) and microglia (Pickford et al., 2011). Injection of recombinant PGRN into the brain causes increased microglial recruitment to the injection site. PGRN deficient mice also develop age-dependent neuroinflammation (Yin et al., 2009, Ahmed et al., 2010, Yin et al., 2010, Ghoshal et al., 2011, Petkau et al., 2011, Wils et al., 2012). All of these data indicate that PGRN is required to promote anti-inflammatory signaling.

It is believed that PGRN controls chronic inflammatory states through blockade of uncontrolled TNFα signaling (Tang et al., 2011). Tang *et. al* has shown recombinant PGRN can attenuate a model of inflammatory arthritis. In fact, a combination of GRNs F, B, A and various linker regions is sufficient to rescue this disease model. The authors believe that PGRN binds to both the TNFR1 and TNFR2 receptors to block TNFα signaling (Tang et al., 2011). While it is undeniable that PGRN can rescue the phenotype, whether or not this effect is mediated through direct binding of PGRN to the TNFRs is

controversial. More likely, PGRN quells the pro-inflammatory state by controlling the levels of all pro-inflammtory cytokines, not just TNFα alone. In fact, it is likely that PGRN promotes the switch from pro-inflammatory cytokine release to anti-inflammatory cytokine release, promoting regeneration and repair of the damage.

Progranulin has been shown to have pro-inflammatory effects in obesity and type II diabetes (Hossein-Nezhad et al., 2012). Serum PGRN concentrations are higher in patients with type II diabetes and correlate with body mass index and macrophage recruitment into adipose tissue (Youn et al., 2009). *Grn*$^{-/-}$ mice were protected from high-fat diet-induced insulin resistance and weight gain. The pro-inflammatory cytokine IL-6 has been implicated as the downstream cytokine that mediates progranulin's induction of insulin resistance (Matsubara et al., 2012); however, it is unclear whether full-length PGRN or GRN elicit the demonstrated effects. These data indicates that progranulin's role in chronic inflammation can be context dependent.

Murine Models of Progranulin Deficiency

Murine progranulin is highly expressed in skin, the gastrointestinal tract, reproductive tissues, and brain, including Purkinje cells, microglia and neurons in the hippocampus and cortex (Daniel et al., 2000). In the periphery, *Grn*$^{-/-}$ mice display bone, adipose, and immune system alterations. Chondrocyte-specific knockdown of *Grn* leads to the reduction of cartilage and decrease in femur growth plate size, indicating that PGRN plays a role in cartilage development (Feng et al., 2010). *Grn*$^{-/-}$ mice are protected from high fat diet-induced insulin resistance and obesity (Matsubara et al., 2012). Finally, *Grn*$^{-/-}$ mice have increased susceptibility to an OVA-induced asthma model (Guo et al., 2012), a collagen-induced arthritis model (Tang et al., 2011), and infection with either

Listeria monoctogenes (Yin et al., 2009) or *Helicobacter pylori* (Wex et al., 2011) providing evidence of multiple deficiencies in the immune response.

Once mutations in *PGRN* were causatively linked to FTD, the race was on to determine PGRN's CNS function. Multiple laboratories took on the task of generating mice with genetic *Grn* deletions in order to study the function of PGRN as well as model FTD (Kayasuga et al., 2007, Yin et al., 2009, Yin et al., 2010, Ghoshal et al., 2011, Petkau et al., 2011, Wils et al., 2012). To date, four PGRN deficient lines, including our own, have been generated and utilized to model aspects of FTD. The only common feature between all lines is the development of social deficits in $Grn^{-/-}$ mice (Yin et al., 2010, Ghoshal et al., 2011, Petkau et al., 2011), although the timing and magnitude of change vary. Other behavioral changes include: impaired learning and memory deficits in the oldest mice (Yin et al., 2010, Ghoshal et al., 2011), depression-like behaviors (Yin et al., 2010), and anxiety alterations (Kayasuga et al., 2007, Yin et al., 2010, Petkau et al., 2011). All of these phenotypes are consistent with various clinical symptoms associated with FTD, which include early behavioral changes and later memory deficits.

These same mouse lines have been aged to look for the development of characteristic FTD pathology. The main pathology associated with murine PGRN deficiency is the development of age-dependent gliosis in the cortex, hippocampus, and thalamus beginning as early as 6 months in the $Grn^{-/-}$ mice (Yin et al., 2009, Ahmed et al., 2010, Yin et al., 2010, Ghoshal et al., 2011, Petkau et al., 2011, Wils et al., 2012). The mice also show the accumulation of ubiquitin-positive aggregates (Yin et al., 2009, Ahmed et al., 2010, Yin et al., 2010, Ghoshal et al., 2011, Petkau et al., 2011, Wils et al., 2012), and it is believed that these aggregates are comprised of the autofluorescent

lipofuscin (Ahmed et al., 2010) and phosphorylated TDP-43 (Yin et al., 2009, Yin et al., 2010), although mislocalized TDP-43 is not present. Ahmed et al. observed vacuolation in the hippocampus of 23-month-old *Grn*$^{-/-}$ mice, but neuronal death and brain mass loss are not apparent in *Grn*$^{-/-}$ mice (Ahmed et al., 2010). Interestingly, all of these pathological findings are absent in the *Grn*$^{+/-}$ mice.

Goal of Our Studies

Our work focuses on examining the cell type specific role of progranulin in the CNS *in vivo*. We sought to determine the importance and/or requirement of either neuronal or microglial PGRN in acute brain injury (chapter 2), aging (chapter 4), and the development of FTD-like phenotypes in progranulin deficient mice (chapter 3). We have demonstrated a clear role for microglial PGRN in regulating neuroinflammation associated with both injury and aging. Future work using the cell type-specific progranulin deficient mice is needed to determine which cell type alterations due to progranulin deficiency initiate the FTD-like phenotype (discussed in chapter 5).

CHAPTER 2

Progranulin Deficiency Promotes Neuroinflammation and Neuron Loss Following Toxin-Induced Injury

Abstract

Progranulin (PGRN) is a widely expressed, secreted protein that is linked to inflammation. In humans, PGRN haploinsufficiency is a major inherited cause of frontotemporal dementia (FTD), but how PGRN deficiency causes neurodegeneration is unknown. Here we show that loss of PGRN results in increased neuron loss in response to injury in the CNS. When exposed acutely to 1-methyl-4-(2'-methylphenyl)-1,2,3,6-tetrahydrophine (MPTP), *Grn*$^{-/-}$ mice showed more neuron loss and increased microgliosis. The mechanism leading to exacerbated neuron loss was not due to selective vulnerability of *Grn*$^{-/-}$ neurons to MPTP, but because of an increased microglial inflammatory response. Consistent with this, conditional mutants lacking PGRN in microglia (*Cd11b-Cre+; Grn*$^{flox/flox}$) exhibited MPTP-induced phenotypes similar to *Grn*$^{-/-}$ mice. Selective depletion of PGRN from microglia in mixed cortical cultures resulted in increased death of wild-type neurons in the absence of injury. Furthermore, *Grn*$^{-/-}$ microglia treated with LPS/IFN-γ exhibited an amplified inflammatory response, and conditioned media from these microglia promoted death of cultured neurons. Our results indicate that PGRN deficiency leads to dysregulated microglial activation and thereby contributes to increased neuron loss with injury. These findings suggest that PGRN deficiency may cause increased neuron loss in other forms of CNS injury accompanied by neuroinflammation.

Introduction

Progranulin (PGRN) is a ~70 kDa secreted protein involved in cellular processes such as wound healing and inflammation (He et al., 2002, He et al., 2003). PGRN has been implicated as a regulator of TNFα-mediated inflammation (Tang et al., 2011) and also has growth factor properties, with roles in cellular proliferation and survival (He et al., 2002). PGRN can be processed to granulin (GRN) peptides (Zhu et al., 2002), which may have different functions (Bateman and Bennett, 1998). PGRN is expressed widely in tissues and circulates in the blood and cerebrospinal fluid (Daniel et al., 2000, Petkau et al., 2010).

Mutations in *GRN* are causally linked to frontotemporal dementia (FTD) (Baker et al., 2006, Cruts et al., 2006, Gass et al., 2006). Various types of mutations have been found that result in *GRN* haploinsufficiency and cause a >50% reduction in circulating PGRN (Finch et al., 2009). PGRN is expressed in neurons and microglia (Petkau et al., 2010); the contribution of PGRN deficiency in these cell types to FTD is unknown. Intracellular aggregates of TDP-43 are found in neurons of subjects with PGRN-deficient FTD, and TDP-43 may contribute to neuron loss (Neumann et al., 2006). However, microglial PGRN expression is increased in Alzheimer's disease and amyotrophic lateral sclerosis (Irwin et al., 2009, Pereson et al., 2009), suggesting that it may play a more general role in neuroinflammation and neurodegeneration.

We and several groups have used murine models to examine the effects of PGRN deficiency in the CNS. Neurons of PGRN knockout ($Grn^{-/-}$) mice develop ubiquitin-positive aggregates and phosphorylated TDP-43, similar to FTD patients with *GRN* mutations (Yin et al., 2009, Ahmed et al., 2010, Yin et al., 2010, Ghoshal et al., 2011,

Petkau et al., 2011, Wils et al., 2012). Neurons from *Grn*$^{-/-}$ mice exhibit reduced survival in culture (Kleinberger et al., 2010). In addition, PGRN deficiency results in gliosis in the CNS of aged mice (L.H.M., unpublished observations) (Yin et al., 2009, Ahmed et al., 2010, Yin et al., 2010, Ghoshal et al., 2011, Petkau et al., 2011, Wils et al., 2012). PGRN expression is also upregulated following axotomy of the sciatic nerve in the peripheral nervous system (Moisse et al., 2009b). These latter observations suggest that PGRN may modulate inflammation in the CNS, consistent with studies showing that PGRN deficiency predisposes macrophages to increased inflammation (Yin et al., 2009).

Here we tested the hypothesis that PGRN attenuates the inflammatory response to CNS injury. We used the acute injury model of 1-methyl-4-(2'-methylphenyl)-1,2,3,6-tetrahydrophine (MPTP), a neurotoxin that targets the dopaminergic neurons of the substantia nigra pars compacta (SNpc). Although MPTP injury is commonly used as a Parkinson's disease model, it provides a reproducible CNS injury with consistent neuron loss and reactive gliosis (Dauer and Przedborski, 2003). We examined the effects of MPTP on neuron survival and microglial activation in PGRN-deficient mice and utilized primary cultures of neurons and microglia to investigate mechanisms.

Results & Discussion

To investigate PGRN expression and function in the CNS, we generated a conditional *Grn* allele and, subsequently, $Grn^{-/-}$ mice by crossing $Grn^{flox/flox}$ mice with β-actin–Cre mice (Lewandoski et al., 2000) (Figures A1.1A–C). In adult mouse brains, PGRN was expressed primarily in neurons and in resting and reactive microglia (Figures A1.1D and A1.2A–C).

Because PGRN is expressed in activated microglia (Moisse et al., 2009b) and antagonizes inflammation (Tang et al., 2011), we hypothesized that PGRN attenuates the inflammatory response to CNS injury. To test this hypothesis, we chose an injury model induced by MPTP, which, at high doses, acutely causes inflammation and death of SNpc dopaminergic neurons (Dauer and Przedborski, 2003). Neuron toxicity is in part due to conversion of MPTP to MPP+, which is taken up by dopaminergic neurons and blocks electron transport (Dauer and Przedborski, 2003). Additionally, microglia are activated and secrete cytotoxic, pro-inflammatory cytokines, such as TNFα (Czlonkowska et al., 1996, Dauer and Przedborski, 2003).

Three-month-old $Grn^{+/+}$, $Grn^{+/-}$, and $Grn^{-/-}$ mice were treated with MPTP or vehicle (PBS) for two days (Figure 2.1A). In vehicle-treated mice of any genotype, the numbers of dopaminergic (tyrosine hydroxylase [TH]-positive) neurons in SNpc were similar, indicating that PGRN deficiency did not affect their survival (Figure 2.1A,B). As expected, MPTP treatment induced ~37% loss of dopaminergic neurons in the SNpc of $Grn^{+/+}$ mice (Figure 2.1B). More strikingly, dopaminergic neurons were reduced by ~66% in $Grn^{-/-}$ mice, and by ~50% in $Grn^{+/-}$ mice. Quantification of Nissl-positive neurons in SNpc showed similar deficits in $Grn^{+/+}$ and $Grn^{-/-}$ mice following MPTP

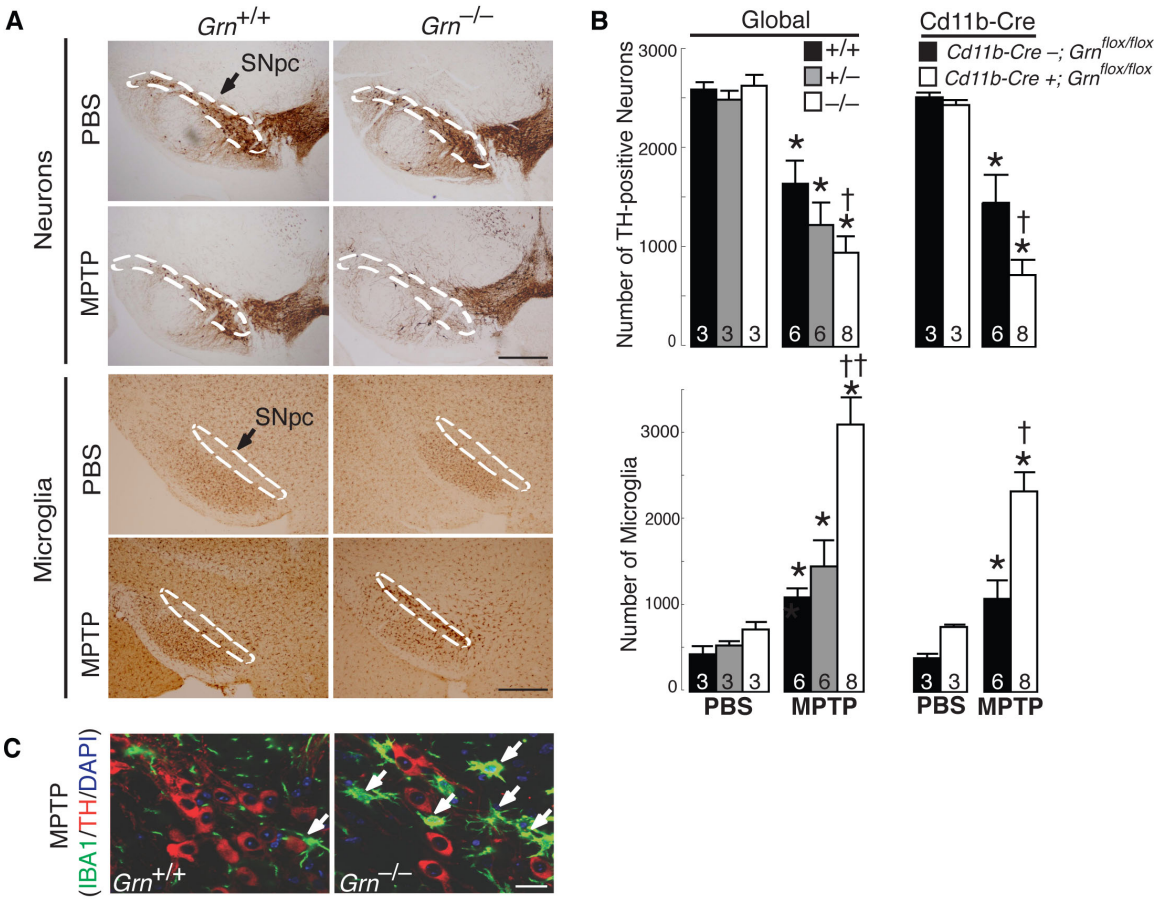

Figure 2.1. Increased neuron death and microglial activation caused by progranulin-deficiency in a model of CNS injury.

(A) Representative SNpc sections showing decreased numbers of TH-positive neurons and increased numbers of IBA1-positive microglia following MPTP exposure in PGRN-deficient mice. Dashed lines denote SNpc. Bar= 500μm. **(B)** Quantification of TH-positive neurons and IBA1-positive microglia in the SNpc in global and microglia-specific PGRN-deficient mouse models. Numbers denote *n* per group. *p < 0.05 for MPTP vs. PBS. †p < 0.05 $Grn^{+/+}$ MPTP vs. $Grn^{-/-}$ MPTP. ††p < 0.01 $Grn^{-/-}$ MPTP vs. either $Grn^{+/+}$ or $Grn^{+/-}$ MPTP. **(C)** Representative confocal images showing that MPTP treatment decreased the number of TH-positive neurons (red) and increased numbers of activated microglia (green) in the SNpc of $Grn^{-/-}$ mice. Arrows indicate activated microglia. Bar= 20μm.

treatment (Figure A1.3A,B). While the numbers of resting microglia showed no detectable differences, MPTP treatment increased activated microglia in SNpc by 2.84-fold in *Grn*$^{-/-}$ mice and 1.33-fold in *Grn*$^{+/-}$ mice, compared with *Grn*$^{+/+}$ mice (Figure 2.1C,D). Most *Grn*$^{-/-}$ microglia were highly ramified and large, indicative of activated microglia (Figure 2.1E) (Czlonkowska et al., 1996).

To further investigate the contribution of PGRN expression in microglia in the MPTP-induced injury model, *Grn*$^{flox/flox}$ mice were crossed with *Cd11b-Cre* mice (Boillée et al., 2006) to generate mice with PGRN deficiency in microglia (*Cd11b-Cre+;Grn*$^{flox/flox}$). Progranulin mRNA levels and secretion was decreased in primary microglia cultured from *Cd11b-Cre+;Grn*$^{flox/flox}$ by ~54% and ~42%, respectively, but not cortical neurons (Figure A1.4A,B). Consistent with the results from *Grn*$^{-/-}$ mice, *Cd11b-Cre+;Grn*$^{flox/flox}$ mice showed similar reduction in dopaminergic neurons (Figure 2.1B, A1.4C) and increased microgliosis after MPTP treatment (Figure 2.1D, A1.4D). Together, these results supported that PGRN deficiency in microglia is sufficient to cause increased inflammation and reduced neuron survival following CNS injury.

To further investigate the effects of PGRN deficiency in microglia, we utilized primary cell culture models. Both primary neurons and microglia expressed *Grn* mRNA, with much higher levels in microglia (Figure 2.2A), which are activated during culturing (Ong et al., 2006). We examined whether PGRN deficiency alters neuron survival in the absence of glia by testing the susceptibility of *Grn*$^{+/+}$ and *Grn*$^{-/-}$ dopaminergic neurons (E13.5) to various doses of MPP+ for three days. Neuron death occurred in a dose-dependent manner following MPP+ exposure, but there were no differences in the

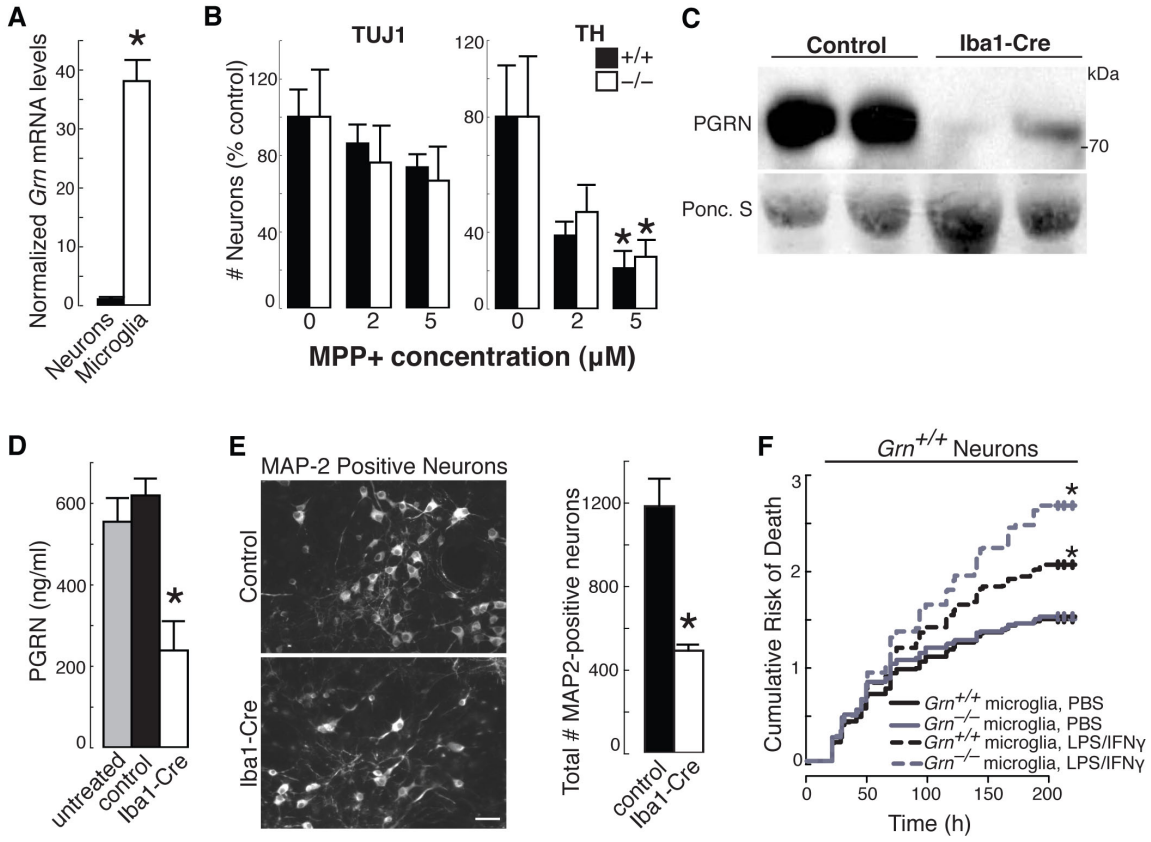

Figure 2.2. Microglial PGRN deficiency increases the death of cultured neurons.

(A) *Grn* mRNA levels in cultured primary neurons and microglia. *p < 0.001 vs. microglia. **(B)** Similar numbers of surviving $Grn^{+/+}$ and $Grn^{-/-}$ midbrain neurons (TUJ1 or TH immunolabelled) following MPP+ treatment. *p < 0.05 5μM vs. untreated. **(C)** Immunoblot showing reduced levels of secreted PGRN in $Grn^{flox/flox}$ mixed cortical cultures infected with Iba1-Cre lentivirus. **(D)** Quantification of secreted PGRN in mixed cortical cultures. *p < 0.01. **(E)** Representative image showing decreased survival of MAP2-positive neurons in mixed cultures lacking microglial PGRN compared to control cultures. *p < 0.001. Bar= 20μm. **(F)** Increased risk of death for wild-type neurons exposed to conditioned media from LPS/IFNγ-treated PGRN-deficient microglia. *p < 0.0001 (log-rank test) LPS/IFNγ-treated conditioned media compared with PBS-treated conditioned media.

numbers of surviving wild-type or PGRN-deficient TH- and TUJ1-positive neurons (Figure 2.2B).

We next asked whether PGRN deficiency in microglia had effects on neuron survival. We isolated mixed cortical cultures–containing neurons, microglia, and astrocytes–from (P0) $Grn^{flox/flox}$ mice and selectively depleted *Grn* in microglia by infecting with lentivirus expressing Iba1-Cre recombinase (Iba1-Cre). Depletion of PGRN from microglia reduced PGRN in the media by ~70% (Figure 2.2C,D) and reduced the survival of MAP2-positive neurons by >50% compared with controls (Figure 2.2E). There were no apparent changes in the numbers of microglia or astrocytes (not shown). Thus, PGRN deficiency in microglia is sufficient to increase death of wild-type neurons in primary cultures.

We hypothesized that the increased neuron death observed when microglia are deficient in PGRN may be attributable to alterations in secreted factors. To test this hypothesis, we collected conditioned media from $Grn^{+/+}$ and $Grn^{-/-}$ microglia treated with either PBS or LPS/IFNγ for 24 hours and then transferred this media to wild-type cortical neurons to assess survival. The cumulative risk of death for each treatment was determined using Kaplan-Meier survival analysis, which assessed the probability of neuron cell death over time (Arrasate and Finkbeiner, 2005, Barmada et al., 2010). There were no differences in survival of neurons exposed to conditioned media of PBS-treated $Grn^{+/+}$ or $Grn^{-/-}$ microglia (Figure 2.2F, solid lines). In contrast, exposure of $Grn^{+/+}$ and $Grn^{-/-}$ microglia to LPS/IFNγ caused significantly more neuron cell death than PBS (Figure 2.2F, dashed lines), and this effect was accentuated with the activated $Grn^{-/-}$ microglia conditioned media (Figure 2.2F, dashed grey line). These results indicate that activated PGRN-deficient microglia likely secrete factors that promote the death of

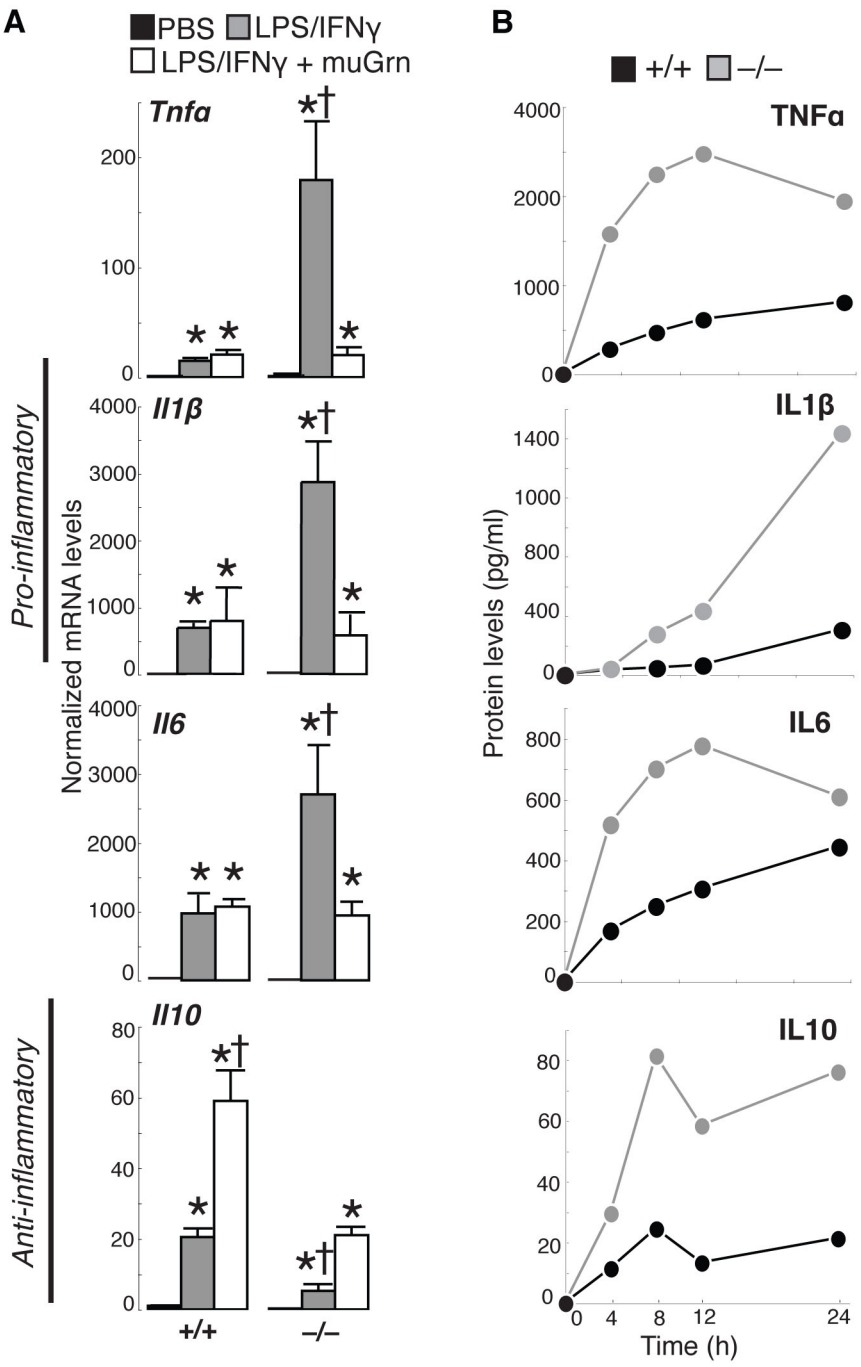

Figure 2.3. Progranulin-deficient microglia exhibit a hyperactivated inflammatory response.

(A) Increased inflammatory cytokine mRNA levels in LPS/IFNγ-treated *Grn*$^{-/-}$ microglia, compared with *Grn*$^{+/+}$ controls, that can be rescued by lentiviral infection of murine PGRN. *$p < 0.05$ compared with LPS/IFNγ. †$p < 0.05$ compared with *Grn*$^{-/-}$ LPS/IFNγ. **(B)** Representative time plots revealing increased secretion of inflammatory cytokines by LPS/IFNγ-treated *Grn*$^{-/-}$ microglia compared with similarly treated *Grn*$^{+/+}$ cultures.

wild-type neurons.

To investigate this phenomenon further, we examined the inflammatory response in primary microglia following 24 hours of treatment with LPS/IFNγ. Similar to findings for PGRN-deficient macrophages (Yin et al., 2009, Tang et al., 2011), *Grn*$^{-/-}$ microglia expressed and secreted increased amounts of the pro-inflammatory cytokines TNFα, IL1β, and IL6 compared with controls (Figure 2.3A,B). *Grn*$^{-/-}$ microglia also expressed less anti-inflammatory *Il10* mRNA after 24 hours (Figure 2.3A), although increased amounts of IL10 were secreted into the media (Figure 2.3B), reflecting differences in the regulation of mRNA versus secreted protein. The increased IL10 secretion was apparently insufficient to dampen the increased inflammatory state of *Grn*$^{-/-}$ microglia. These data indicate that *Grn*$^{-/-}$ microglia are prone to a hyperactive pro-inflammatory state upon activation, and this hyperactivation likely contributes to the death of neurons. These data also suggest that a function of PGRN is to dampen the activation state of microglia upon stimulation. Supporting this, lentiviral mediated overexpression of murine PGRN was sufficient to normalize cytokine mRNA levels in *Grn*$^{-/-}$ microglia (Figure 2.3A, A.5A,B).

In this study, we tested the effects of PGRN deficiency on MPTP treatment, a well-established model of CNS injury that precipitates both neuron death and microglial activation (Dauer and Przedborski, 2003). Our data indicate that PGRN deficiency results in an exaggerated, prolonged inflammatory response in activated microglia, and that this mechanism likely contributes to enhanced neuron death following injury. We examined TNFα as a potential mediator of this effect. TNFα signalling contributes to the demise of SNpc dopaminergic neurons following MPTP treatment (Ferger et al., 2004) and induces

apoptosis in neurons (McGuire et al., 2001). Additionally, mice lacking both TNFR1 and TNFR2 are protected against MPTP-induced dopaminergic neuron death (Sriram et al., 2006). PGRN has been reported to bind TNFα receptors and block signalling (Tang et al., 2011), suggesting that PGRN-deficiency may lead to uncontrolled TNFα signalling. However, we found that the addition of Etanercept, soluble TNFR2, did not attenuate neuron death in our system (Figure A1.6). We are unable to distinguish whether this was due to inadequate TNFα blockade or whether other factors–such as increased cytokines or excitatory factors, or decreased trophic factors–are responsible for the increased neuron death.

Our findings suggest that progranulin deficiency may predispose microglia to hyperactivation and neuron death in FTD. Indeed, microglial activation is found in humans with FTD (Ahmed et al., 2007) and in murine models of PGRN deficiency (Yin et al., 2009, Ahmed et al., 2010, Yin et al., 2010, Ghoshal et al., 2011, Petkau et al., 2011, Wils et al., 2012). However, our findings do not exclude that PGRN deficiency in neurons may also be an important contributing factor. Several studies have demonstrated that PGRN has important neurotrophic properties (Kleinberger et al., 2010, Xu et al., 2011), and indeed, we found small reductions in the survival of *Grn*$^{-/-}$ cortical neurons cultured in nutrient-rich (B27) or nutrient-depleted (N2) media (Table A1.1). Nevertheless, our results reveal a role for PGRN in attenuating neuroinflammation and suggest that this mechanism contributes to neurodegeneration in progranulin-deficient FTD. Further, PGRN may attenuate inflammation and neuron death in other forms of neurodegeneration or CNS injury. Therapies aimed at raising PGRN levels (Capell et al.,

2011, Cenik et al., 2011) in the CNS therefore may prove useful as therapies for FTD and other forms of CNS injury.

Methods

Experimental procedures are described in detail in Supplemental Methods.

Generation of PGRN-deficient mice. A targeting vector was generated with loxP sites flanking the *Grn* coding sequence. $Grn^{floxflox}$ mice were bred with mice expressing Cre recombinase under *β-actin* (Lewandoski et al., 2000), or *Cd11b* (Boillée et al., 2006) promoters.

Acute MPTP treatment. Three-month-old mice were treated with four i.p. injections per day for two days with MPTP (4 μg/g body weight) (Sigma) or PBS. Stereological counting was used to quantify dopamine neurons and microglia in the SNpc.

Primary Cultures. Ventral midbrain, cortical neuron, mixed cortical, and microglial cultures were prepared from E13.5 or E16-18 embryos, and P0 or P2-P4 pups, respectively.

Neuron Survival Assays. Pure cortical cultures were transfected with EGFP, microglial conditioned media was added, and cells were imaged every 24 hours using an automated microscopy system (Arrasate and Finkbeiner, 2005) to assess neuron death.

Cytokine Analysis. Primary microglia were stimulated with PBS or 100 ng/ml LPS (Sigma) and 100 U/ml IFNγ (Sigma). Secreted cytokine levels were measured using the Mouse Pro-inflammatory 7-plx cytokine ELISA kit (Meso Scale Discovery).

Statistics. Results are means ± SEM unless stated. Differences between two groups were assessed with unpaired, two-tailed *t* tests. Comparisons involving more than two groups used an ANOVA with Tukey's post-hoc test. $P < 0.05$ was considered significant. Tests were performed with InStat or StatView software; neuron survival analysis data utilized R.

Study Approval. All procedures were approved by the University of California, San Francisco IACUC and followed the NIH Guide for Care and Use of Laboratory Animals.

Chapter 3

Dissociation Between Frontotemporal Dementia–like Deficits and Neuroinflammation in Progranulin Haploinsufficient Mice

Abstract

Frontotemporal dementia (FTD) is a fatal neurodegenerative disease characterized by changes in social and emotional function. Heterozygous loss-of-function mutations in *GRN,* the progranulin gene, are a common cause of the disorder, but the mechanism by which progranulin haploinsufficiency causes neuronal dysfunction in frontotemporal dementia are unclear. Homozygous progranulin knockout ($Grn^{-/-}$) mice have been studied as a model of this disorder and show behavioral deficits and a neuroinflammatory phenotype with robust microglial activation. However, homozygous *GRN* mutations causing complete progranulin deficiency were recently shown to cause a different neurological disorder, neuronal ceroid lipocusicinosis, suggesting that the total absence of progranulin may have effects distinct from those of haploinsufficiency. Here we studied $Grn^{+/-}$ mice, which model progranulin haploinsufficiency. We found that $Grn^{+/-}$ mice developed age-dependent social and emotional deficits potentially relevant to frontotemporal dementia. However, unlike $Grn^{-/-}$ mice, deficits in $Grn^{+/-}$ mice occurred in the absence of gliosis or increased tumor necrosis factor–α. Instead, we found neuronal abnormalites in the amygdala, an area of selective vulnerability in FTD, in $Grn^{+/-}$ mice. Our findings indicate that FTD-related deficits due to progranulin haploinsufficiency can develop in the absence of detectable gliosis and neuroinflammatory changes, thereby dissociating microglial activation from functional deficits and suggesting an important effect of progranulin deficiency on neurons.

Introduction

Frontotemporal dementia (FTD) is a devastating neurodegenerative disease and the leading cause of dementia in patients younger than 60 years of age (Vossel and Miller, 2008). Patients suffering from FTD experience incapacitating behavioral changes, which commonly include social withdrawal and emotional blunting (Rascovsky et al., 2011). These symptoms result from dysfunction of a brain network called the salience network, which includes the amygdala, anterior cingulate cortex, insular cortex, limbic ventral striatum, and other regions (Seeley et al., 2009, Zhou et al., 2010b). Although the mechanisms leading to this dysfunction are unclear, mutations in the *GRN* gene encoding progranulin are one of the most common causes of inherited FTD (Gass et al., 2006, Gijselinck et al., 2008). Almost all FTD-associated *GRN* mutations result in a null allele causing haploinsufficiency with reduced progranulin levels in brain and plasma (Finch et al., 2009).

Progranulin is a multifunctional protein expressed in neurons and microglia (Petkau et al., 2010). In neurons, progranulin has neurotrophic and neuroprotective properties and regulates synaptic function (Van Damme et al., 2008, Ryan et al., 2009, Tapia et al., 2011). However, considerable attention has focused on progranulin's role in microglia and its connection to neuroinflammation. Progranulin-deficient macrophages, when stimulated, have exaggerated inflammatory and phagocytic responses (Yin et al., 2009, Kao et al., 2011). And a recent report found that progranulin binds to tumor necrosis factor (TNF) receptors and competitively antagonizes the proinflammatory actions of TNF-α, so progranulin deficiency increases inflammation (Tang et al., 2011).

Homozygous progranulin knockout ($Grn^{-/-}$) mice have also suggested a role for gliosis and inflammation in progranulin-deficient FTD. $Grn^{-/-}$ mice develop an FTD-like pattern of behavioral disturbances, with social and emotional abnormalities and only mild or late hippocampal memory dysfunction (Kayasuga et al., 2007, Yin et al., 2010, Ghoshal et al., 2011). $Grn^{-/-}$ mice also have robust, age-dependent microgliosis and astrogliosis (Yin et al., 2009, Ahmed et al., 2010, Yin et al., 2010, Ghoshal et al., 2011). These data suggest that glial overactivation and neuroinflammation due to progranulin deficiency could mediate FTD-related neuronal dysfunction in $Grn^{-/-}$ mice and patients with *GRN* mutations. However, the connection between gliosis and FTD-related neuronal dysfunction remains correlative, and no data indicate a causal role for microglial overactivation in progranulin-deficient mice or FTD patients.

To date, studies of murine progranulin deficiency have focused on homozygous knockout mice, and relatively few data are available for the phenotype of $Grn^{+/-}$ mice. However, in humans, progranulin haploinsufficiency causes FTD, while homozygous progranulin deficiency causes another disorder, neuronal ceroid lipofuscinosis (Smith et al., 2012). Thus, haploinsufficiency and complete deficiency of progranulin have different effects, indicating a need for closer examination of possible FTD-related phenotypes in $Grn^{+/-}$ mice.

To determine whether progranulin haploinsufficiency in mice causes FTD-related behavioral deficits and whether those deficits involve gliosis and neuroinflammation, we studied behavior, physiology, neuropathology, and inflammatory mediators in multiple cohorts of $Grn^{+/-}$ mice at different ages. Our findings shed new light on the relationship

between behavioral abnormalities and inflammatory changes with progranulin haploinsufficiency.

Materials and Methods

Generation of progranulin-deficient mice

Mice with a floxed *Grn* allele ($Grn^{+/F}$ mice) were generated by homologous recombination in RF8 ES cells (129Sv/Jae) (Martens et al., 2012). $Grn^{+/-}$ mice were produced by breeding $Grn^{+/F}$ mice with mice expressing Cre recombinase in the germline (Tg(ACTB-cre)2Mrt/J, JAX #003376). Deletion of progranulin was observed at the mRNA and protein levels in multiple tissues (Martens et al., 2012); progranulin brain mRNA levels in $Grn^{+/-}$ mice were somewhat less than 50% of normal and plasma levels were approximately 50% of normal (Figure A2.1). Mice for this study were generated by breeding $Grn^{+/-}$ mice, except Fig. 1E, for which the mice were a product of a cross between $Grn^{+/+}$ and $Grn^{+/-}$ mice. $Grn^{+/F}$ mice that had not been crossed to Cre and, thus, had a floxed *Grn* allele but normal progranulin levels were used as controls in Fig. 3.1F. Figure A2.3 utilized an independent line of progranulin-deficient mice (Kayasuga et al., 2007).

Males and females were used for all experiments except electrophysiology and Golgi staining, which used only males. Males and females were analyzed separately and presented together if there were no significant main effect for sex. Two cohorts of mice were tested on a mixed background that included 129Sv (on which the floxed line was originally created), FVB/N (the background strain of the Cre transgenic mice), and C57BL/6 (to which the original $Grn^{+/-}$ mice were crossed to expand the line for experiments). Subsequently, after 10 generations of backcrosses, a third cohort was tested on a congenic C57BL/6 background. All mice used were Cre-negative and verified Disc-1 wild-type (Disc-1 deletion is endogenous to 129 substrains (Clapcote and Roder, 2006).

Animals were housed in a pathogen-free barrier facility with a 12-h light/12-h dark cycle and *ad libitum* access to food (NIH-31 Open Formula Diet, Harlan #7917) and water. All behavior experiments were conducted during daylight hours under normal room lighting conditions. All experiments were approved by the Institutional Animal Care and Use Committees of the University of Alabama at Birmingham or the University of California, San Francisco.

Three-chamber sociability

Mice were tested for social interaction time in a three-chamber sociability test adapted from Moy *et al*. (Moy et al., 2004) with minor modifications. Testing was conducted under red light. The test boxes were fabricated from white plexiglass at the UAB machine shop and did not contain bedding. After 30–90 minutes of habituation to the testing room, a mouse was placed in the center chamber with the two outside chambers containing empty wire cages (Spectrum Diversified Designs). Mice were allowed to explore all three chambers for 10 minutes. After 10 minutes, a novel mouse (8-month-old, male, C57BL/6 mouse that had been habituated to being in the wire cage) and an inanimate object (matchbox car or block) were placed under the wire cages. The test mouse was allowed to explore for 10 minutes. The time spent interacting with the novel mouse and the inanimate object was scored either by a blinded observer with a stopwatch or a video tracking system (CleverSys, Inc.). A sociability ratio was calculated for each mouse by dividing the time spent interacting with the other mouse by the time spent interacting with the inanimate object. To show data from multiple cohorts, the sociability ratio was normalized with 100% as the average sociability ratio of wild-type mice in each cohort.

Pheromone preference

To test for pheromone preference, time spent investigating stimuli containing urine and water was measured. Urine was collected and combined from 10 male C57BL/6 mice and subsequently frozen until testing. Urine or water (50 μL) was spotted onto small pieces of filter paper, which were then dried. The filter papers were inserted into histology cassettes to prevent direct contact, and cassettes containing urine and water were placed into opposite corners of a standard mouse cage with bedding. The test mouse was placed into the cage for 5 minutes and time spent within 5 cm of each stimulus was recorded with video tracking software (Clever Sys., Inc.).

Tube test of social dominance

Mice were tested for social dominance in a tube test adapted from Lindzey et al. (Lindzey et al., 1961). Mice were placed, head first, into opposing sides of a clear plastic tube (3.81 cm I.D. X 30.5 cm in length) and released simultaneously. The trial ended when two paws of one mouse left the tube. The mouse remaining in the tube at the end of the trial was deemed the winner. A trial was aborted if the mice crossed each other or no mouse left the tube in two minutes. The tube was cleaned with 70% ethanol and dried between trials. Data were analyzed using a chi-squared test.

Fear conditioning

Experiments were conducted in Quick Change Test chambers (Med Associates). For the acquisition of fear conditioning, mice were placed in the chambers and allowed to acclimate for 180 seconds. After acclimation, a conditioned stimulus (white noise at 75 Db) was given for 20 seconds co-terminating with a 0.5-mA foot shock (2 seconds). This stimulus was given a total of three times with a 40-second inter-stimulus interval. Videos

were recorded and the time the mice spent immobile was measured by a blinded observer. The mice were then returned to their home cage. To test for cued-based conditioning, mice were tested 24 hours after training. For this test, the chambers' context was made novel with a triangular, opaque white plexiglass insert and a spearmint scent. Mice were placed in the chamber for 6 minutes with the white noise auditory cue given for the last 3 minutes. Freezing was measured before and during the cue. The chamber was cleaned with 70% ethanol between mice during the training and with isopropanol during the cued testing.

Developmental Milestones

The assessment of developmental milestones began on postnatal day two. Pups were monitored daily for weight and attainment of physical milestones, such as incisor eruption, pinnae detachment, and opening of eyes. Further, pups were evaluated for reflexes and coordinated movements. For grasp reflex, forepaws were gently stroked with the wooden end of a swab; achievement of the milestone was registered if a grasping motion was observed. For surface righting, pups were placed in bedding with their ventral side up and timed until they successfully righted themselves. To assess cliff avoidance, pups were placed at the edge of a 6-cm high Styrofoam platform, with head and paws hanging over the edge. The time it took to back away from the edge was measured and achievement of the milestone was recorded if the time was less than 10 seconds. Negative geotaxis was measured by placing a pup facing downward on a coarse surface at an angle of 30^{o}. The time it took for a pup to right itself was scored and achievement of the milestone was recorded when the time was less than 10 seconds. To examine visual placing, pups were lowered downward by their tails toward a surface.

When the pup raised their head and extended their forelimbs towards the surface, achievement of the milestone was recorded. To evaluate air righting, pups were held 30 cm above a well bedded surface and dropped ventral side up. Achievement of the milestone was recorded on the day the pups were able to land on their feet. The bar hanging milestone was tested by allowing the mice to grasp a small bar and measuring the amount of time they could remain suspended without falling. Achievement of the milestone was scored if they could remain suspended.

Open field

Total ambulatory distance and anxiety were measured on the open field (Med Associates). Mice were placed in the open field for 15-minute trials. Activity was measured via infrared beam breaks by automated tracking software. The apparatus was cleaned with 70% ethanol between trials.

Rota-rod

Motor cooridination was measured on a rota-rod treadmill (Med Associates). Mice were allowed to acclimate to the testing room for 60 minutes before testing. For testing, mice were place on an accelerating rota-rod (3.5-35 rpm) for a maximum of 5 minutes. The trial ended when a photobeam under the apparatus was broken by the falling mouse. Testing consisted of two blocks of three trials separated by 3 hours. A 10-minute resting period was given between the three trials in each block.

Water maze

Spatial learning and memory were assessed with the Morris Water Maze as described (Scearce-Levie et al., 2008). All mice were single-housed for at least 5 days before testing. Hidden platform training consisted of 4 days of training with six trials

each day (three in the morning and three in the afternoon). The platform sat 1.5 cm below the surface of the opaque water (20^{o}C) in a fixed location. Each mouse was placed in the maze, initially facing the outer wall, at a drop-off point that changed semi-randomly for each trial. A trial ended when the mouse located the platform and remained motionless on the platform for 2 seconds. If the mouse did not find the platform in 60 seconds, they were led to the platform then removed from the pool. Performance was measured with an EthoVision video-tracking system (Noldus Information Technology). A probe trial was conducted 1 day after conclusion of training. The platform was removed and each mouse was placed into the maze opposite of where the platform resided. Each trial lasted 60 seconds. The latency to find the platform was analyzed using a two-way ANOVA with repeated measures.

Electrophysiology

Electrophysiology was performed on acute hippocampal slices from 12-month-old mice. Mice were sacrificed by decapitation and brains immediately placed in ice-cold cutting solution (110 μM sucrose, 60 μM NaCl, 3 μM KCl, 1.25 μM NaH_2PO_4, 28 μM $NaHCO_3$, 2 μM $CaCl_2$, 7 μM $MgCl_2$, 5 μM glucose, and 0.6 μM ascorbate). Transverse slices (400 μm thick) were prepared on a Vibratome (The Vibratome Company) and the hippocampus was dissected from the slice in a room temperature solution of 50% cutting solution and 50% ACSF (125 μM NaCl, 2.5 μM KCl, 1.25 μM NaH_2PO_4, 25 μM $NaHCO_3$, 2 μM $CaCl_2$, 1 μM $MgCl_2$, 25 μM glucose). Slices were then equilibrated for 45 minutes in room temperature ACFS, followed by 1 hour in 32^{o}C ACSF. All solutions were saturated with 95% O_2 and 5% CO_2. Electrophysiology measurements were made in an interface chamber (Fine Science Tools) as described (Levenson et al., 2004).

Hippocampal slices were constantly perfused at a rate of 1 mL/min with 30°C ACSF. Extracellular stimuli were applied to the Schaffer-collaterals along the border of areas CA1 and CA3 (Model 2200 stimulus isolator, A–M Systems) with an enameled, bipolar platinum-tungsten (92%:8%) electrode. fEPSPs were recorded in stratum radiatum with a glass recording electrode (1–3 MΩ) filled with ACSF. Clampex was used for data acquisition and Clampfit used for data analysis (Molecular Devices). Input/output curves were generating by applying a range of stimuli from 0.5V to 30V in 1V increments. Intensities were averaged over three sweeps. The stimulus intensity that evoked 50% of the maximal fEPSP slope was used for subsequent stimulations. Paired-pulse facilitation was measured by applying consecutive stimuli at a range of interstimulus intervals (10, 20, 50, 100, 150, 200, 250, 300 ms). After 20 minutes of baseline recording, LTP was induced by applying two 100-Hz, 1-second stimulus trains, 20 seconds apart. Recordings were taken every 20 seconds, and data were averaged into 2-minute intervals. Data from paired pulse facilitation and LTP were analyzed using a two-way ANOVA with repeated measures.

Spine density

Mouse brains were processed for morphological assessment with the FD Rapid GolgiStain Kit (FD NeuroTechnologies) according to the manufacturer's protocol. Mice were sacrificed with 100 mg/kg Fatal-Plus (Vortech Pharmaceuticals) and decapitated, and brains were removed. Hemibrains were submerged in impregnation solution for 14 days then transferred to a cryoprotectant for an additional 7 days. Next, brains were cut into 200-µm sections with a cryostat (Leica) and mounted on gelatin-coated slides. After mounting, the slides were rinsed in ddH_2O and incubated in developing solution. After

development, the sections were rehydrated with increasing concentrations of ethanol and cleared with xylene. Lastly, slides were coverslipped using EUKITT mounting medium (Electron Microscopy Sciences).

Microscopy was performed on a MicroBrightField system (MBF Bioscience). Image stacks were taken of 10–40 µm segments of second-order apical dendrites on CA1 pyramidal neurons at 100X (oil-immersion). All image stacks were manually traced using Neurolucida and analyzed using Neurolucida Explorer.

Immunohistochemistry

Immunohistochemistry was performed on free-floating 30-µm thick coronal sections as described (Palop et al., 2011). To obtain sections, mice were sacrificed as described above and transcardially perfused with normal saline. Brains were removed, drop-fixed in 4% paraformaldehyde in phosphate buffer (PB: 80 mM Na_2HPO_4, 200 mM NaH_2PO_4, pH 7.4), and placed at 4^{o}C for 48 hours. After two phosphate-buffered saline (PBS) washes, the brains were transferred to 30% sucrose in PBS for 48 hours or until they sank. 30-µm sections were then cut on a sliding microtome with freezing stage (Leica). The sections were placed in cryoprotectant (30% ethylene glycol, 30% glycerol, 40% PBS, v/v/v) and held at –20^{o}C until use.

Sections were washed free of cryoprotectant with PBS. Endogenous peroxidase activity was quenched with 3% H_2O_2 and 10% methanol in PB, followed by blocking with 10% normal goat serum (Vector Laboratories), 1% dry milk, and 0.2% gelatin to prevent nonspecific binding. Primary antibodies were used at the following concentrations diluted in PBS: 3% normal goat serum and 0.2% gelatin: Iba1 (1:5000; Wako), GFAP (1:5000; Dako), c-fos (1:10,000; EMD Millipore). Species-specific

biotinylated secondary IgG (1:5000; Vector Laboratories) was applied and the Vectastain Elite avidin-biotin horseradish peroxidase complex kit (Vector Laboratories) was used for amplification. Diaminobenzidine:tetrahydrochloride was added for detection and sections were mounted with cover glass using Cytoseal 60 (Electron Microscopy Sciences). For analysis of Iba1 and GFAP, photomicrographs of 3 sections per mouse were collected on an upright microscope (Zeiss) with a 10X objective. Thresholds were set to include only GFAP or Iba1 positive pixels. The total number of GFAP or Iba1 positive pixels per image were quantified then averaged for the 3 images. Autofluorescent images were taken on an upright microscope (Zeiss) equipped with a FITC (Ex 480/30 Em 535/40) filter cube. Pixel densities were calculated using Image J software.

Quantitative real-time PCR

TNF-α mRNA levels were quantified using qPCR. RNA was first prepared using Trizol reagent (Invitrogen), according to manufacturer's protocol. From the prepared RNA, cDNAs were generated with SuperScript III and random primers (Invitrogen). cDNAs were quantified using LightCycler 480 Probes master mix (Roche) and Taqman Gene Expression Assays for TNF-α (Mm00443258_m1), progranulin (Mm00433848_m1), and β-actin (Mm00607939_s1). Amplification was performed on a Roche LightCycler 480, and data were quantified using the ΔΔCt method (User Bulletin #2, Applied Biosystems).

Novel/social environment

Mice were exposed to a novel and social environment as previously described (Scearce-Levie et al., 2008). Briefly, two mice of the same genotype and opposite sex were placed in a cage with a new type of bedding and novel olfactory, tactile, and visual

stimuli for 2 hours prior to sacrificing. Control mice were left in their home cage, undisturbed for 3 days prior to sacrifice.

For neuron counts, sections were immunostained for c-fos or NeuN as described above, then scanned with a slide scanner (Electron Microscopy Sciences). Three serial sections, 300 microns apart, in which the caudate/putamen and amygdala were clearly defined (between 1.0 and 1.8 mm posterior to bregma) were chosen. Cells were manually counted by an observer blind to genotype using landmarks as described in Figure A2.4. Any cell touching a line was excluded from the count. Data are represented as a sum of all cells counted through the 3 sections.

Data Analysis

All experiments were conducted by observers blinded to genotype. All data represent means ± SEM. Data were analyzed using GraphPad Prism or SPSS, and statistical comparisons were made with ANOVA with Dunnet's *post-hoc* test for multiple comparisons unless otherwise stated. A $p < 0.05$ was considered significant. Outliers more than two standard deviations from the mean were excluded for all behavioral assays.

Results

Progranulin Haploinsufficiency Causes Social Dysfunction

Social withdrawal is a common symptom of FTD. To test social withdrawal in progranulin-deficient mice, we used the three-chamber sociability test (Moy et al., 2004). This test measures the sociability of a mouse when given the choice between interacting with another mouse versus an inanimate object. We tested two separate cohorts of 6–7-month-old wild-type ($Grn^{+/+}$), $Grn^{+/-}$, and $Grn^{-/-}$ mice on a mixed genetic background. As expected, $Grn^{+/+}$ mice spent more time interacting with the other mouse than with the object (average conspecific:inanimate ratio 2.75±0.23), and $Grn^{-/-}$ mice showed reduced sociability (Fig. 3.1A). Interestingly, $Grn^{+/-}$ mice also showed reduced sociability to a similar extent as $Grn^{-/-}$ mice (Fig. 3.1A).

We confirmed this finding in a third cohort of mice on a congenic C57BL/6 background. When tested at 4 months, the congenic cohort showed no abnormalities (Fig. 3.1B), indicating that the sociability deficits in progranulin-deficient mice are age-dependent, not developmental. When the same cohort was tested at 9 months, $Grn^{+/-}$ mice showed reduced sociability, just as on the mixed background (Fig. 3.1C). On both genetic backgrounds, similar deficits were observed in males and females.

This abnormality in progranulin-deficient mice could be due to either a true social deficit or an inability to detect pheromones, an olfactory cue critical for social behavior. To distinguish between these possibilities, we determined the preference to explore a pheromone-scented stimulus over a control without pheromones. $Grn^{+/+}$ mice spent more time investigating the pheromone-positive stimulus, and similar results were observed in

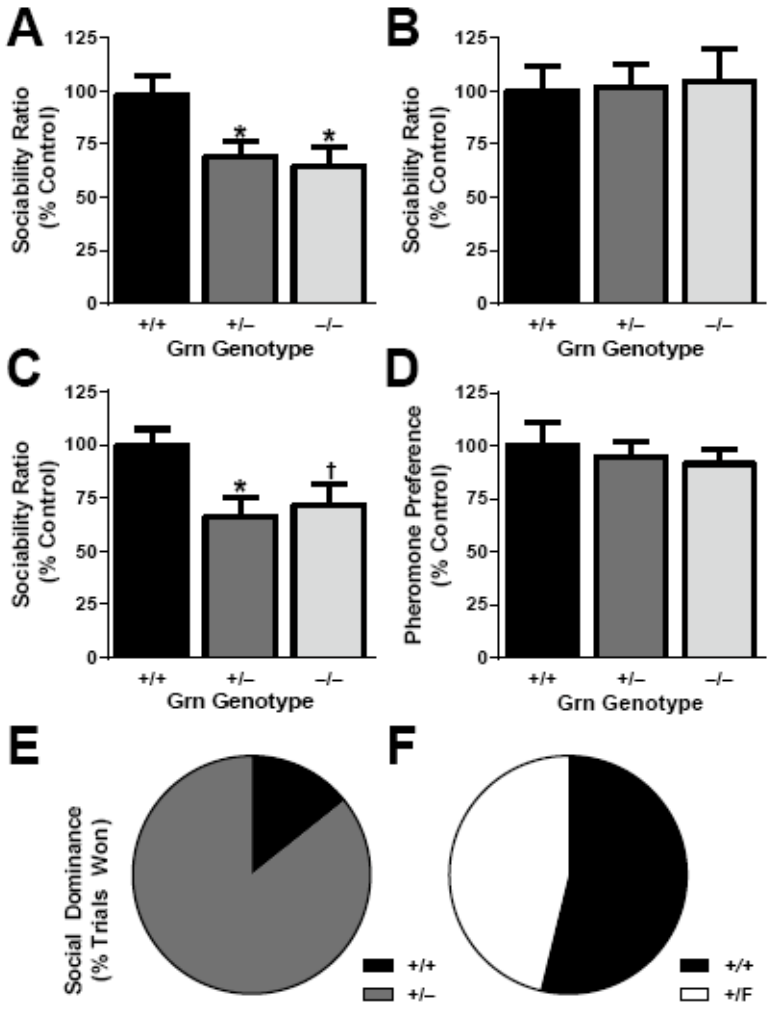

Figure 3.1 Progranulin haploinsufficiency causes social deficits.

(A–C) Three-chamber sociability test, with sociability ratio (time spent investigating another mouse divided by time spent investigating an inanimate object) expressed as percent of control. (A) On a mixed background at 6–7 months, $Grn^{+/-}$ mice and $Grn^{-/-}$ mice had lower sociability than $Grn^{+/+}$ mice (ANOVA, $p < 0.01$; * $p < 0.05$ by Dunnett's post-hoc test; $N = 51–58$ mice per genotype). (B) On a congenic C57BL/6 background at 4 months, there were no sociability deficits (ANOVA, $p = 0.9644$; $N = 15–18$ mice per genotype). (C) On a congenic C57BL/6 background at 9 months, $Grn^{+/-}$ mice and $Grn^{-/-}$ mice had lower sociability than $Grn^{+/+}$ mice (ANOVA, $p < 0.05$; * $p < 0.05$, † $p = 0.051$ by Dunnett's post-hoc test; $N = 17–18$ mice per genotype). (D) No deficit in pheromone preference was observed in progranulin-deficient mice ($N = 17$ mice per genotype; mixed background at 7–8 months). (E,F) Social interactions were further tested with the tube test of social dominance at 4–6 months old. (E) $Grn^{+/-}$ mice won 86% (12/14) of trials against $Grn^{+/+}$ mice ($\chi^2 = 7.143$, $p < 0.01$). (F) $Grn^{+/F}$ controls, which have normal progranulin levels, won 46% (6/13) of trials against $Grn^{+/+}$ mice, no different from

chance. Male and female mice were used for both social tests. No sex-dependent effects were observed so the data from males and females were combined.

Grn$^{+/-}$ and *Grn*$^{-/-}$ mice (Fig. 3.1D). Thus, progranulin deficiency does not impair olfactory detection of, or preference for, pheromones. We conclude that the deficits in the three-chamber test reflect social dysfunction.

To confirm that *Grn*$^{+/-}$ mice have social deficits, we used the tube test for social dominance (Lindzey et al., 1961). In this test, a wild-type and a test mouse of the same sex enter opposite ends of a plastic tube. The mice cannot pass each other inside the tube, so one mouse must turn around to exit. In the absence of social abnormalities, each genotype should "win" 50% of trials. However, when *Grn*$^{+/-}$ mice were paired against *Grn*$^{+/+}$ mice, *Grn*$^{+/-}$ mice won 86% of the time (12/14 trials; Fig. 3.1E). As a control, we tested mice in which one *Grn* allele was floxed, but not deleted by Cre (*Grn*$^{+/F}$ mice), so progranulin levels in these mice are normal. *Grn*$^{+/F}$ controls did not show abnormalities, winning 46% of trials which was not different from chance (6/13 trials; Fig. 3.1F). Thus, in multiple cohorts of mice on different genetic backgrounds, *Grn*$^{+/-}$ mice have impaired social behavior.

Progranulin Haploinsufficiency Impairs Fear Conditioning

Emotional impairment is also common in FTD patients (Rosen et al., 2004), including impairment of fear conditioning (Hoefer et al., 2008). To examine the effect of progranulin haploinsufficiency on fear conditioning, we performed classical cued fear conditioning. Cued fear conditioning requires an association between an aversive stimulus and an auditory cue and depends on the amygdala but is hippocampus-independent (Maren et al., 1996, Logue et al., 1997). The amount of time a mouse is immobile after being presented with the auditory cue 24 hours post-training is a measure

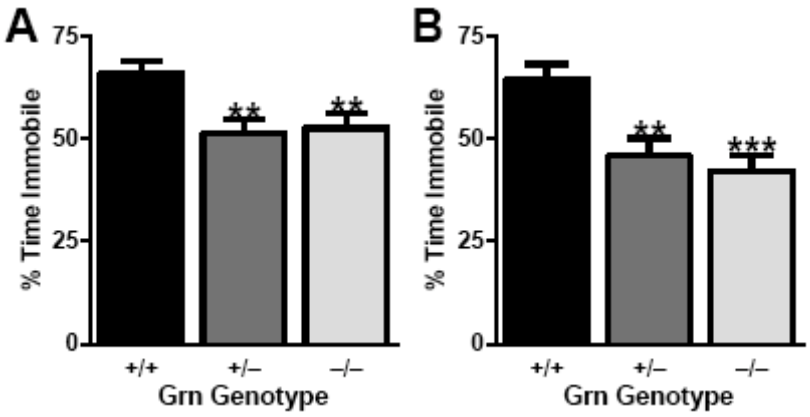

Figure 3.2 Progranulin haploinsufficiency impairs fear conditioning.

12-month-old mice from a mixed (A, $N = 26$-51 mice per genotype) or congenic (B, $N = 9$-10 mice per genotype) background were tested for cued fear conditioning one day after training. A significant effect of progranulin deficiency was observed in mice on both backgrounds (ANOVA, $p < 0.01$). Both $Grn^{+/-}$ and $Grn^{-/-}$ mice spent significantly less time immobile than $Grn^{+/+}$ mice (** $p < 0.001$, *** $p < 0.0001$ by post-hoc test).

of fear memory. On the mixed background, both *Grn*$^{+/-}$ and *Grn*$^{-/-}$ mice had impaired fear conditioning, with a decrease in the percent time spent immobile during the auditory cue (Fig. 3.2A). Similar results were obtained on a congenic C57BL/6 background (Fig. 3.2B). For each cohort, deficits in *Grn*$^{+/-}$ mice were equivalent to those in *Grn*$^{-/-}$ mice. As with the sociability assay, no abnormalities in fear conditioning were observed at 4 months of age, no significant sex effects were observed (data not shown). Therefore, in multiple cohorts of mice on different genetic backgrounds, *Grn*$^{+/-}$ mice have emotional dysfunction.

Sparing of Other Domains in Progranulin-deficienct Mice

We also examined a variety of other behavioral measures to determine if the social and emotional abnormalities in *Grn*$^{+/-}$ mice reflected more global neuronal dysfunction. Progranulin-deficient mice had no detectable abnormalities in postnatal development (Fig. 3.3A–C), consistent with the findings that social and emotional deficits did not develop until after four months. We also observed no deficits in adult mice in locomotor activity (Fig. 3.3D–F) or anxiety-related behavior (Fig. A2.2).

FTD causes significant social and emotional dysfunction, but hippocampal function is relatively preserved in the early stages of disease (Kril and Halliday, 2011). To investigate hippocampal function in progranulin-deficient mice, we performed a rigorous battery of behavioral, electrophysiological, and structural analyses. First, we used the Morris water maze to test spatial memory in 7-month-old mice. *Grn*$^{+/-}$ and *Grn*$^{-/-}$ mice learned to find the hidden platform just as well as *Grn*$^{+/+}$ mice (Fig. 3.4A). During the probe trial, all three groups spent more time in the target quadrant than the

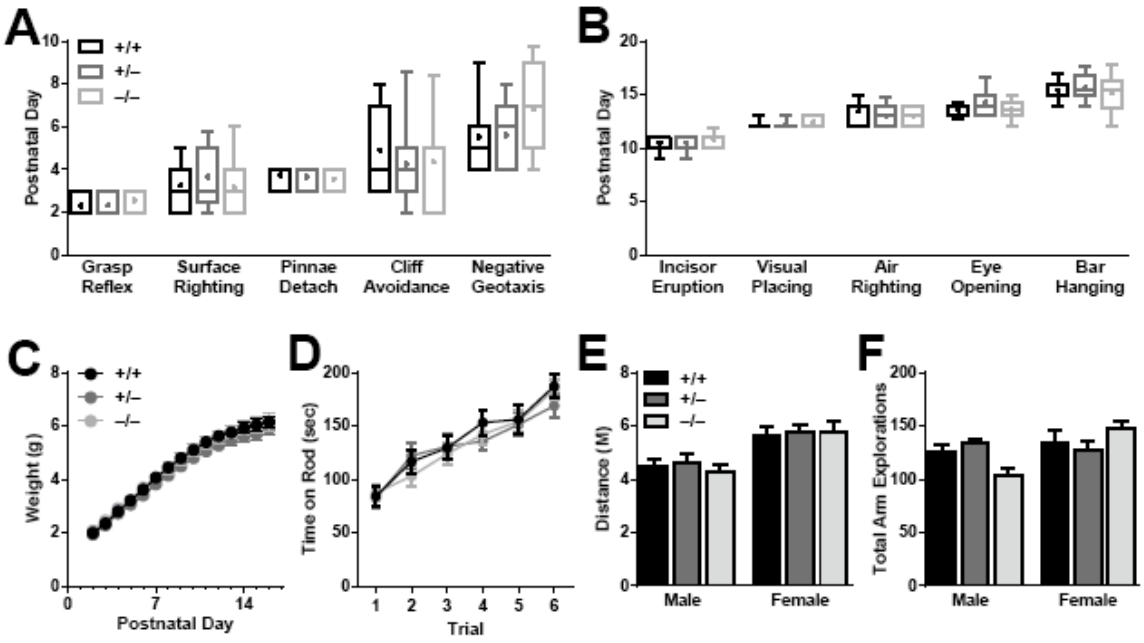

Figure 3.3 Progranulin deficiency does not affect postnatal developmental or motor/exploratory behavior.

(A and B) Box-and-whisker plots representing the age at which early (A) and late (B) milestones were attained for each genotype. Boxes indicate the 75th and 25th percentiles, with a horizontal line at the median and a dot at the mean; whiskers represent the 10th and 90th percentiles (N = 11–21 mice per genotype). (C) Weight gain for the first 16 postnatal days (N = 11–21 mice per genotype). (D) No differences were observed in motor performance on the rotarod. Data are represented as time spent on the rod before falling (N = 30 mice per genotype). (E) No differences were observed in exploratory behavior in the open field. Data are represented as total distance traveled during 15 min (congenic C57BL/6 background; N = 12–15 mice per genotype; age 9 months). (F) No differences were observed in total arm explorations during 10 min in the elevated plus maze (congenic C57BL/6 background; N = 14–15 mice per genotype; age 9 months).

other quadrants (Fig. 3.4B). Next, we recorded electrophysiological responses at the Schaffer collateral–CA1 synapse in acute hippocampal slices. Progranulin deficiency caused no changes in basal synaptic transmission, determined by input/output curves (Fig. 3.4C), long-term potentiation (Fig. 3.4D), or paired-pulse facilitation (Fig. 3.4E). Finally, we evaluated the morphology of hippocampal CA1 pyramidal neurons and found that progranulin deficiency did not affect spine density in this region (Fig. 3.4F). Furthermore, we confirmed that progranulin deficiency does not alter hippocampal spine density in an independent line of progranulin knockout mice produced by another group (Fig. A2.3). We conclude that the hippocampus is relatively spared by progranulin deficiency at ages when deficits are seen in more FTD-related regions.

Murine Progranulin Haploinsufficiency Does Not Cause Gliosis or Lipofuscinosis

Our analysis of $Grn^{+/-}$ mice indicates that they display an FTD-like phenotype with social and emotional dysfunction and relative preservation of other domains. To begin determining how progranulin haploinsufficiency causes deficits in these mice, we looked for gliosis and neuroinflammation, which in other lines was present in $Grn^{-/-}$ mice but absent in $Grn^{+/-}$ mice (Ahmed et al., 2010). As expected, $Grn^{-/-}$ mice had significant microgliosis in multiple brain regions including thalamus (Fig. 3.5A, B), hippocampus (Fig. 3.5C), and cortex (Fig. 3.5D), but not in the amygdala (data not shown). And consistent with prior studies, $Grn^{+/-}$ mice did not have microgliosis (Fig. 3.5A–D). Other measures of neuroinflammation had the same pattern of abnormalities in $Grn^{-/-}$ but not $Grn^{+/-}$ mice, including TNF-α mRNA levels (Fig. 3.5E–G) and astrocytosis (Fig. 3.5H–K). While not surprising given prior studies, the differences in

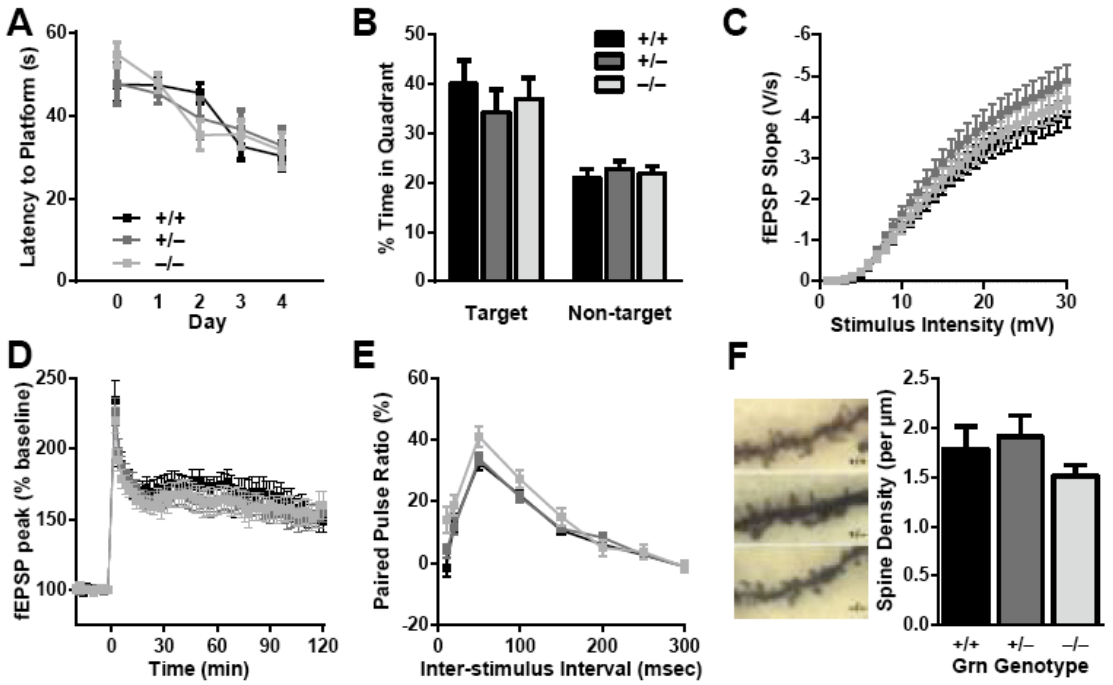

Figure 3.4 Progranulin-deficient mice have normal hippocampal function and spine density.

(A) Learning curves on the Morris water maze hidden platform task were not affected by progranulin deficiency. (B) Dwell time in the target quadrant on a probe trial conducted 24 hours after completion of training was not affected by progranulin deficiency (N = 14 mice per genotype; age = 7 months). (C–E) Extracellular field recordings in area CA1 of acute hippocampal slices (N = 31–40 slices from 5–6 mice per genotype; age = 12 months). (C) Progranulin deficiency did not affect baseline synaptic transmission, assessed by input–output curves. (D) Progranulin deficiency did not affect LTP, either early or late stages. (E) Progranulin deficiency did not affect paired-pulse facilitation. (F) Progranulin deficiency did not affect hippocampal spine density in second-order apical dendrites of Golgi-stained CA1 pyramidal neurons (N = 9–10 neurons from two mice per genotype; age = 12 months).

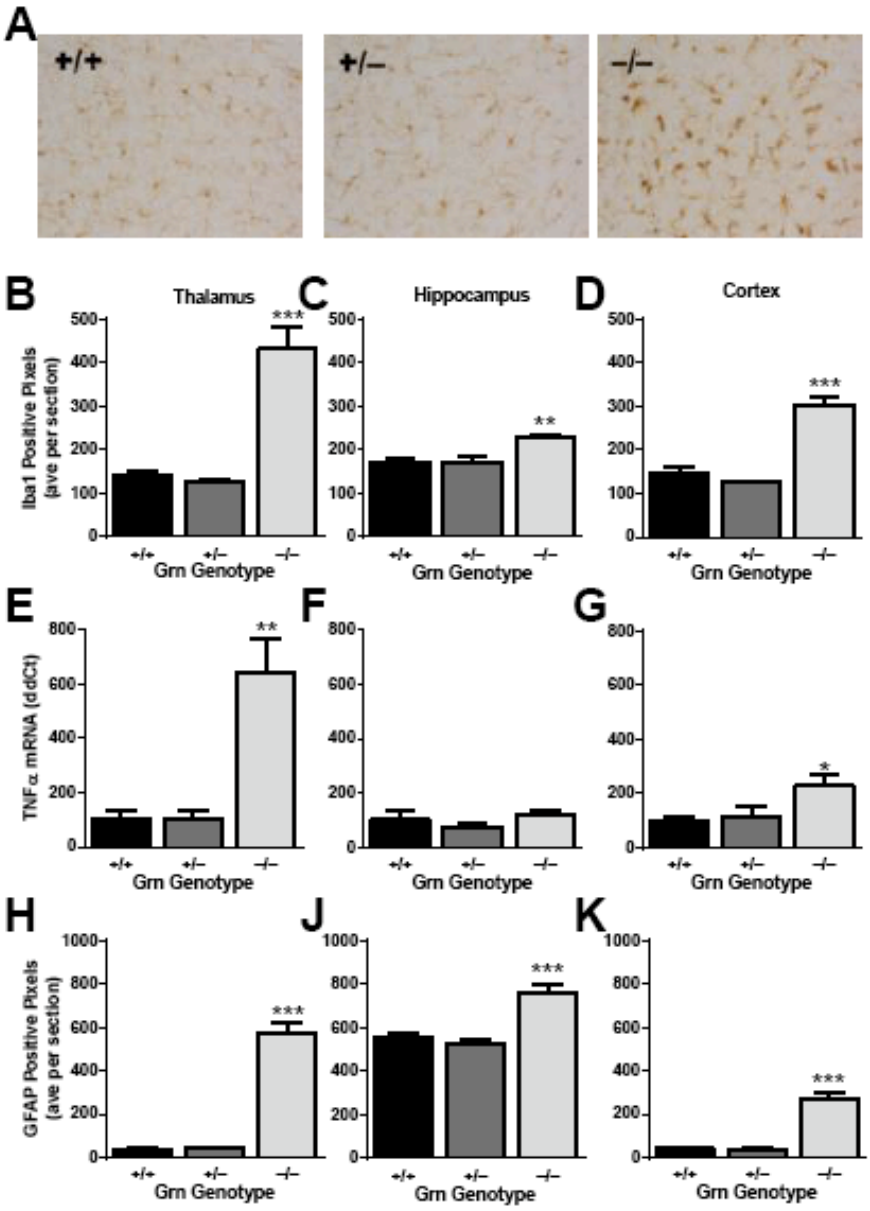

Figure 3.5 Absence of neuroinflammation in *Grn*$^{+/-}$ mice with FTD-related behavioral abnormalities.

(A) Representative images of Iba1 immunohistochemistry in the thalamus of control and progranulin-deficient mice. (B–D) Quantification of Iba1 immunoreactivity in various brain regions ($N = 6$ mice per genotype; age = 12 months). (B) *Grn*$^{-/-}$, but not *Grn*$^{+/-}$, mice had microgliosis in thalamus (ANOVA, $p < 0.0001$; on post-hoc tests only *Grn*$^{-/-}$ mice differ from other groups, *** $p < 0.0001$). (C) *Grn*$^{-/-}$, but not *Grn*$^{+/-}$, mice had microgliosis in hippocampus (ANOVA, $p < 0.005$; on post-hoc tests only *Grn*$^{-/-}$ mice differ from other groups, ** $p < 0.001$). (D) *Grn*$^{-/-}$, but not *Grn*$^{+/-}$, mice had microgliosis in cortex (ANOVA, $p < 0.0001$; on post-hoc tests only *Grn*$^{-/-}$ mice differ from other groups, *** $p < 0.0001$). (E–G) qPCR analysis of TNF-α mRNA levels in various brain

regions (N = 5–6 mice per genotype; age = 19 months). (E) $Grn^{-/-}$, but not $Grn^{+/-}$, mice had increased TNF-α in thalamus (ANOVA, $p < 0.005$; on post-hoc tests only $Grn^{-/-}$ mice differ from other groups, ** $p < 0.001$). (F) There were no significant differences in TNF-α in hippocampus. (G) $Grn^{-/-}$, but not $Grn^{+/-}$, mice had increased TNF-α in cortex (ANOVA, $p < 0.05$; on post-hoc tests only $Grn^{-/-}$ mice differ from other groups, * $p < 0.05$). (H–K) Quantification of GFAP immunoreactivity in various brain regions (N = 6 mice per genotype; age = 12 months). (H) $Grn^{-/-}$, but not $Grn^{+/-}$, mice had astrocytosis in thalamus (ANOVA, $p < 0.0001$; on post-hoc tests only $Grn^{-/-}$ mice differ from other groups, *** $p < 0.0001$). (J) $Grn^{-/-}$, but not $Grn^{+/-}$, mice had astrocytosis in hippocampus (ANOVA, $p = 0.0001$; on post-hoc tests only $Grn^{-/-}$ mice differ from other groups, *** $p < 0.001$). (K) $Grn^{-/-}$, but not $Grn^{+/-}$, mice had astrocytosis in cortex (ANOVA, $p < 0.0001$; on post-hoc tests only $Grn^{-/-}$ mice differ from other groups, *** $p < 0.0001$).

neuroinflammation between *Grn*$^{-/-}$ and *Grn*$^{+/-}$ mice becomes quite interesting in light of the presence of behavioral deficits in *Grn*$^{+/-}$ mice. The dissociation between functional impairment and microgliosis in *Grn*$^{+/-}$ mice suggests that neuroinflammation is likely not driving the functional deficits due to progranulin haploinsufficiency in these mice.

Because homozygous *GRN* mutations in humans cause neuronal ceroid lipofuscinosis (Smith et al., 2012) and *Grn*$^{-/-}$ mice display autofluorescent lipofuscin granules in the hippocampus (Ahmed et al., 2010, Petkau et al., 2011) we quantified these deposits in our mice. The density of autofluorescent granules was increased not only in the hippocampus of *Grn*$^{-/-}$ mice, but also in the frontal cortex, thalamus, and amygdala (Fig. 3.6). However, these deposits were not increased above normal levels in *Grn*$^{+/-}$ mice (Fig. 3.6). These data also dissociate lipofuscin pathology from the functional deficits in *Grn*$^{+/-}$ mice and suggest that lipofuscinosis does not contribute to the impairments caused by progranulin haploinsufficiency.

Progranulin Haploinsufficiency Impairs Amygdala Function

Given the dissociation between neuroinflammation and functional deficits, we turned our attention from microglia to neurons, which are the other major cell type expressing progranulin in the brain (Petkau et al., 2010). We exposed mice to a novel environment with various stimuli including a conspecific of the same genotype and opposite sex for two hours prior to sacrifice, then stained for the immediate early gene, c-Fos, to identify activated neurons (Scearce-Levie et al., 2008). We focused on the amygdala for several reasons. First, amygdala dysfunction could account for the social and emotional abnormalities we observed in progranulin-deficient mice, as regulation of social interactions and emotion are core functions of the amygdala

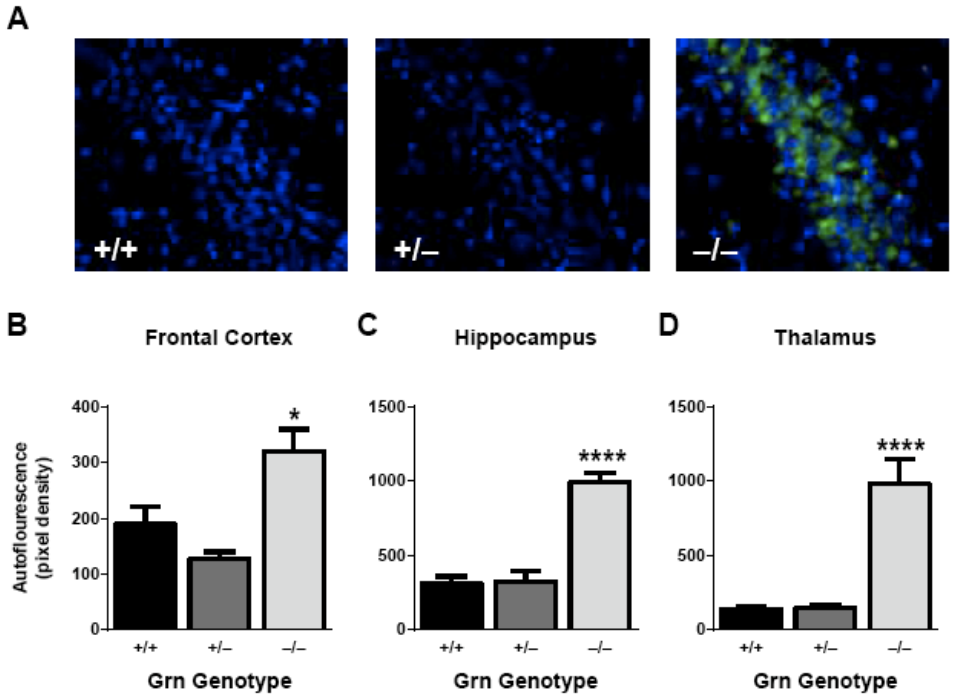

Figure 3.6 Absence of lipofuscinosis in *Grn*$^{+/–}$ mice.

(A) Representative images of autofluorescent lipofuscin granules in the CA3 region of the hipocampus. (B–E) Quantification of autofluorescence in various brain regions (N = 6–8 mice per genotype; age = 12 months). Increased autofluorescence was observed in *Grn*$^{–/–}$, but not *Grn*$^{+/–}$ mice (ANOVA, $p < 0.001$; on post-hoc tests only *Grn*$^{–/–}$ mice differ from other groups, * $p < 0.05$; **** $p < 0.0001$).

(LeDoux, 2003, Adolphs, 2010). Specifically, amygdala dysfunction has shown to decrease sociability in the three-chamber test (Moya et al., 2011) and impair fear conditioning (Maren et al., 1996). Second, the amygdala plays a major role in social and emotional symptoms of FTD (Liu et al., 2004, Hoefer et al., 2008, Kipps et al., 2009). Third, the amygdala is a component of the salience network, which is selectively vulnerable in FTD (Seeley et al., 2009, Zhou et al., 2010a).

Under resting, home-cage conditions, there were few c-Fos–positive neurons (Fig. 3.7A–C). In *Grn*$^{+/+}$ mice, exposure to a novel environment activated neurons in the central nucleus of the amygdala and the adjacent amygdalostriatal transition area (Fig. 3.7A). In contrast, both *Grn*$^{+/-}$ and *Grn*$^{-/-}$ mice had reduced activation, to a similar extent, in this area (Fig. 3.7A). This region of the amygdala is a primary output of other amygdala nuclei (LeDoux, 2007) and is critically involved in fear and social behavior (LeDoux, 2007, Bosch et al., 2010).The impairment of neuronal activity was selective to the amygdala as no differences were observed in the adjacent caudate/putamen (Fig. 3.7B) or in the dentate gyrus (Fig. 3.7C). The reduced neuronal activity was not due to decreased interactions during exploration of the novel environment (Fig. 3.7D). Furthermore, the total number of amygdala neurons, assessed by NeuN immunohistochemistry, was unchanged (Fig. 3.7E), indicating that the observed abnormality reflects a functional impairment of neuronal activation, not neuronal loss. Thus, while *Grn*$^{+/-}$ mice do not have gliosis or lipofuscinosis, they do have neuronal dysfunction in the amygdala, a region critical for normal social and emotional function (Adolphs, 2010, Bickart et al., 2011) that is strongly affected in FTD (Rabinovici and Miller, 2010).

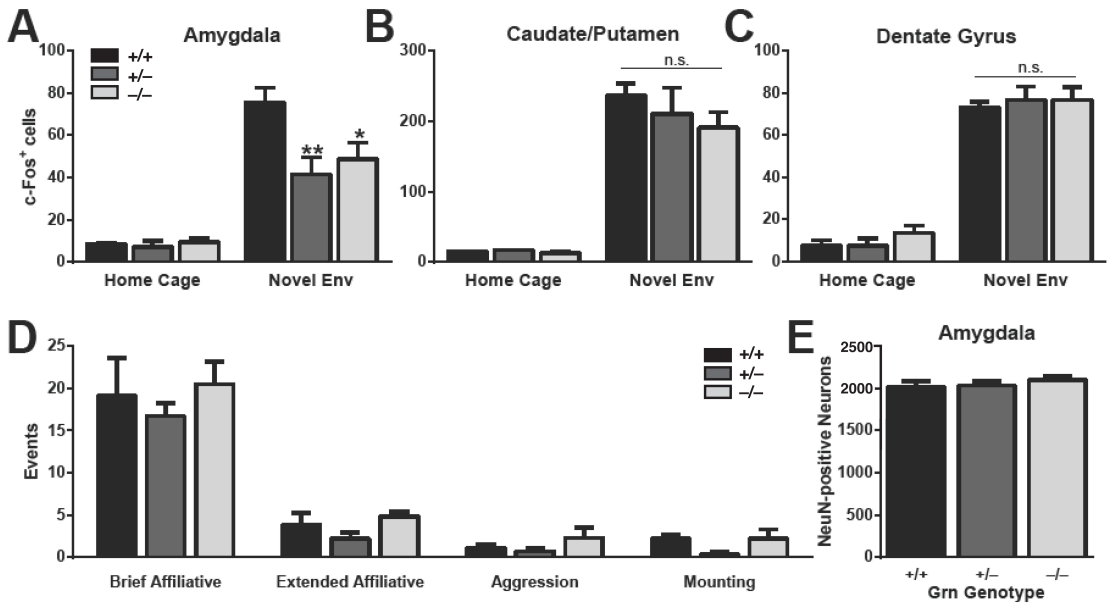

Figure 3.7 Decreased neuronal activation in the amygdala of *Grn*$^{+/-}$ mice.

(A-C), Active c-Fos–positive neurons were counted in various brain regions. Under resting, home-cage conditions, few neurons were c-Fos–positive. (A) Fewer c-Fos–positive neurons were present in the amygdala of *Grn*$^{+/-}$ and *Grn*$^{-/-}$ mice after two hours in a novel environment (ANOVA, $p<0.05$; ** $p < 0.01$; * $p < 0.05$ vs. *Grn*$^{+/+}$ mice on *post-hoc* test). There was no difference in the number of c-Fos–positive neurons in the (B) caudate/putamen or (C) dentate gyrus of the hippocampus. (D) There were no differences between groups in the number of social interactions of various types during the two hours in the novel environment. (E) There were no differences in total NeuN-positive amygdala neuron counts of progranulin-deficit mice, so the decrease in c-Fos–positive neurons cannot be attributed to neuron loss, but rather to impaired activation.

Discussion

In this study, we demonstrate that progranulin haploinsufficiency in *Grn*$^{+/-}$ mice causes neuronal dysfunction potentially related to FTD, but with mechanistically informative differences from existing *Grn*$^{-/-}$ models with complete progranulin deficiency. We found that *Grn*$^{+/-}$ mice have social and emotional dysfunction without detectable differences in hippocampal function or other behavioral abnormalities. However, neuronal dysfunction in *Grn*$^{+/-}$ mice occurs without neuroinflammation (microgliosis, increased TNF-α, and astrogliosis), indicating that these abnormalities found in *Grn*$^{-/-}$ mice do not mediate the FTD-like dysfunction due to progranulin haploinsufficiency in *Grn*$^{+/-}$ mice. Instead, we found decreased neuronal activity in the amygdala of *Grn*$^{+/-}$ (and *Grn*$^{-/-}$) mice, suggesting important neuronal effects from progranulin haploinsufficiency.

Behavioral Abnormalities in Progranulin Mouse Models

Most reports on the three previously published progranulin knockout mouse lines have focused on homozygous *Grn*$^{-/-}$ mice. To our knowledge, there is just one study reporting behavioral data from *Grn*$^{+/-}$ mice, which examined only sexual behavior, aggression, and anxiety (Kayasuga et al., 2007). There were no significant abnormalities in *Grn*$^{+/-}$ mice, although they trended toward abnormal sexual behavior that was intermediate between *Grn*$^{+/+}$ and *Grn*$^{-/-}$ mice (Kayasuga et al., 2007). Other behavioral studies included only *Grn*$^{-/-}$ mice. Of note, in the line utilizing a gene trap construct, progranulin levels were not reduced in heterozygous mice (Petkau et al., 2011), limiting their usefulness to model haploinsufficiency.

We found that progranulin haploinsufficiency in mice produces key features of FTD. Impaired social function is a cardinal symptom of FTD (Rascovsky et al., 2011). We observed social deficits in *Grn*$^{+/-}$ mice in multiple cohorts of mice on two different genetic backgrounds (Fig. 3.1). These deficits were apparent with both the three-chamber sociability test and the tube test. Social dysfunction is the most consistently observed abnormality in progranulin-deficient mice. Although different groups have used different assays, each of the four *Grn*$^{-/-}$ lines now published has social deficits. One study previously showed deficits on the three-chamber sociability test in a different *Grn*$^{-/-}$ line (Yin et al., 2010). Deficits in that study appeared at one month of age, but we found the sociability deficit to be age-dependent, with deficits emerging after 4 months (Fig. 3.1B,C). Two other *Grn*$^{-/-}$ lines had social deficits on the resident-intruder test (Kayasuga et al., 2007, Ghoshal et al., 2011, Petkau et al., 2011).

Impairment of emotion, particularly "negative" emotions such as fear, is another common feature of FTD (Werner et al., 2007, Kipps et al., 2009). We tested classical fear conditioning, which is impaired in FTD patients (Hoefer et al., 2008). *Grn*$^{+/-}$ and *Grn*$^{-/-}$ mice had impaired fear conditioning, again on both genetic backgrounds (Fig. 3.2).
In addition to social and emotional deficits, FTD is characterized by relative preservation, in early stages, of other cognitive domains including learning and memory. We observed no deficits in learning and memory, hippocampal physiology, or hippocampal spine density in *Grn*$^{+/-}$ or *Grn*$^{-/-}$ mice (Fig. 3.4). These results corroborate previous work indicating that deficits in hippocampal-dependent learning and memory, if present, do not occur until much later than social abnormalities in *Grn*$^{-/-}$ mice (Yin et al., 2010, Ghoshal et al., 2011). One study using a gene trap that expresses LacZ in place of progranulin

found hippocampal synaptic deficits and spine loss in *Grn*$^{-/-}$ mice (Petkau et al., 2011); we did not observe these changes in two different lines of *Grn*$^{-/-}$ mice (Fig. 3.4 and Fig. A2.3). It is possible that the abnormalities observed in the gene trap line result from overexpression of LacZ rather than from progranulin deficiency.

Progranulin Deficiency, Inflammation, and FTD

Evidence from *Grn*$^{-/-}$ mice suggested that progranulin deficiency fosters inflammatory changes that could contribute to FTD. Stimulating *Grn*$^{-/-}$ macrophages leads to exaggerated release of neurotoxic cytokines (Yin et al., 2009) and accelerated phagocytosis (Kao et al., 2011). *Grn*$^{-/-}$ mice also display striking, age-dependent microgliosis and astrogliosis (Ahmed et al., 2010, Yin et al., 2010, Ghoshal et al., 2011)(Fig. 5). Recent studies showed that progranulin attenuates the activation of TNF-α receptors and that loss of this anti-inflammatory effect of progranulin increases susceptibility to inflammatory arthritis in *Grn*$^{-/-}$ mice (Tang et al., 2011). Consistent with a role of progranulin in attenuating inflammation, we found increased TNF-α mRNA in the brains of *Grn*$^{-/-}$ mice (Fig. 3.5E–G).

However, our findings indicate that inflammatory changes are not necessary for the FTD-like dysfunction induced by progranulin haploinsufficiency. Middle-aged *Grn*$^{+/-}$ mice had similar social and emotional dysfunction as *Grn*$^{-/-}$ mice (Figs. 3.1 and 3.2) but no apparent microgliosis, increased TNF-α, or astrogliosis (Fig. 3.5). Others have also found that *Grn*$^{+/-}$ mice do not develop gliosis (Ahmed et al., 2010). Because the FTD-like behavioral abnormalities did not differ between *Grn*$^{+/-}$ and *Grn*$^{-/-}$ mice, our data suggest that gliosis and increased TNF-α, while present in *Grn*$^{-/-}$ mice, are not required for associated behavioral deficits. Of course, these findings do not rule out a role for TNF

signaling in the deficits in *Grn*$^{+/-}$ mice; it is possible that reduced progranulin levels in *Grn*$^{+/-}$ mice increase TNF receptor signaling without elevation of TNF-α levels.

While our data indicate that gliosis is not necessary for deficits in mice with progranulin haploinsufficiency, microgliosis and astrogliosis are present at autopsy in FTD patients with progranulin haploinsufficiency (Mackenzie and Rademakers, 2007). This may reflect the fact that while we are studying the initial sequelae of progranulin haploinsufficiency in mice, the human tissue is from end-stage disease and the gliosis may represent a reactive change to neuronal injury that developed over many years. Thus, although our data suggest that gliosis is not necessary for early dysfunction due to progranulin haploinsufficiency, it is possible that in FTD patients, gliosis exacerbates neuronal injury, perhaps creating a vicious circle leading to further reactive gliosis and additional injury. Indeed, murine progranulin deficiency predisposes to increased neuroinflammation in response to CNS injury (Martens et al., 2012). Causality is difficult to dissect in human subjects, and cell type–specific knockout mice in which progranulin is selectively reduced in neurons or microglia will further illuminate the contribution of each cell type to the progression of FTD.

Haploinsufficiency vs. Complete Progranulin Deficiency

The early finding that *Grn*$^{+/-}$ mice lacked many neuropathological abnormalities seen in *Grn*$^{-/-}$ mice (Ahmed et al., 2010) suggested that *Grn*$^{-/-}$ mice may be superior to *Grn*$^{+/-}$ mice as a tool for studying FTD. The recent discovery that patients completely lacking progranulin due to homozygous *GRN* mutations develop a different disease, neuronal ceroid lipofuscinosis (Smith et al., 2012), calls for reevaluating this idea. Complete progranulin deficiency produces a more aggressive disorder (the siblings with

homozygous *GRN* mutations developed a syndrome of vision loss, seizures, and cerebellar ataxia in their 20's) with a different pathophysiology (lysosomal storage disorder) than progranulin haploinsufficiency. Thus, we should expect that some phenotypes of $Grn^{-/-}$ mice will not be applicable to FTD. The lipofuscinosis in $Grn^{-/-}$ mice (Ahmed et al., 2010, Petkau et al., 2011)(and Fig. 6) is almost certainly one example. Further work is needed to determine whether the neuroinflammatory changes in $Grn^{-/-}$ mice are mechanistically related to progranulin haploinsufficient FTD, or only to neuronal ceroid lipofuscinosis.

$Grn^{+/-}$ mice have advantages and disadvantages for studying FTD. The lack of TDP-43 pathology in $Grn^{+/-}$ mice makes them an incomplete model of FTD due to progranulin deficiency and limits their use for addressing how progranulin impacts TDP-43. However, this is not an irredeemable weakness. There are now several examples of dissociation between the functional effects of proteins involved in neurodegenerative disease and their neuropathological aggregates, including beta-amyloid plaques, tau tangles (Santacruz et al., 2005), and huntingtin inclusion bodies (Arrasate et al., 2004). Thus, the lack of TDP-43 aggregates does not necessarily preclude using $Grn^{+/-}$ mice to study how progranulin haploinsufficiency produces social and emotional dysfunction, which should be an important goal for future research.

The chief advantage of $Grn^{+/-}$ mice for studying FTD is that one progranulin allele remains intact, which may enable their use for evaluating of potential therapeutics. Increasing progranulin levels from the normal allele is perhaps the most straightforward strategy for treating FTD due to *GRN* mutations. Several progranulin expression–raising compounds have been identified, including amiodarone and the histone deacetylase

inhibitor, SAHA (Capell et al., 2011, Cenik et al., 2011), which are both already FDA-approved for other indications. It may also be possible to target specific miRNAs to elevate progranulin levels (Jiao et al., 2010, Wang et al., 2010). The presence of multiple functional outcome measures relevant to FTD in *Grn*$^{+/-}$ mice may make them a useful tool for preclinical studies of potential therapies for treating patients with progranulin mutations.

Chapter 4

Age-dependent Neuroinflammation, Vascular Alterations, and OCD-like Behaviors in a Mouse Model of Progranulin Deficiency

Summary

Frontotemporal dementia (FTD) disease pathology includes both neuron loss and neuroinflammation, and similar to other neurodegenerative diseases, age is the biggest known risk factor. Understanding the role of PGRN deficiency in aging is critical to uncovering the disease mechanism that will aid in the determination of potential therapeutic targets. It has been determined that PGRN deficient mice mimic aspects of human FTD, but it is currently unclear what cellular alteration triggers the pathology associated with the aging mice and human disease. We therefore are performing an extensive aging study of our global PGRN-deficient mouse model, as well as cell-specific models, in order to determine the sequence of cellular and regional changes that cause the pathological phenotypes. So far, we have demonstrated that gliosis occurs at an early age and precedes neuron loss and vascular changes in the thalamus. Further analysis is required to investigate early neuronal dysfunction in these mice. It is unclear whether or not any or all of these changes can be linked to the OCD-like behaviors that develop the $Grn^{-/-}$ mice.

Introduction

Similar to all other neurodegenerative diseases, aging is the number one risk factor for frontotemporal dementia (FTD). When mutations in the progranulin (*PGRN*) gene were causatively linked to FTD in 2006, the CNS function of PGRN was not well understood (Baker et al., 2006, Cruts et al., 2006). All that was known at the time was that PGRN haploinsuffiency led to the development of FTD with ubiquitin-positive, TDP-43 containing aggregates in neurons and microglia, and neuroinflammation in the affected brain regions, frontal cortex and temporal lobes (Mackenzie, 2007).

We and others have developed PGRN deficient mouse models in order to begin to elucidate the CNS function of PGRN and to determine if murine PGRN deficiency recapitulates certain aspects of human FTD. To date, $Grn^{-/-}$ mice were shown to have social and anxiety deficits (Kayasuga et al., 2007, Yin et al., 2010, Ghoshal et al., 2011) (chapter 3), slight neuronal dysfunction in the hippocampus (Petkau et al., 2011) and amygdala (chapter 3), as well as age-dependent regional gliosis, accumulation of ubiquitin-positive aggregates of cytoplasmic, phosphorylated TDP-43, and accumulation of lipofuscin (Yin et al., 2009, Ahmed et al., 2010, Yin et al., 2010, Ghoshal et al., 2011, Petkau et al., 2011, Wils et al., 2012). All of these findings resemble aspects of the human disease, although the majority of these changes are identified in $Grn^{-/-}$, but not in $Grn^{+/-}$ mice.

The one characteristic that is the most obvious and found in all of the PGRN-deficient mouse models is age-dependent regional gliosis in the hippocampus, cortex, and thalamus (Yin et al., 2009, Ahmed et al., 2010, Yin et al., 2010, Ghoshal et al., 2011, Petkau et al., 2011, Wils et al., 2012). We have also demonstrated that following brain

injury, microglial PGRN is critical for the regulation of the neuroinflammatory response and that uncontrolled PGRN-deficient neuroinflammatory response is detrimental to neuron survival. Therefore, even if the underlying changes in PGRN deficiency are functional changes in neurons, blocking neuroinflammatory response may have benefical effects on the aging pathology of the *Grn*$^{-/-}$ mice.

In this study, we set out to perform an extensive pathological analysis of our aging PGRN-deficient mice as well as microglia- and neuron-specific PGRN-deficient mice start uncovering the first cellular alterations associated with PGRN deficiency. These studies will allow us to determine in which cell type PGRN deficiency is most critical for the development of the aging related phenotypes.

Results

We utilized our model of murine PGRN deficiency to investigate the aging phenotypes associated with global, as well as CNS cell-type specific, PGRN deficiency (Martens et al., 2012). *Grn*$^{+/+}$, *Grn*$^{+/-}$, and *Grn*$^{-/-}$ littermate mice were aged in a barrier facility to 4, 7, 12, and 19 months of age. At 15-18 months of age, approximately 1/3 of the *Grn*$^{-/-}$ mice developed severe skin lesions on the head and back (Figure 4.1A). Interestingly, this same line of mice housed at the Palo Alto VA animal facility has a 30% penetrance of the lesion phenotype in the *Grn*$^{-/-}$ mice at 11-12 months of age, which reaches 100% penetrance by 14-15 months (personal communication Eva Czirr, postdoc in Tony Wyss-Coray's lab, Stanford). As obsessive-compulsive behavior is a known symptom of frontotemporal dementia (FTD), we hypothesized that the lesions may be due to compulsive grooming by the mice. Indeed, singly housed *Grn*$^{-/-}$ mice spent more time grooming themselves compared to *Grn*$^{+/+}$ mice as early as 5-months-old (Figure 4.1B). Interestingly, the incidence of compulsive grooming increases with age in the *Grn*$^{-/-}$ mice, as they groom themselves about twice as much as *Grn*$^{+/+}$ mice at 18-months-old. These data indicate that PGRN deficient mice have another FTD-like behavioral phenotype that worsens with age.

It is known that changes in the corticostriatal circuitry in mice can lead to the development of obsessive-compulsive disorder (OCD)-like behaviors, such as compulsive grooming. Mice with genetic disruptions in *Sapap3* (Welch et al., 2007) and *Slitrk5* (Shmelkov et al., 2010) result in neuronal phenotypes that cause OCD-like behaviors. While disruption of hematopoietic *Hoxb8* is sufficient to induce OCD-like

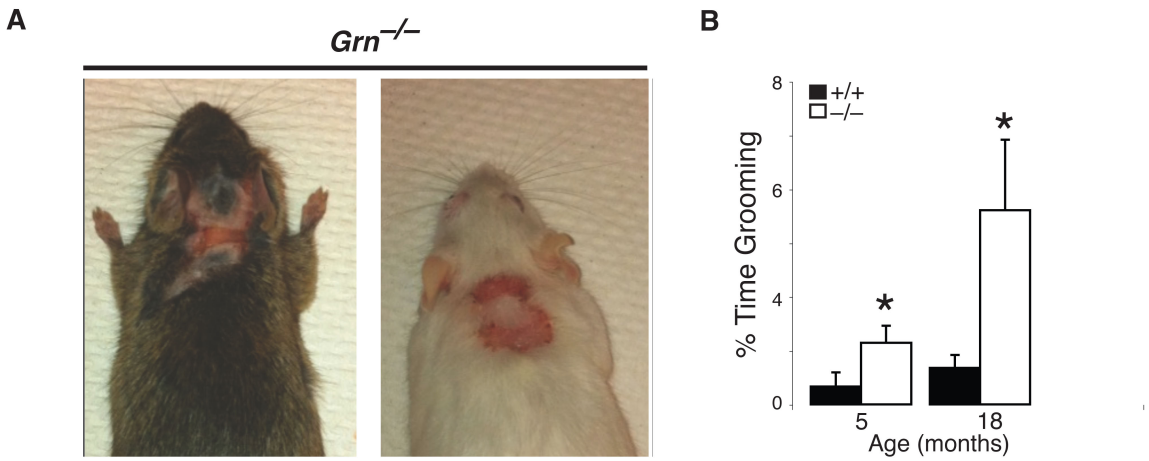

Figure 4.1 OCD-like behaviors in PGRN-deficient mice.

(A) Images of typical location and severity of skin lesions found on ~1/3 of 15-18-month-old *Grn*$^{-/-}$ mice. **(B)** Singly-housed *Grn*$^{-/-}$ mice groom more than *Grn*$^{+/+}$ mice and the grooming becomes more excessive with age. 6-10 mice per genotype/age. Non-parametric Mann-Whitney *$p < 0.05$.

behaviors in mice, which can be rescued with a bone marrow transplant (Chen et al., 2010). Pathological characterization of aged PGRN deficient mice by our group (Filiano, submitted) and others (Yin et al., 2009, Ahmed et al., 2010, Yin et al., 2010, Ghoshal et al., 2011, Petkau et al., 2011, Wils et al., 2012) have shown gliosis in the cortex, hippocampus, and thalamus, with no obvious neuronal death in mice at 12-months-old. The gliosis is evident as early as 6 months of age (Ahmed et al., 2010). To further characterize our aging model of PGRN-deficiency, pathological analysis of brain tissue was performed at 4, 7, 12, and 19-months-old. Consistent with previous studies, we also found an age-dependent gliosis in *Grn*$^{-/-}$ mice. Interestingly, however, the gliosis continued to worsen in 19-month-old *Grn*$^{-/-}$ mice. While the gliosis appeared to diffusely affect the entire brain, three regions in the *Grn*$^{-/-}$ mice showed most pronounced microgliosis, including the caudate putamen, thalamus, and cerebellum (Figure 4.2A). The number of microglia in the caudate putamen of *Grn*$^{-/-}$ mice is significantly increased at 12 and 19-months-old compared to *Grn*$^{+/+}$ mice (Figure 4.2B). In the thalamus, where there seems to be the most neuroinflammation, the number of microglia is significantly increased over *Grn*$^{+/+}$ mice as early as 4 months of age, and this difference significantly increases with age (Figure 4.2B). We also examined the amount of astrogliosis in the aging brains of PGRN-deficient mice. Similar to the microgliosis, there is astrogliosis in the caudate putamen and thalamus of 19-month-old *Grn*$^{-/-}$ mice (Figure 4.2C). Quantification of the number of astrocytes in each region shows that there is a significant increase in the number of astrocytes in the *Grn*$^{-/-}$ mice compared with *Grn*$^{+/+}$ mice starting at 7-months-old and increasing over time (Figure 4.2D). We also quantified the numbers of microglia and astrocytes in *Grn*$^{+/-}$ mice with age, and did not a change.

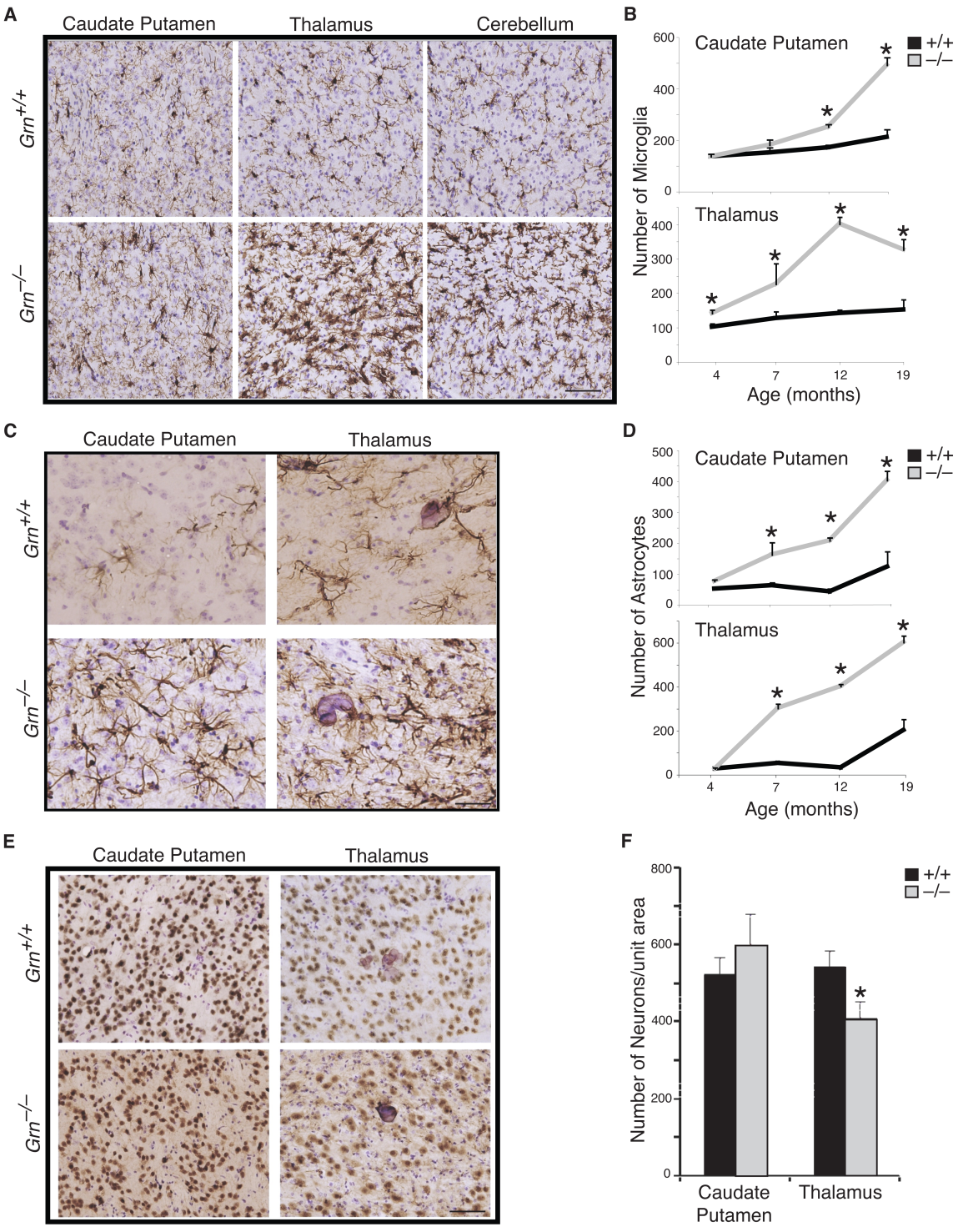

Figure 4.2 Region-specific gliosis PGRN-deficient mice.

(A) Representative sections showing increased numbers and activation of IBA1-positive microglia in the caudate putamen, thalamus, and cerebellum of 19-month-old PGRN-deficient mice. Scale bar = 500 μm. **(B)** Quantification of IBA1-positive microglia in the

caudate putamen and thalamus of aging $Grn^{+/+}$ and $Grn^{-/-}$ mice. Analysis of 2-3 sections per mouse/genotype/age (n= 3-4 mice per genotype/age). Student's T-test *p < 0.01 $Grn^{-/-}$ compared with $Grn^{+/+}$ mice. **(C)** Representative sections showing increased numbers of GFAP-positive astrocytes in the caudate putamen and thalamus of 19-month-old PGRN-deficient mice. Scale bar = 500 μm. **(D)** Quantification of GFAP-positive astrocytes in the caudate putamen and thalamus of aging $Grn^{+/+}$ and $Grn^{-/-}$ mice. Analysis of 2-3 section per mouse/genotype/age (n= 3-4 mice per genotype/age). Student's T-test *p < 0.01 $Grn^{-/-}$ compared with $Grn^{+/+}$ mice. **(E)** Representative sections showing numbers of NeuN-positive neuronal nuclei in the caudate putamen and thalamus of 19-month-old PGRN-deficient mice. Scale bar = 500 μm. **(F)** Quantification of NeuN-positive neuronal nuclei in the caudate putamen and thalamus of 19-month-old $Grn^{+/+}$ and $Grn^{-/-}$ mice. Analysis of 2-3 sections per mouse/genotype/age (n= 3-4 mice per genotype/age). Student's T-test *p < 0.05 $Grn^{-/-}$ compared with $Grn^{+/+}$ mice.

It is known that chronic, uncontrolled neuroinflammation can contribute to neuron loss associated with neurodegenerative disease (Glass et al., 2010). We examined whether neuron loss occurred in the regions with gliosis. At 19 months, there was no difference in the postmortem brain weight of $Grn^{+/+}$ and $Grn^{-/-}$ mice (data not shown) and no **overt** loss of neurons in the caudate putamen or thalamus of $Grn^{-/-}$ mice compared with $Grn^{+/+}$ mice (Figure 4.2E). While modest reduction in the number of $Grn^{-/-}$ NeuN-positive neurons was present in the thalamus, there was no change in neuron number in the caudate putamen despite of the gliosis present there (Figure 4.2F).

Neuronal death is the most obvious result of neuronal dysfunction, but loss of synapses/spines and/or changes in dendritic arborization generally precede the neuron death. We used Golgi staining to begin investigating neuron structures in the PGRN-deficient mice. The Golgi staining in the thalamus of 19-month-old mice poorly impregnated neurons, but affectively infiltrated the vasculature. The thalamic vasculature in the $Grn^{-/-}$ mice was markedly altered and reduced (Figure 4.3A). Vascular markers, such as VEGF, CD31, and smooth muscle actin (SMA), also indicated abnormal vasculature architecture, as well as gliosis surrounding the abnormal vessels (Figure 4.3B). In $Grn^{+/+}$mice, astrocytes in the thalamus surround large, CD31-positive arteries, whereas in the $Grn^{-/-}$ mice the astrocytes are found ubiquitously, including on blood vessels. The vessels in the $Grn^{-/-}$ thalamus are thinner and CD31 is dispersed in an abnormal pattern (Figure 4.3B). Tracing of the vasculature revealed that the total length of the vessel branches was significantly reduced, as well as the average length between the branches in the 19-month-old $Grn^{-/-}$ mice (Figure 4.3C). This was not the case for the

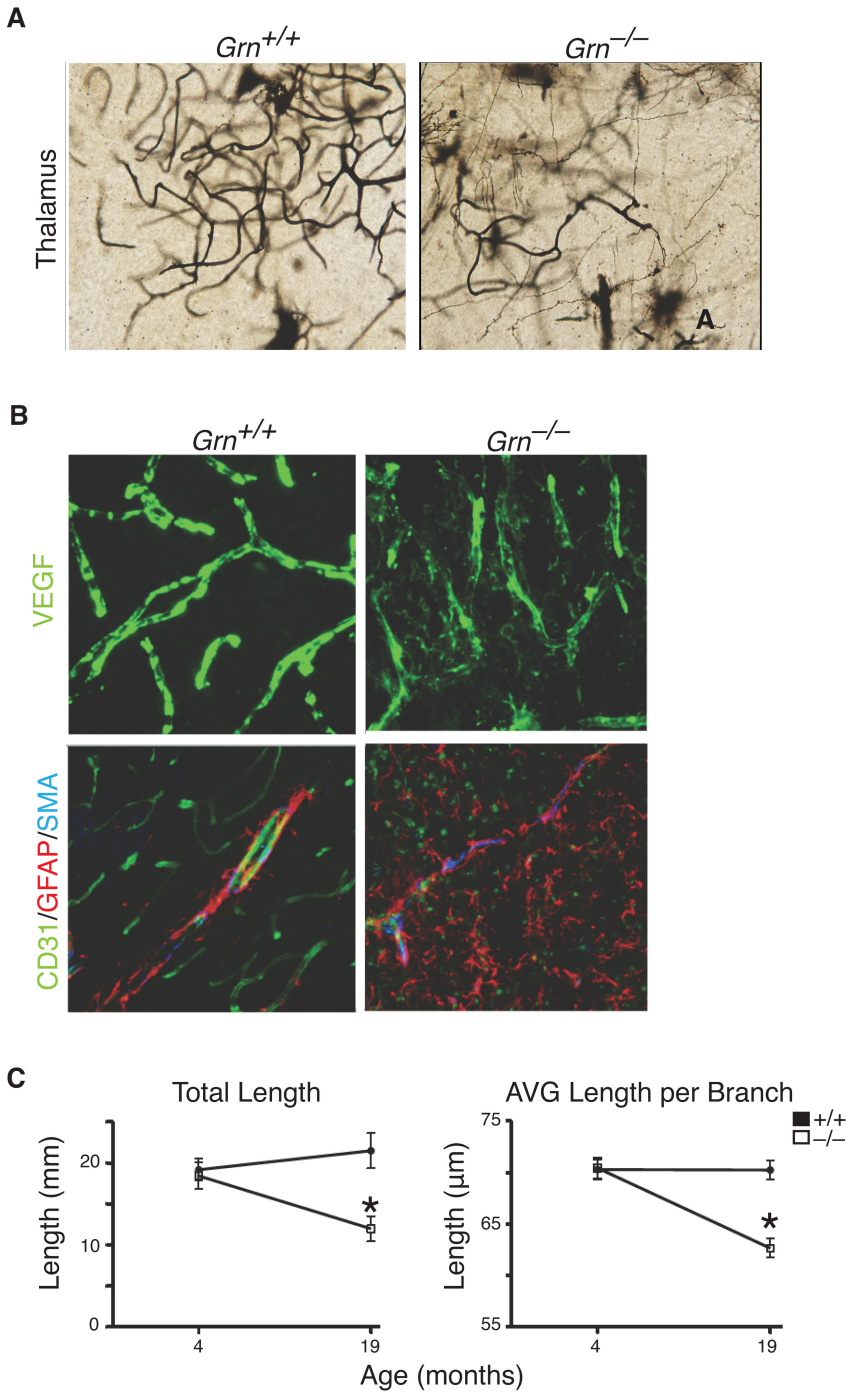

Figure 4.3 Loss of progranulin leads to an abnormal vascular phenotype.

(A) Representative image of Golgi staining highlighting the reduced vasculature in the thalamus of 18-month-old *Grn*$^{-/-}$ mice. **(B)** Confocal microscopy images of altered vascular markers in the thalamus of 18-month-old *Grn*$^{-/-}$ mice. **(C)** Quantification of vasculature changes in 18-month-old *Grn*$^{-/-}$ mice. ANOVA *p < 0.01 *Grn*$^{-/-}$ compared with *Grn*$^{+/+}$ mice.

4-month-old *Grn*$^{-/-}$ mice, where there was no difference in the thalamic vessel structure (Figure 4.3C). These results indicate that the vascular changes observed in the 19-month-old mice occur with age, and may be due to the neuroinflammation that occurs in the *Grn*$^{-/-}$ mice.

To gain more insight into the overall changes occurring in PGRN-deficient CNS with age we performed Weighted Correlation Network Analysis (WGCNA) using gene expression data (Rosen et al., 2011) from 2, 6, 9, 12, and 18-month-old *Grn*$^{+/+}$, *Grn*$^{+/-}$, and *Grn*$^{-/-}$ mice looking at 3 brain regions: the cortex, hippocampus, and cerebellum. We were interested in networks that changed with age in the PGRN deficient mice. Only one network fit these criteria for each of the three brains regions, and included genes known to play a role in inflammation. Only *Grn*$^{-/-}$ mice showed inflammatory changes that were significantly different than *Grn*$^{+/+}$ mice with age (Figure 4.1A). As *Grn*$^{-/-}$ mice age, the gene expression of many genes known to play a role in inflammation is significantly upregulated compared to the *Grn*$^{+/+}$ and *Grn*$^{+/-}$ mice. Principal component analysis was performed to linearly depict the variance seen within the inflammatory network (Figure 4.4B) and nicely demonstrates a steady increase in inflammatory gene expression as the *Grn*$^{-/-}$ mice age in all three regions of the brain examined. The WGCNA generates a list of significant gene ontology (GO) categories for each of the gene networks analyzed that is based on the significantly changing genes in that particular network. Figure 4.4C lists GO categories that are overrepresented in the inflammatory module of the WGNCA for the PGRN-deficient mice. One gene that is overrepresented in many of the significant GO categories

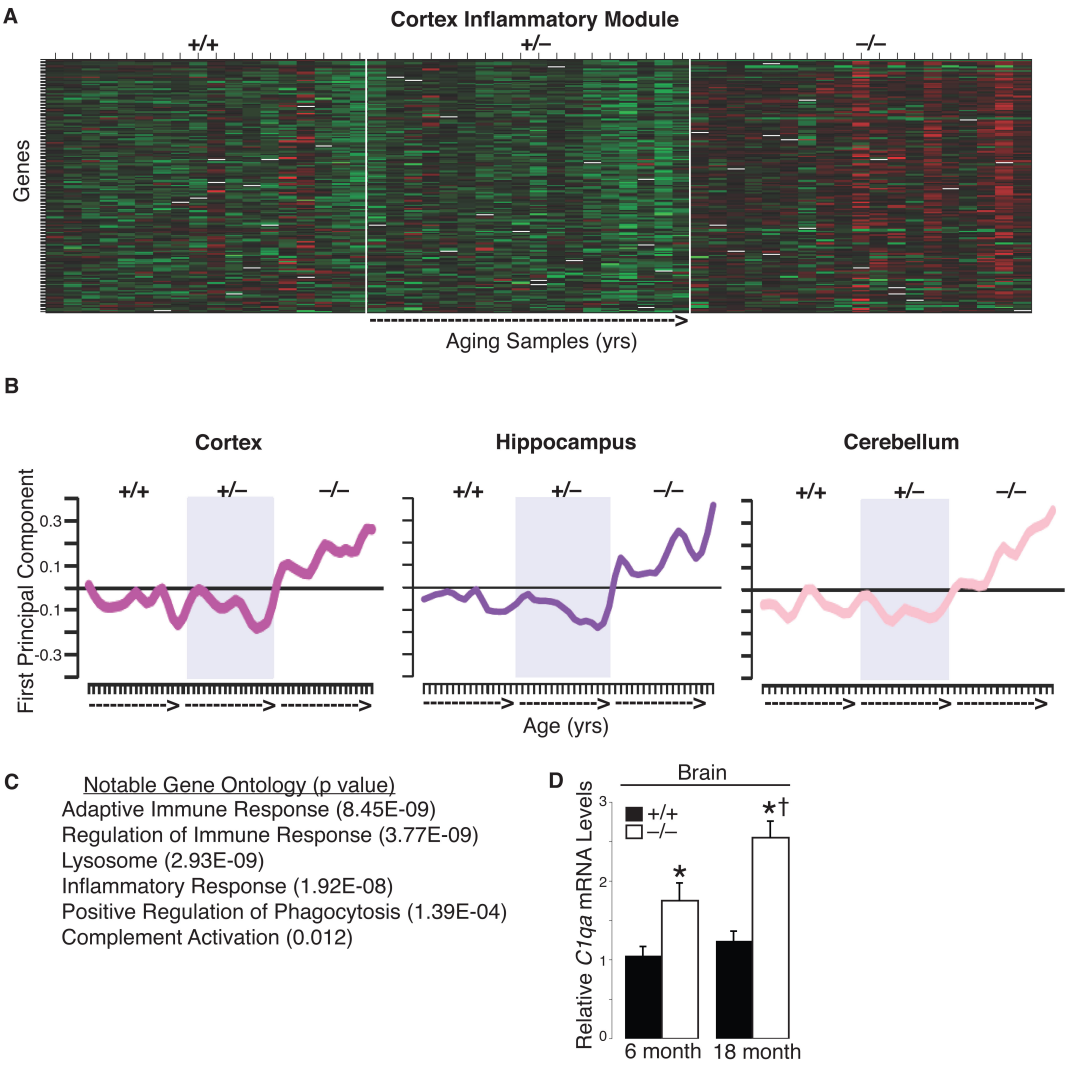

Figure 4.4 WGCNA analysis of aging PGRN-deficient mice.

WGCNA analysis was performed using the microarray data from PGRN-deficient mice at ages 2, 6, 9, 12, and 18 months of age. The only module that demonstrates a significant difference between the *Grn*$^{+/+}$ and *Grn*$^{-/-}$ mice due to aging is the inflammatory module. (**A)** Heat map depicting the differential expression of the genes included in the inflammatory module for the cortex. Red= increased gene expression; green= decreased gene expression. **(B)** Principal component analysis was used to linearly depict the variance observed in the inflammatory module for the three brain regions analyzed. In all three regions there is an increase in inflammatory gene expression as the *Grn*$^{-/-}$ mice age compared with *Grn*$^{+/+}$ and *Grn*$^{+/-}$ mice. **(C)** List of pertinent significant gene ontonology categories represented in the inflammatory module. **(D)** Validation of increased *C1qa* mRNA in the aging *Grn*$^{-/-}$ mice. ANOVA *p < 0.05 *Grn*$^{-/-}$ versus *Grn*$^{+/+}$ mice; †p < 0.05 6-month *Grn*$^{-/-}$ compared with 18-month *Grn*$^{-/-}$ mice.

associated with the inflammatory network is *C1qa*, complement component 1, q subcomponent, A chain. It is known that endothelial cells express complement receptors, and complement binding increases ICAM-1 expression. ICAM-1 is a marker of vascular inflammation (Alexander et al., 2008), and can potentially contribute to the vascular changes in the thalamus of the aged $Grn^{-/-}$ mutants. In aggregate, the results of the WGCNA support the role of PGRN in neuroinflammation and aging.

Discussion & Future Directions

Our findings provide clear evidence that *Grn*$^{-/-}$ mice develop prominent neuroinflammation, cerebrovascular alterations, and modest neuron loss, which potentially contribute to the OCD-like behaviors that occur with age. It is unclear how all of these changes are linked and whether or not they are causative of one another. Further analysis of the aging phenotypes of these mice is necessary to determine which alterations occur first.

We hypothesize that neuronal dysfunction in the cortico-striatial-thalamic pathway in the *Grn*$^{-/-}$ mice results in the OCD-like behaviors. It is unclear whether neuronal changes in these brain regions precede the neuroinflammation or vice versa. We believe, though, that the uncontrolled inflammation in these regions contributes to the worsening of the phenotype with age, as the increased inflammation causes more neuronal dysfunction over time. It is possible that if mice were aged longer, we would begin to see overt neuron loss in these regions.

Evidence supporting this hypothesis is that skin lesions appear at different times when the same strain of mice is housed in different facilities. The Gladstone animal facility is a antiseptic barrier facility where the mice are exposed to very few pathogens. The facility at the Palo Alto VA is not as clean and mice are exposed to more pathogens, possibly triggering earlier inflammation in the *Grn*$^{-/-}$ mice.

The lesions themselves could also be linked to a wound healing defect in these mice, as PGRN is known to play a role in the wound healing process (He et al., 2003). Therefore, the skin and wound healing capacity of the *Grn*$^{-/-}$ mice needs to be examined

at a young age. Alterations in the wound healing response of the *Grn*$^{-/-}$ mice, if present, could partially explain why the lesions develop following compulsive grooming.

The evidence for early neuronal dysfunction needs to be explored in the PGRN deficient mice. The Golgi-positive neurons in the caudate putamen need to be examined for spine number and type alterations, as well as any changes to the dendritic arborization in the 4, 12, and 19-month-old *Grn*$^{+/+}$, *Grn*$^{+/-}$, and *Grn*$^{-/-}$ mice. Alterations in synapse numbers could also be performed by quantifying synaptophysin staining in the various brain regions. Electron microscopy in the PGRN deficient mice would also permit structural analysis of synapses. Finally, electrophysiological analysis of the neurons in the thalamus and caudate putamen at various ages would demonstrate whether or not there are true functional changes in the neurons that occur with age.

The chronic neuroinflammation observed may contribute to the vascular changes observed in the *Grn*$^{-/-}$ mice since no changes are observed in the younger mice. An overabundance of inflammatory factors secreted by reactive microglia and astrocytes contribute to the vascular alterations and dysfunction (Grammas, 2011). It is known that complement receptors are expressed on endothelial cells and can cause an inflammatory phenotype in the vasculature (Lister and Hickey, 2006). The progressive gliosis may also cause changes in the maintenance of the blood-brain barrier, thereby destabilizing the vasculature. Finally, PGRN is known to play are role in angiogenesis, especially in tumor biology (He et al., 2002), indicating that PGRN deficiency may cause alterations in the repair of the damaged vasculature. No matter what the cause of the vascular changes, these changes may also contribute to the neuronal dysfunction due to hypoperfusion of the affected brain regions and/or leakage of toxic cells and factors from the periphery.

Overall, more work is required to determine when, where, and in which cell type the first aging alterations due to PGRN deficiency occur. Although, simply controlling the local neuroinflammation may be sufficient to slow or prevent the exaggeration of the underlying dysfunction. Once these questions are answered it will be key to determine whether microglia- or neuron-specific PGRN deficient mice mimic any of the aging characteristics observed in the global knockout mice.

Methods

Progranulin deficient mice. The *Grn* mice were generated as previously described (Martens et al., 2012). Briefly, a Grn^{flox} allele was created by flanking the entire murine *Grn* coding sequence with loxP sites. The mice were then bred with mice expressing Cre recombinase driven by either the *β-actin, Cd11b, CamKIIα,* or *Nestin* promoter to generate global or cell-type specific PGRN deficient mice. $Grn^{+/+}$, $Grn^{+/-}$, and $Grn^{-/-}$ littermates were aged in a barrier facility and maintained on a regular chow diet. All mice utilized for these experiments existed on a mixed background (62.5% C57BL/6J, 12.5% 129Sv/Jae, and 25% FVB).

Grooming behavior characterization. A new homecage was created for each mouse by singly housing them at least 24 hours prior to the experiment. The mice were acclimated to a quiet, dark room with a red light for an hour prior to videotaping. Cages were opened and food racks were removed so that the mice could be videotaped from above. Each mouse was videotaped for five minutes alone in order to assess grooming behavior. A mouse of similar age and sex was then added to the cage and their interactions were recorded for an additional five minutes. Mice were returned to their original group housing following the experiment. Males were only put back together if they had been separated for less than five days. Videos were later scored for grooming behavior, which consisted of cleaning/scratching of the face, hind leg scratching, or grooming of the fur with teeth.

Immunohistochemisty. Mice were perfused with PBS followed by 4% PFA (Electron Microscopy Sciences, Hatfield PA) at 4, 7, 12, and 19-months-old. The brains were extracted and fixed in 4% PFA overnight, rocking at room temperature. The brains were

cryoprotected in 15% sucrose, followed by 30% sucrose for 24 hours each, rocking at room temperature. The brains were then embedded in OCT and cut into 40 μm sections for pathology analysis. Free floating sections were stained as previously described (Zhang et al., 2007). The following primary antibodies were incubated overnight at room temperature: IBA1 (Wako, 1:5000), GFAP (Dako, 1:5000), NeuN (Millipore, 1:1000).

Stereological Quantification. Stereological counting of IBA1-, GFAP-, and NeuN-positive cells in the thalamus and caudate putamen (2-3 serial sections per region) was performed at 100X magnification using the StereoInvestigator Software, version 9 (MBF Bioscience, Williston VT) (Zhang et al., 2007).

Golgi Staining. Three mice per genotype were sacrificed at 4, 12, and 19-months-old for Golgi staining using the FD Rapid GogliStain Kit (FD NeuroTechnologies, Columbia MD). Briefly, the brains were extracted and washed in PBS prior fixation in 5 ml of Golgi impregnation solution for two weeks. The impregnantion solution was changed after the first 24 hours. The brains were then cryoprotected for two weeks at 4°C. Again, the cryoprotectant was replaced after the first 24 hours. The brains were then embedded and cut into 100 nm sections for analysis. Vascular analysis in the thalamus was performed using the NeuroLucida Software (MBF Bioscience).

Microarray & WGCNA. The microarray data for the 2, 6, and 9-month-old mice has been previously published (Rosen et al., 2011). The 12- and 18-month-old data has recently been added to the dataset. Briefly, mice were perfused with PBS, brains were extracted, and hemibrains were frozen. The frozen hemibrains were dissected into the cortex, hippocampus, and cerebellum and homogenized using the Bullet Blender (Next Advance, Averill Park, NY) in Trizol (Invitrogen, Grand Island, NY). RNA integrity was insured

by running samples on a Bioanalyzer (Aligent, Santa Clara, CA). Samples were hybridized to Illumina (San Diego, CA) Mouse8 version 2 microarray chips as previously described (Rosen et al., 2011). Network anlysis was performed as previously described (Zhang and Horvath, 2005) and module merging was accomplished using the WGCNA package in R (Rosen et al., 2011). Differentially expressed genes within a given module were compared against the murine background for enrichment within gene ontology (GO) anlaysis (Rosen et al., 2011).

Real-time PCR. RNA was reverse-transcribed using the SuperScript III First Strand Synthesis System (Invitrogen). The primers used for qPCR were as follows, *Cyclo* (F 5'-tggaagagcaccaagacaaca-3', R 5'-tgccggagtcgacaatgat-3') and *C1qa* (F 5'-aacctcggataccagtcc -3', R 5'-atggggctccaggaaatc -3'). SYBR green master mix (Qiagen, Valencia, CA) reactions were run on an ABI Prism 7700 (Applied Biosystems, Carlsbad, CA). The data was normalized to the internal standard and subsequently normalized to an experimental control (ΔΔCT method, Invitrogen).

Statistical Analysis. The results are represented as mean ± SEM. Comparisons between two or more groups with normally distributed data used an ANOVA with Tukey's posthoc test. Non-normally distributed data sets comparing two groups used the non-parametric Mann-Whitney test. $P < 0.05$ was considered significant. Tests were performed with InStat software.

Chapter 5

Insights into Progranulin Biology

In the previous chapters I have highlighted published (chapter 2), submitted (chapter 3), and ongoing (chapter 4) work. While much of the data I have generated have been covered, I would like to highlight a few key pieces of unpublished data that if further investigated may provide mechanistic insight into progranulin CNS biology. The data vignettes also highlight some of the open questions remaining in the PGRN field.

Progranulin regulates the microglial inflammatory response

We and others have demonstrated that PGRN plays a role in CNS inflammation as PGRN-deficient mice develop age-dependent microgliosis and astrocytosis (Yin et al., 2009, Ahmed et al., 2010, Yin et al., 2010, Ghoshal et al., 2011, Petkau et al., 2011), peripheral microglia upregulate PGRN expression following activation (Moisse et al., 2009a), and PGRN-deficient macrophages (Yin et al., 2009) and microglia exhibit an exaggerated pro-inflammatory response that is toxic to neurons (see chapter 2; Figures 2.2, 2.3) (Martens et al., 2012). In Figure 2.2, we show that conditioned media from activated $Grn^{-/-}$ microglia is significantly more toxic to wild-type neuron survival than conditioned media from activated $Grn^{+/+}$ microglia.

In order to gain more insight into the regulation of the microglial inflammatory response we performed a timecourse of microglial activation and transferred the conditioned media at various time points to wild-type neurons. The conditioned media from activated microglia of either genotype is always more toxic to the neurons compared with the PBS control (Figure 5.1, Table 5.1). At each time point, the

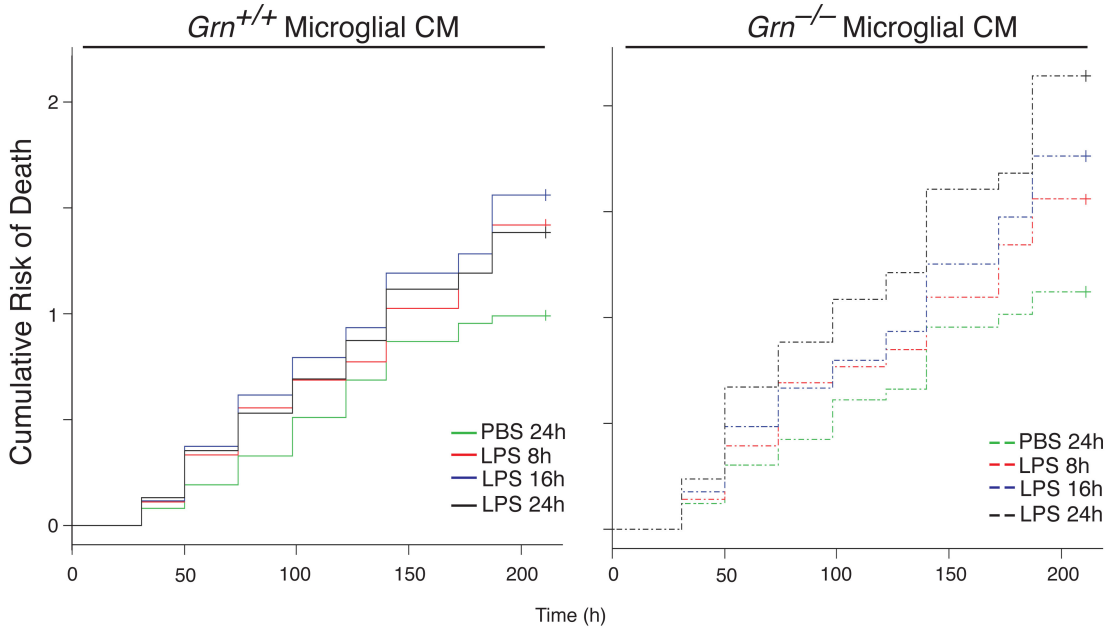

Figure 5.1 *Grn*$^{-/-}$ microglial conditioned media accumulates cytotoxic factors over time that contribute to increased death of wild-type neurons.

Activated *Grn*$^{-/-}$ microglia continually secrete cytotoxic factors over time that accumulate in the conditioned media and cause in increased risk of death of wild-type neurons compared with *Grn*$^{+/+}$ microglia.

Condition	HR	P value
WT PBS (24h)	1	Ref
KO PBS (24h)	1.15	0.35
WT LPS/IFN (8h)	1.38	0.02
KO LPS/IFN (8h)	1.54	0.002
WT LPS/IFN (16h)	1.54	0.002
KO LPS/IFN (16h)	1.72	0.0001
WT LPS/IFN (24h)	1.4	0.01
KO LPS/IFN (24h)	2.2	<0.00001

Table 5.1 *Grn*$^{-/-}$ microglial conditioned media causes an increased risk of death of wild-type neurons over time.

Hazard ratios indicating the risk of neuron death when treated with microglial conditioned media. P values were determined using a log-rank test. HR, hazard ratio.

conditioned media from LPS/IFNγ-treated *Grn*$^{-/-}$ microglia is more toxic to the neurons than activated *Grn*$^{+/+}$ microglial conditioned media (Figure 5.1, Table 5.1). Interestingly, the *Grn*$^{+/+}$ microglia conditioned media at 24 hours resulted in less neuron death than 16 hour conditioned media (Figure 5.1, Table 5.1), indicating that *Grn*$^{+/+}$ microglia are beginning to quell their pro-inflammatory response and turn on their anti-inflammatory reparative response (Glass et al., 2010) by this time point. Clearly, this regulation of the inflammatory response is NOT occurring in the *Grn*$^{-/-}$ microglia, as the toxicity to the neurons continues to increase after 24 hours (Figure 5.1, Table 5.1). This data provides strong evidence that the *Grn*$^{-/-}$ microglial pro-inflammatory response is unregulated. Therefore, PGRN plays a role in quelling the pro-inflammatory response, thereby allowing an anti-inflammatory response to take place in order to control and clean up the damage evoked during the injury and pro-inflammatory period.

To prove that PGRN is involved in regulating the switch from the pro- to anti-inflammatory response we would need to show that not only are there increased amounts of pro-inflammatory cytokines in the *Grn*$^{-/-}$ microglial conditioned media (Figure 2.3), but also an altered cytokine milieu. This could be accomplished by using more extensive cytokine arrays (Luminex or Affimatrix Antibody Arrays) or mass spectrometry. This information would permit therapeutic targeting of specific pathways downstream of PGRN. Regulating the amount and type of cytokines secreted by microglia, including PGRN, is critical for a proper neuroinflammatory response to occur, thereby preventing chronic neuroinflammation that leads to neurodegeneration.

Methods: *Grn*$^{+/+}$ and *Grn*$^{-/-}$ microglia were harvested as described in Appendix I (Supplemental Methods). Briefly, microglia were treated with PBS or 100 ng/ml LPS (Sigma) and 100 U/ml interferon-γ (Sigma) for 8, 16, or 24 hours. Conditioned media was collected, pooled, and centrifuged to remove any cells. The media was then transferred to wild-type primary cortical neurons (DIV5) that had been transfected with EGFP. The neurons were then imaged daily for 9 days in order to assess cell survival (see Appendix I for details).

Microglia conditioned media affects Grn$^{+/+}$ and Grn$^{-/-}$ neuron survival differently

We and others have shown a basal deficit in the survival of *Grn*$^{-/-}$ neurons *in vitro* (Table A1.1) (Kleinberger et al., 2010, Xu et al., 2011). We had not determined whether or not this difference in *Grn*$^{+/+}$ and *Grn*$^{-/-}$ neuron survival also increased the risk of death following treatment with activated *Grn*$^{+/+}$ and *Grn*$^{-/-}$ microglial conditioned media (as seen in Figure 2.2F). The basal increase in risk of death of *Grn*$^{-/-}$ neurons is not observed when treated with microglial conditioned media (Figure 5.3). This may be due to sensitivity issues as high numbers of neurons were required to detect the significant difference observed in Table A1.1. Interestingly, unlike *Grn*$^{+/+}$ neurons, there is not an increased risk of death to *Grn*$^{-/-}$ neurons when exposed to activated *Grn*$^{-/-}$ microglial conditioned media (Figure 5.2). Instead the amount of neuron death is similar to cells treated with *Grn*$^{+/+}$ microglial conditioned media. The **only** difference between these two cultures is that **neuronal** PGRN is present in the wild-type primary neuron cultures. This data suggests that neuronal PGRN may be detrimental to survival in the setting of neuroinflammation.

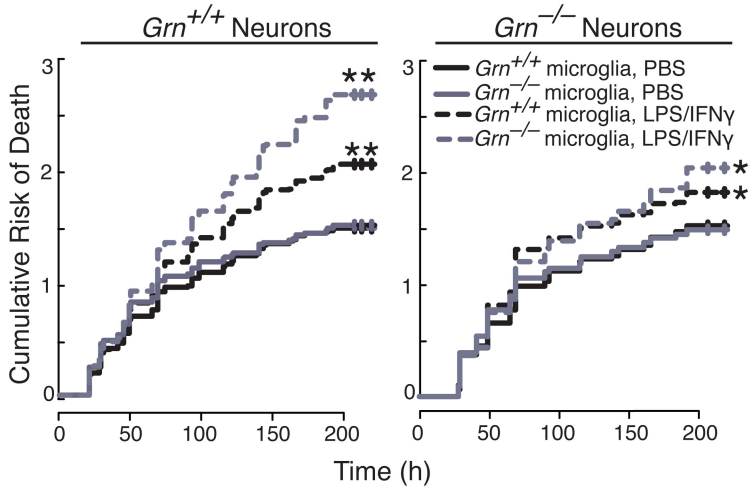

Figure 5.2 Microglial conditioned media has differential effects on wild-type and progranulin-deficient neurons.

Conditioned media from activated $Grn^{-/-}$ microglia causes an increased risk of death of $Grn^{+/+}$ neurons compared with activated $Grn^{+/+}$ microglial conditioned media (left). This increased risk of death does NOT occur in $Grn^{-/-}$ neurons (right). * $p < 0.001$, ** $p < 0.0001$ log-rank test. Representative experiment that was repeated three times.

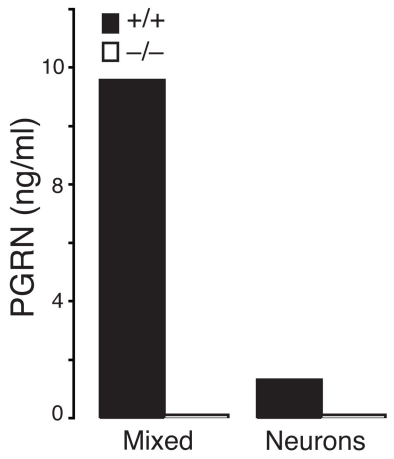

Figure 5.3 Cortical neurons secrete very little progranulin *in vitro.*

Primary cortical neurons secrete ~10 times less PGRN compared with primary mixed cortical cultures containing neurons, astrocytes, and microglia. Adipogen murine PGRN ELISA.

One hypothesis is that neurons secrete PGRN in response to stress. The data in Figure 5.2 may suggest that injured/dying neurons may secrete PGRN in an effort to signal for help from the surrounding neurons and glia. However, primary cortical neurons secrete very little PGRN compared to mixed cortical cultures containing neurons, astrocytes, and microglia (Figure 5.3). It is currently unknown whether neuronal PGRN secretion can be modulated by stress.

Another hypothesis in that GRNs have differential effects on neuron survival. In the setting of inflammation, as mimicked by the stimulated microglial conditioned media, the secreted neuronal PGRN is likely cleaved by proteases, with potentially more proteases secreted by the $Grn^{-/-}$ microglia. The resulting granulins (GRNs) may play a role in adding to the increased neuron death. It is also possible that other neuronal secreted factors may also contribute to the increased risk of death. Analysis of the conditioned media (now microglial and neuronal) to determine whether different proteins are secreted from the $Grn^{+/+}$ and $Grn^{-/-}$ neurons in response to the cytotoxic microglial conditioned media should be performed. This experiment may provide evidence that activated microglia secrete proteases that cause increased cleavage of PGRN into GRNs, and possibly even specific GRN species that are detrimental to neuron survival.

A potential therapeutic strategy may be to target proteases that are upregulated in the $Grn^{-/-}$ microglia conditioned media to regulate GRNs levels. It is unclear what the specific proteases are that cleave PGRN in the CNS, besides MMP-12 (Suh et al., 2012). Elastase is believed to be secreted by microglia and secretory leukocyte protease inhibiotor (SLPI) by astrocytes, but there is little supporting *in vivo* evidence (Ahmed et

al., 2007). There are many other microglial proteases that could cleave PGRN, and perhaps into specific GRN combinations.

The specific GRN receptors on neurons and microglia are also unknown. It has been shown that GRNs E and C promote neuron survival (Ryan et al., 2009, Gass et al., 2012). However, it is unknown whether these GRNs bind different receptors or induce different signaling cascades than those that may be detrimental to neuron survival. Neurons and microglia may also have different GRN receptor levels and therefore utilize different GRNs for various cellular functions. Determining the function and receptors for GRNs on both neurons and microglia will provide insight into the protein species to rescue with and/or which receptors to block with a therapeutic. Unfortunately, the reagents to specifically and reliably detect GRNs do not yet exist.

Methods: See chapter 2 and Appendix I.

Recombinant progranulin is not sufficient to rescue the PGRN-deficient exaggerated myeloid pro-inflammatory response

In 2006, it was clearly shown that mutations in *PGRN* lead to haploinsufficiency of the protein and cause FTD (Baker et al., 2006, Cruts et al., 2006). One potential therapeutic strategy was to determine whether providing PGRN to patients would be enough to prevent disease. Many companies and laboratories have generated recombinant PGRN (rPGRN) in order to rescue PGRN-deficient phenotypes. rPGRN, as well as rGRN E and C, has been shown to increase survival and neurite length of wild-type neurons (Van Damme et al., 2008, Ryan et al., 2009, Gass et al., 2012). Xu et al. demonstrated that rPGRN was sufficient to rescue glutamate excitotoxicity, oxidative stress, and MPP+

induced neuron cell death by activating the ERK and Akt signaling pathways (Xu et al., 2011). Gass et al. also demonstrated that rPGRN, GRNE and GRNC were sufficient to rescue neuronal outgrowth and branching deficits seen in *Grn*$^{-/-}$ neurons (Gass et al., 2012). Tang et al. demonstrated *in vivo* that i.p. administration of rPGRN can rescue a model of collagen-induced arthritis. They also showed that rPGRN can block TNFα-induced signaling in immortalized macrophages (Tang et al., 2011).

We wanted to determine whether or not rPGRN was capable of rescuing the *Grn*$^{-/-}$ microglial/macrophage hyperactivation phenotype. The majority of work was performed using bone marrow-derived macrophages (BMDMs) because of the low numbers of microglia obtained by primary culture. Pre- and co-treatment of LPS/IFNγ-stimulated *Grn*$^{-/-}$ BMDMs with murine rPGRN (400 ng/ml) (R&D Systems) is not sufficient to quell the pro-inflammatory phenotype of increased *Il1β* and *Tnfα* mRNA (Figure 5.4). It also had no effect on wild-type cells (data not shown). This dose was also not sufficient to rescue the *Grn*$^{-/-}$ microglia phenotype (data not shown). Treatment with rPGRN in this experimental paradigm does not rescue *Grn*$^{-/-}$ myeloid phenotypes.

In collaboration with Malu Tansey's lab at Emory University we have more exhaustively tested differentially tagged and prepared versions of rPGRN (both human and mouse) from different companies and laboratories. Again, we showed that pre- and/or co-treatment with ANY preparation of rPGRN is insufficient to rescue the pro-inflammatory phenotype of PGRN-deficient BMDMs at various time points and doses (there was no effect on wild-type cells) (Chen et al, unpublished). Chen et al. also could not replicate the PGRN/TNFR interaction. Together this data suggest that rPGRN is not a reliable therapeutic candidate for quelling neuroinflammation.

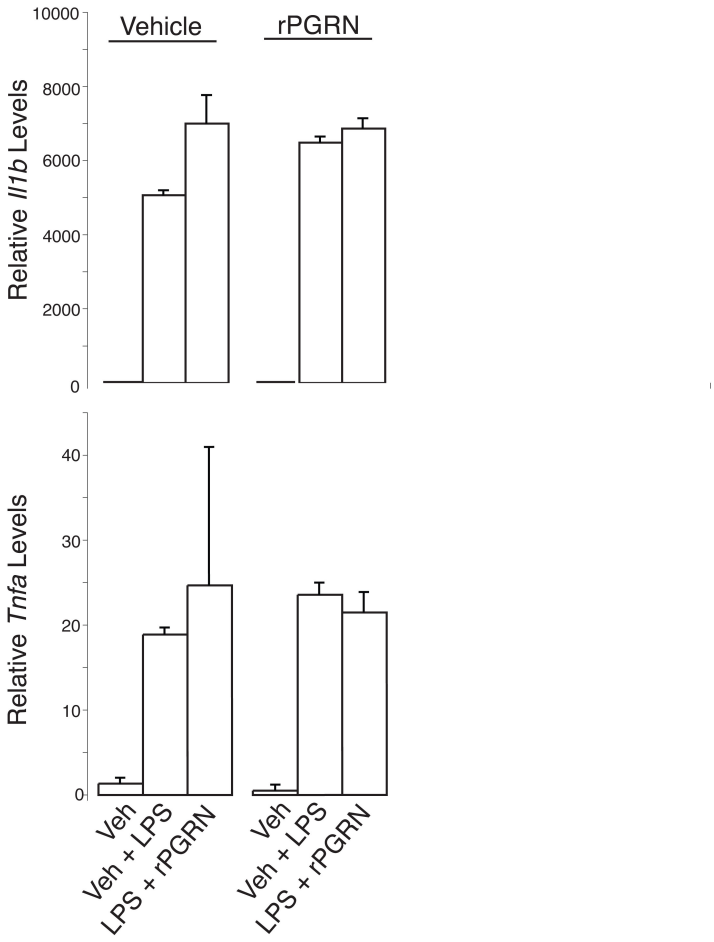

Figure 5.4 Recombinant PGRN is not sufficient to rescue the increased pro-inflammatory response of *Grn*$^{-/-}$ bone marrow-derived macrophages.

Neither co- (left) nor pre-treatment (right) with recombinant PGRN rescues *Grn*$^{-/-}$ BMDM cytokine mRNA levels following LPS treatment. (Representative experiment)

We do know, however, that expression of PGRN using lentivirus can rescue the *Grn*$^{-/-}$ microglial phenotype (Figure 2.3) and that exogenous PGRN is sufficient to rescue neuronal phenotypes (Van Damme et al., 2008, Ryan et al., 2009, Xu et al., 2011, Gass et al., 2012). There are multiple potential explanations for these discrepancies. First, there may be different PGRN:GRN ratios in the myeloid and neuronal experiments. The rPGRN may be quickly cleaved into granulins due to increased protease secretion by the BMDMs and microglia *in vitro* because there is a higher level of basal activation than *in vivo*. The full-length protein is likely more stable in the neuronal experiments as neurons do no secrete many proteases (Brown and Neher, 2010). Therefore, neither the myeloid or neuronal experiments may accurately reflect *in vivo* settings.

Second, the expression level of PGRN and GRN receptors may all also be different on neurons and myeloid cells. It is currently known that PGRN receptors, sortilin1 and TNFR, have different expression levels on neurons and microglia (McCoy and Tansey, 2008, Hu et al., 2010). The function of granulins is currently unclear due to lack of reliable reagents and unknown receptors. Some granulins have been deemed pro- and others anti-inflammatory with little convincing evidence (Jian et al., 2012) and not all have been tested for survival function.

Third, intracellular PGRN may have a function since expression is capable of rescuing the phenotype. At one time there was a focus on Nogo as a potential PGRN receptor, and this receptor is expressed intracellularly in the ER (Basar Cenik, unpublished). It is also known that neuronal sortilin1 endocytoses PGRN, indicating another, yet unknown, role of intracellular PGRN (Hu et al., 2010).

Finally, the exogenous PGRN may not rescue the microglial phenotypes in our hands as we have yet to establish a robust bioassay for the recombinant protein. We have tried various assays, such as proliferation of R- cells or SW13 cells (He and Bateman, 2003), Erk and Akt activation in HEK and RAW cells, and rescue of the myeloid hyperactivation. All of these assays lack robustness, as rPGRN gives a 10% boost, but positive controls give a 70-80% boost in proliferation or activity. There has also been the issue of reproducibility between experiments and preparations of rPGRN. Currently, we have moved away from using recombinant protein to rescue any PGRN-deficient phenotypes.

Methods: *Grn*$^{+/+}$ and *Grn*$^{-/-}$ bone marrow was harvested and plated in non-tissue culture treated 10 cm dishes in RPMI supplemented with 20% FBS, P/S, and 10 ng/ml GM-CSF (Peprotech, Rocky Hill NJ). When the cells were confluent (~ 1 week), they were scraped using a cell lifter, spun down, and resuspended in M-SFM supplemented with P/S. The cells were plated at a density of $1x10^{-6}$ cells/well in 6-well dishes and allowed to rest overnight. The BMDMs were then pretreated with 400 ng/ml murine rPGRN (R&D, Minneapolis, MN) for 8 hours. The cells were then stimulated with either PBS or 100 ng/ml LPS plus 100 U/ml IFNg with or without fresh rPGRN overnight in M-SFM supplemented with P/S. RNA isolation, cDNA synthesis, and QPCR was performed as described in chapter 2 and Appendix I.

What disease are we modeling with $Grn^{-/-}$ mice?

As indicated in the chapter 1, two patients have recently been identified to be homozygous for a mutation in *PGRN* (Smith et al., 2012). The two patients presented with visual distortion and eventual failure as well as seizures, cerebellar ataxia, and cognitive deterioration in their 20s. Sequencing identified a 4 bp deletion that resulted in a frameshift and trunctated PGRN protein at residue 272. It is known that patients heterozygous for the c.813-816 deletion get FTD (Smith et al., 2012).

Unlike patients with PGRN haploinsuffficiency that results in FTD, these patients develop a condition known as neuronal ceroid lipofuscinosis (NCL). NCLs are neurodegenerative disorders that result from accumulation of lipofuscin in neurons due to lysosomal dysfunction. Lipofucsin results from the oxidation of lipids that may be due to cellular damage to membrane, mitochondria and/or lysosomes (Kohlschutter and Schulz, 2009).

The discovery of these two patients has led the FTD field to question what disease the $Grn^{-/-}$ mice model. In comparison to human FTD, the $Grn^{-/-}$ mice have altered social behavior (Yin et al., 2010, Ghoshal et al., 2011), inflammation in regions that would be characteristic of areas affected in the human condition, and accumulation of ubiquitin positive aggregates, as well as some phospho-TDP-43 deposits in the thalamus. They also develop OCD-like behaviors (chapter 4). We have demonstrated that haploinsufficient mice have altered social and emotional dysfunction similar to the $Grn^{-/-}$ mice, without the associated inflammation (chapter 3).

In comparison to patients with NCL, the mice have accumulation of lipofuscin as early as 3 weeks of age (Michael Ward, unpublished data) that gets progressively worse

with age. The lipofuscin seems to accumulate in a region-specific manner that correlates with the age-dependent inflammation observed in the *Grn*$^{-/-}$ mice. There is retinal accumulation of lipofuscin, but death of neurons does not occur until 18 months (M. Ward, unpublished). It is unknown whether the neuron death observed in the retina causes blindness in the *Grn*$^{-/-}$ mice. The mice perform normally on the rotarod at 12-months-old, but their gait has not been assessed. We also have not observed convulsive seizures, but this has not been specifically tested using EEG. Furthermore, the *Grn*$^{-/-}$ mice live to be at least 18-20 months old. I believe that we are modeling aspects of both diseases and further investingation of specific NCL-related alterations in needed in order to conclude for which disease the *Grn*$^{-/-}$ mice are a better model.

We do see lysosomal dysfunction that progresses with age in the *Grn*$^{-/-}$ mice. This is apparent by the upregulation of genes with known lysosomal function in all three brain regions analyzed (Table 5.1). (All of the significant gene ontology (GO) categories are associated with the WGCNA inflammatory network discussed in chapter 4.) This does not occur in the heterozygous mice and is likely due to the accumulation of lipofuscin. In the CNS, we see accumulation of lipofuscin in neurons at 6 month (and earlier) in the cortex, hippocampus, thalamus (Figure 5.5), and retina (M. Ward, unpublished). The accumulation may be more widespread and therefore needs to be examined further. In older mice, microglia also possess autofluorescent lipofuscin in these brain regions and the retina (data not shown, M. Ward, unpublished). It is likely that the microglia are phagocytosing the lipofuscin, but they could be developing lysosomal dysfunction. These findings need to be further investigated to determine which cell type the lysosomal dysfunction contributes to disease: neuron cell death,

inflammation in the microglia, or both. The lysosomal dysfunction may contribute to both NCL and FTD.

Brain Region	GO Term	P Value	Genes
Cortex	Lysosome	2.93E-09	*Ctsz, Lamp2, Cd68, Laptm5, Hpse, Hexa, Gusb, Hs-dmb1, Cd63, Man2b1, Dpp7, Slc15a3*
	Lysosome	7.01E-06	*Slc11a1, Ctsz, Lamp2, Cd68, Laptm5, Hexa, Gusb, Cd63, Man2b1*
	Lysosome-associated Membrane Protein	0.025	*Lamp2, Cd68*
	Lysosome	0.05	*Laptm4b, Abcb9, Smpd1, Arsa*
Hippocampus	Lysosome	5.49E-10	*Tcirg1, Cln3, Ctsz, Gusb, Hexa, Cd63, Gns, Slc11a1, Lamp2, Cd68, Laptm5, Ctse, Man2b1, Ctsh*
	Lysosome	1.44E-09	*Cln3, Ctsz, Gusb, Hexa, Cd63, Gns, Lamp2, Cd68, Laptm5, Man2b1, Slc15a3, Dpp7, Ctsh*
	Lysosome	0.005	*5430435G22RIK, Plekhf1, Slc29a3, Fnbp1, Litaf, Tmem74*
	Lysosome-associated Membrane Protein	0.03	*Lamp2, Cd68*
Cerebellum	Lysosome	1.57E-13	*Ctsz, Hexa, Gusb, Hexb, 0610031J06RIK, Ctss, Cd63, Dnase2a, Glb1, Lamp1, Lamp2, Cd68, Laptm5, Hpse, Man2b1, Slc15a3, Dpp7, Ctsh, Gba*
	Lysosome-associated Membrane Protein	8.11E-04	*Lamp1, Lamp2, Cd68*
	Lysosome Organization	0.03	*Hexa, Hexb, Gba*

Table 5.2 Signficant lysosomal GO categories in aging *Grn*$^{-/-}$ mice.

There are a number of GO categories that contain lysosomal genes that are significant in the inflammatory network in all three brain regions analyzed in the *Grn*$^{-/-}$ mice. All of

the genes listed are upregulated in the aged *Grn*$^{-/-}$ mice, suggesting a lysosomal dysfunction.

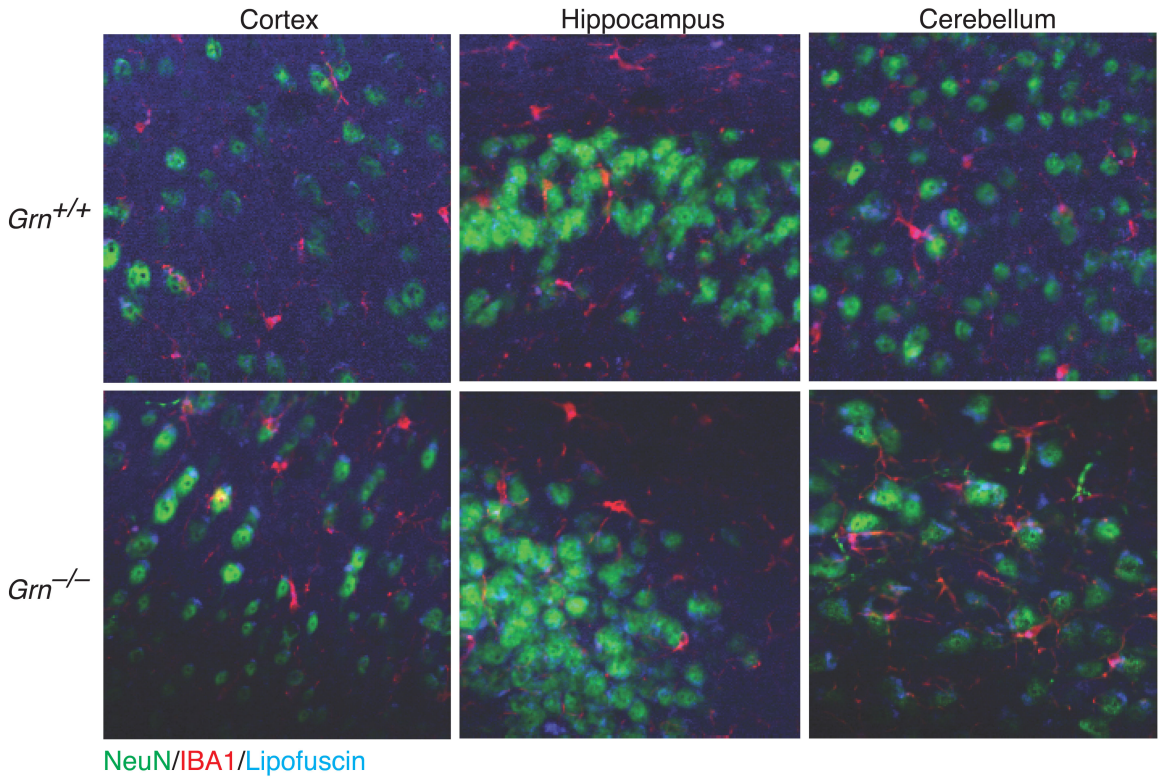

Figure 5.5 Lipofuscin accumulates in neurons of *Grn*$^{-/-}$ mice.

Representative images of lipofuscin (autofluorescent, blue) in 6-month-old *Grn*$^{-/-}$ mouse cortical, hippocampcal, and thalamic neurons (NeuN, green) compared with *Grn*$^{+/+}$ mice. Microgliosis (IBA1, red) is also evident in the thalamus due to altered microglial morphology in the *Grn*$^{-/-}$ mice.

Grn$^{+/-}$ *mice do not have FTD-like pathology*

Mutations in *PGRN* are known to cause FTD due to haploinsufficiency of the progranulin protein (Baker et al., 2006, Cruts et al., 2006). *Grn*$^{+/-}$ mice, which would be the predicted murine model for the disease, do not possess any of the gross pathology associated with FTD at 19-months-old (chapter 3, chapter 4, data not shown). Although *Grn*$^{-/-}$ mice do possess many of the pathological hallmarks associated with FTD, it is unclear whether they are the best model of the human FTD. These findings raise the question as to why the *Grn*$^{+/-}$ mice do not model FTD.

PGRN mutation carriers have a 75% reduction in full-length plasma PGRN levels (Finch et al., 2009). It is unknown whether there is a similar reduction in the brain. The *Grn*$^{+/-}$ mice have a 60% reduction in mRNA (Figure A1.1C, A2.1A-C) and plasma PGRN levels, as measured by an ELISA manufactured by Adipogen (Figure A1.1E). When the plasma of the same line of mice is tested using an in-house ELISA, the *Grn*$^{+/-}$ mice have a 50% reduction in plasma PGRN levels (Figure A2.1D). It is unclear whether either ELISA is detecting only full-length PGRN. Either way, the *Grn*$^{+/-}$ mice do not have as severe of a reduction in plasma PGRN levels as human mutation carriers. The amount of PGRN reduction in the murine brain has not been thoroughly quantified, although Ahmed et al shows a greater than 50% reduction in PGRN staining in the brains of *Grn*$^{+/-}$ mice by quantifying PGRN immunohistochemistry (Ahmed et al., 2010). This reduction is much less in older mice (Ahmed et al., 2010), indicating that murine CNS PGRN levels increase with age. This 50-60% reduction may not be enough to mimic human FTD, especially if the *Grn*$^{+/-}$ mice are increasing levels with age. This increase also seems to occur in patients (Chen-Plotkin et al., 2008), but in patients it is attributed

to neuroinflammation, which is not present in the *Grn*$^{+/-}$ mice. We have generated a mouse carrying the human R493X mutation. These mice phenocopy the PGRN-deficient mice PGRN levels (data not shown). A transgenic mouse expressing PGRN driven by a weak or titratable promoter on the *Grn*$^{-/-}$ background may be required to generate a mouse with PGRN levels similar to mutation carriers.

In humans, the first neurons to demonstrate vulnerability in FTD are von Economo neurons (VENs) found in the anterior cingulated cortex (ACC) and frontal insula (Seeley et al., 2006). VENs are large, bipolar neurons in layer 5b that exist in minicolumns in the ACC and frontal insula only. Evolutionarily, VENs are only found in the most encephalized and socially complex mammals (Seeley et al., 2006). They are also more abundant in the right hemisphere, which is believed to control social and emotional behaviors, and is the hemisphere that degenerates in behavioral FTD (Rosen et al., 2002). Mice do not have VENs and, interestingly, both hemispheres are equally affected by age-dependent pathological changes in the *Grn*$^{-/-}$ mice. This suggests that mice may not be capable of fully mimicking all aspects of human FTD.

We do have evidence of early neuron functional changes in the amygdala of the PGRN-deficient mice (Figure 3.7), which is their social-emotional center. These neuronal changes correlate with behavioral alterations (chapter 3). It may be that 18-20 months is not enough time for the *Grn*$^{+/-}$ mice to develop FTD-associated pathology [a normal laboratory mouse can live up to three years (http://research.jax.org/faculty/harrison/ger1vi_LifeStudy2.html)]. It would be interesting to see if pathology could be triggered by a CNS injury, such as neuroinflammatory stimulus, traumatic brain injury, or seizure.

Cell-specific PGRN-deficient mice

The aging characterization of cell-specfic PGRN-deficient mice is critical for determining in which cell type PGRN-deficiency causes the age-dependent changes seen in the global $Grn^{-/-}$ mice described in chapters 2-4. Since PGRN is expressed by neurons and microglia we have bred the $Grn^{flox/flox}$ mice with mice expressing Cre-recombinase driven by the neuron-specific promoters *CamKIIα* (hippocampal and cortical neurons) (Tsien et al., 1996), *Nestin* (pan-neuronal Cre) (Tronche et al., 1999), and the myeloid-specific promoters *Cd11b* (basally expressed on microglia) (Boillée et al., 2006) and *LysM* (activation-induced microglial expression) (Clausen et al., 1999) (Figure 5.6). We have examined plasma PGRN levels in the *CamKIIα-, Nestin,* and *Cd11b-Cre* lines. In all three lines, there is no difference in circulating PGRN levels between Cre+ and Cre– mice. We hypothesized that there may be a reduction in circulating PGRN levels in the *Cd11b-Cre* mice since PGRN levels should be reduced in all cells of the myeloid lineage, including monocytes and macrophages that contribute to the plasma, although this was not the case (Figure 5.7). We also chose to look at an older age to see if there was an age-dependent decrease in plasma PGRN levels because *Cd11b* expression can change slightly with activation state; again, this was not the case (Figure 5.7). Therefore, these cell types do not contribute a significant amount of PGRN to the circulation.

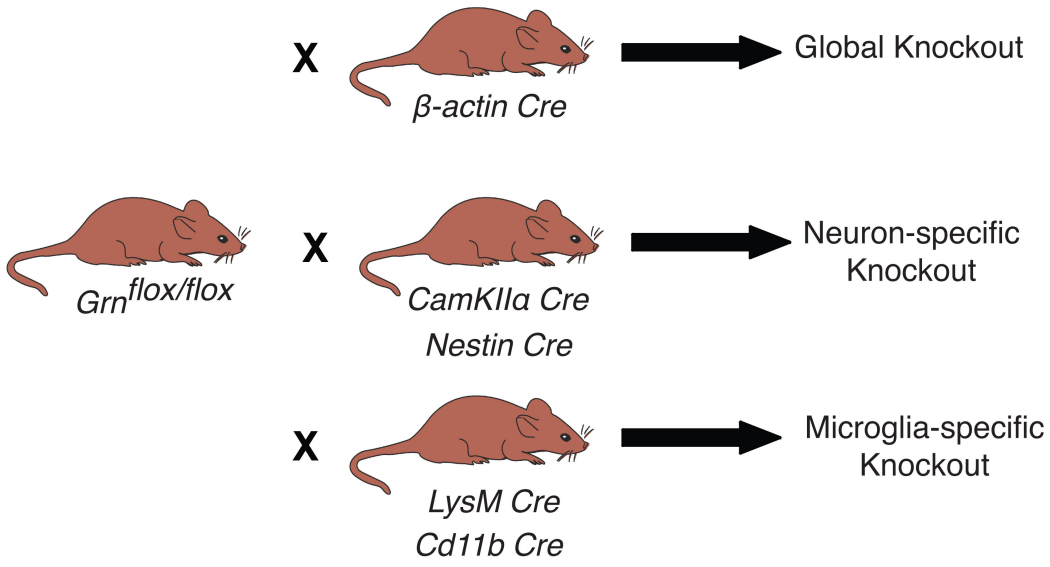

Figure 5.6. Generation of progranulin deficient mouse lines using various promoters to drive Cre recombinase expression.

The *Grn*$^{flox/flox}$ mice were bred with mice expressing Cre recombinase driven by various promoters in order to generate global or cell-specific PGRN deficiency.

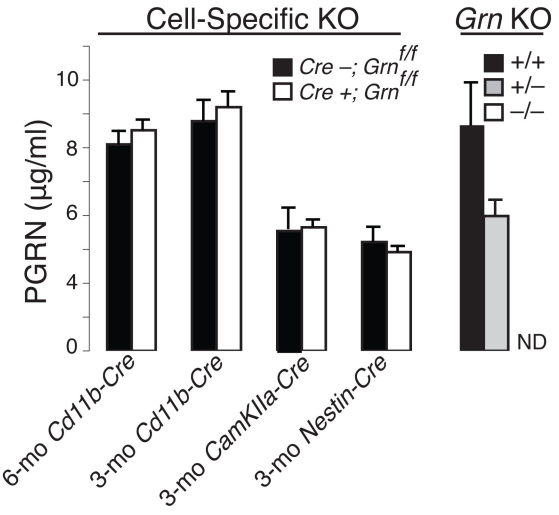

Figure 5.7. The cell-specific progranulin deficient mice do not have altered plasma PGRN levels.

A murine PGRN ELISA was used to quantify the plasma PGRN levels in the cell-specific progranulin deficient mouse lines. There was no difference in plasma PGRN levels between *Cre*+ or *Cre*– mice in any of the cell-specific lines. $N = 6$ mice per genotype.

Interestingly, the *CamKIIα-* and *Nestin-Cre* lines have significantly lower circulating PGRN levels compared with *Cd11b-Cre* and $Grn^{-/-}$ mice (Figure 5.7). These plasma samples were collected at different times of the day- *Cd11b-Cre* and $Grn^{-/-}$ mice in the morning and *CamKIIα-* and *Nestin-Cre* mice in the afternoon. This suggests that there may be a diurnal cycle of PGRN expression. Alternatively, these mice do not exist on a congenic background, a potential modifying polymorphism in another gene may affect PGRN levels. It would be interesting to see if different congenic strains of mice have different circulating PGRN levels. If so, we may be able to find another gene that modifies PGRN levels besides *Sortilin1* and *Tmem106b* (Hu et al., 2010, Van Deerlin et al., 2010).

The efficiency of the Cre recombinase needs to be characterized in all of these mice in order to know whether or not we can believe the aging phenotypes that we observe. Brain mRNA and protein PGRN levels need to evaluated, perhaps even in a regional manner as the *CamKIIα-Cre* mice should only lack PGRN in the hippocampus, cortex, and amygdala (Tsien et al., 1996). Immunohistochemistry for PGRN should be performed to determine which cell populations have lost expression. The caveat with these findings is that PGRN is a secreted protein that is known to be endocytosed through the sortilin-1 receptor, so cells that are expected to lack PGRN may still take up the protein. It will be more informative to isolate the cells *in vitro* to assess mRNA and protein levels, both secreted and intracellular. We have determined the *in vitro* PGRN levels in the *Cd11b-Cre* line; microglia have ~50% reduction in PGRN, while neuronal PGRN is unchanged (Figure A1.4A,B). Determining the *in vivo* microglial PGRN levels at both young and older ages using a Percoll microglia isolation method will tell us

whether or not there are differences in the degree of PGRN deficiency with changes in the activation state of the microglia. Determining the Cre efficiency is critcal for the proper interpretation of ALL future data.

The behavioral and pathological analysis of these mice are ongoing. The *CamKIIα-Cre* line is being characterized by the Roberson lab (UAB). The *CamKIIα-Cre*+ mice have amygdala dysfunction without neuroinflammation similar to $Grn^{+/-}$ mice (Anthony Filiano, unpublished). The *LysM-Cre* line is being characterized by the Gan lab (Gladstone). The *LysM-Cre*+ mice have social deficits and neuroinflammation similar to $Grn^{-/-}$ mice, although the phenotype requires an i.p. injection of LPS (S. Sakura Minami, unpublished). In collaboration with the Huang lab (UCSF) we have determined that 15-month-old *CamKIIα-* and *Cd11b-Cre* mice do not display OCD-like behaviors (data not shown). We are currently assessing the inflammatory, vascular, and neuronal phenotypes in the aged *Cd11b-Cre* mice. The *Nestin-Cre* mice are still aging. Once all of the data has been collected it will be interesting to see which, if any, cell-specific PGRN-deficient mice display FTD-like behavioral and pathological phenotypes, or whether a PGRN deficiency in both neurons and microglia is required for the development of the phenotypes. I hypothesize that a small neuronal change triggers the uncontrolled neuroinflammation, causing even more neuronal damage. Therefore, the introduction of an inflammatory stimulus may be enough to trigger the disease phenotypes, but may lack the regional specificity.

Summary

Overall, lots of progress in elucidating the CNS function of progranulin has been made since *GRN* mutations were causatively linked to FTD in 2006. I believe the data in this chapter indicates that more knowledge about PGRN CNS biology is essential prior to even just upregulation of PGRN levels as a therapy. The largest gaps in knowledge include: cell-type specific PGRN function in neurons and microglia *in vivo*; cell-type specific receptor levels; CNS GRN species, receptors, and cell-type specific function; and determining the best murine model of PGRN deficiency. Increased information in these areas will permit the most efficient and accurate targeting of therapeutics for PGRN deficient FTD.

References

Adolphs R (What does the amygdala contribute to social cognition? Ann N Y Acad Sci 1191:42-61.2010).

Ahmed Z, et al. (Progranulin in frontotemporal lobar degeneration and neuroinflammation. Journal of neuroinflammation 4:7.2007).

Ahmed Z, et al. (Accelerated Lipofuscinosis and Ubiquitination in Granulin Knockout Mice Suggests a Role for Progranulin in Successful Aging. Am J Pathol.2010).

Alexander JJ, et al. (The complement cascade: Yin-Yang in neuroinflammation--neuro-protection and -degeneration. J Neurochem 107:1169-1187.2008).

Almeida S, et al. (Induced pluripotent stem cell models of progranulin-deficient frontotemporal dementia uncover specific reversible neuronal defects. Cell Rep 2:789-798.2012).

Arrasate M, Finkbeiner S (Automated microscope system for determining factors that predict neuronal fate. Proc Natl Acad Sci USA 102:3840-3845.2005).

Arrasate M, et al. (Inclusion body formation reduces levels of mutant huntingtin and the risk of neuronal death. Nature 431:805-810.2004).

Bai X-H, et al. (ADAMTS-7, a direct target of PTHrP, adversely regulates endochondral bone growth by associating with and inactivating GEP growth factor. Mol Cell Biol 29:4201-4219.2009).

Baker M, et al. (Mutations in progranulin cause tau-negative frontotemporal dementia linked to chromosome 17. Nature 442:916-919.2006).

Barmada SJ, et al. (Cytoplasmic mislocalization of TDP-43 is toxic to neurons and enhanced by a mutation associated with familial amyotrophic lateral sclerosis. Journal of Neuroscience 30:639-649.2010).

Bateman A, Bennett HP (Granulins: the structure and function of an emerging family of growth factors. J Endocrinol 158:145-151.1998).

Bickart KC, et al. (Amygdala volume and social network size in humans. Nat Neurosci 14:163-164.2011).

Boillée S, et al. (Onset and progression in inherited ALS determined by motor neurons and microglia. Science 312:1389-1392.2006).

Bosch OJ, et al. (Maternal behaviour is associated with vasopressin release in the medial preoptic area and bed nucleus of the stria terminalis in the rat. J Neuroendocrinol 22:420-429.2010).

Brown GC, Neher JJ (Inflammatory neurodegeneration and mechanisms of microglial killing of neurons. Mol Neurobiol 41:242-247.2010).

Butler GS, et al. (Pharmacoproteomics of a metalloproteinase hydroxamate inhibitor in breast cancer cells: dynamics of membrane type 1 matrix metalloproteinase-mediated membrane protein shedding. Mol Cell Biol 28:4896-4914.2008).

Cabal-Hierro L, Lazo PS (Signal transduction by tumor necrosis factor receptors. Cell Signal 24:1297-1305.2012).

Capell A, et al. (Rescue of Progranulin Deficiency Associated with Frontotemporal Lobar Degeneration by Alkalizing Reagents and Inhibition of Vacuolar ATPase. Journal of Neuroscience 31:1885-1894.2011).

Cenik B, et al. (SAHA (VORINOSTAT) upregulates progranulin transcription: a rational therapeutic approach to frontotemporal dementia. J Biol Chem.2011).

Chen J, et al. (SIRT1 protects against microglia-dependent amyloid-beta toxicity through inhibiting NF-kappaB signaling. J Biol Chem 280:40364-40374.2005).

Chen SK, et al. (Hematopoietic origin of pathological grooming in Hoxb8 mutant mice. Cell 141:775-785.2010).

Chen-Plotkin AS, et al. (Variations in the progranulin gene affect global gene expression in frontotemporal lobar degeneration. Human Molecular Genetics 17:1349-1362.2008).

Clapcote SJ, Roder JC (Deletion polymorphism of Disc1 is common to all 129 mouse substrains: implications for gene-targeting studies of brain function. Genetics 173:2407-2410.2006).

Clausen BE, et al. (Conditional gene targeting in macrophages and granulocytes using LysMcre mice. Transgenic Res 8:265-277.1999).

Cohen TJ, et al. (TDP-43 functions and pathogenic mechanisms implicated in TDP-43 proteinopathies. Trends in Molecular Medicine 17:659-667.2011).

Coppola G, et al. (Gene expression study on peripheral blood identifies progranulin mutations. Ann Neurol 64:92-96.2008).

Cruts M, et al. (Null mutations in progranulin cause ubiquitin-positive frontotemporal dementia linked to chromosome 17q21. Nature 442:920-924.2006).

Cruts M, Van Broeckhoven C (Loss of progranulin function in frontotemporal lobar degeneration. Trends Genet 24:186-194.2008).

Cuevas-Antonio R, et al. (Expression of progranulin (Acrogranin/PCDGF/Granulin-Epithelin Precursor) in benign and malignant ovarian tumors and activation of MAPK signaling in ovarian cancer cell line. Cancer Invest 28:452-458.2010).

Czlonkowska A, et al. (Microglial reaction in MPTP (1-methyl-4-phenyl-1,2,3,6-tetrahydropyridine) induced Parkinson's disease mice model. Neurodegeneration 5:137-143.1996).

Daniel R, et al. (Cellular localization of gene expression for progranulin. J Histochem Cytochem 48:999-1009.2000).

Dauer W, Przedborski S (Parkinson's disease: mechanisms and models. Neuron 39:889-909.2003).

DeJesus-Hernandez M, et al. (Expanded GGGGCC hexanucleotide repeat in noncoding region of C9ORF72 causes chromosome 9p-linked FTD and ALS. Neuron 72:245-256.2011).

Eriksen JL, Mackenzie IRA (Progranulin: normal function and role in neurodegeneration. J Neurochem 104:287-297.2008).

Farkas LM, et al. (Transforming growth factor-beta(s) are essential for the development of midbrain dopaminergic neurons in vitro and in vivo. J Neurosci 23:5178-5186.2003).

Feng JQ, et al. (Granulin epithelin precursor: a bone morphogenic protein 2-inducible growth factor that activates Erk1/2 signaling and JunB transcription factor in chondrogenesis. FASEB J 24:1879-1892.2010).

Ferger B, et al. (Genetic ablation of tumor necrosis factor-alpha (TNF-alpha) and pharmacological inhibition of TNF-synthesis attenuates MPTP toxicity in mouse striatum. J Neurochem 89:822-833.2004).

Finch N, et al. (Plasma progranulin levels predict progranulin mutation status in frontotemporal dementia patients and asymptomatic family members. Brain.2009).

Gao X, et al. (Progranulin promotes neurite outgrowth and neuronal differentiation by regulating GSK-3β. Protein Cell 1:552-562.2010).

Gass J, et al. (Mutations in progranulin are a major cause of ubiquitin-positive frontotemporal lobar degeneration. Human Molecular Genetics 15:2988-3001.2006).

Gass J, et al. (Progranulin regulates neuronal outgrowth independent of Sortilin. Mol Neurodegener 7:33.2012).

Ghidoni R, et al. (Low plasma progranulin levels predict progranulin mutations in frontotemporal lobar degeneration. Neurology 71:1235-1239.2008).

Ghoshal N, et al. (Core features of frontotemporal dementia recapitulated in progranulin knockout mice. Neurobiology of disease.2011).

Gijselinck I, et al. (Granulin mutations associated with frontotemporal lobar degeneration and related disorders: an update. Hum Mutat 29:1373-1386.2008).

Glass CK, et al. (Mechanisms underlying inflammation in neurodegeneration. Cell 140:918-934.2010).

Grammas P (Neurovascular dysfunction, inflammation and endothelial activation: implications for the pathogenesis of Alzheimer's disease. J Neuroinflammation 8:26.2011).

Guo Z, et al. (Prevention of LPS-induced acute lung injury in mice by progranulin. Mediators Inflamm 2012:540794.2012).

He Z, Bateman A (Progranulin gene expression regulates epithelial cell growth and promotes tumor growth in vivo. Cancer Res 59:3222-3229.1999).

He Z, Bateman A (Progranulin (granulin-epithelin precursor, PC-cell-derived growth factor, acrogranin) mediates tissue repair and tumorigenesis. J Mol Med 81:600-612.2003).

He Z, et al. (Progranulin (PC-cell-derived growth factor/acrogranin) regulates invasion and cell survival. Cancer Res 62:5590-5596.2002).

He Z, et al. (Progranulin is a mediator of the wound response. Nat Med 9:225-229.2003).

Hoefer M, et al. (Fear conditioning in frontotemporal lobar degeneration and Alzheimer's disease. Brain 131:1646-1657.2008).

Hossein-Nezhad A, et al. (Obesity, inflammation and resting energy expenditure: possible mechanism of progranulin in this pathway. Minerva Endocrinol 37:255-266.2012).

Hu F, et al. (Sortilin-mediated endocytosis determines levels of the frontotemporal dementia protein, progranulin. Neuron 68:654-667.2010).

Hutton M, et al. (Association of missense and 5'-splice-site mutations in tau with the inherited dementia FTDP-17. Nature 393:702-705.1998).

Hynes MA, et al. (Neurotrophin-4/5 is a survival factor for embryonic midbrain dopaminergic neurons in enriched cultures. J Neurosci Res 37:144-154.1994).

Irwin D, et al. (Progranulin (PGRN) expression in ALS: an immunohistochemical study. Journal of the Neurological Sciences 276:9-13.2009).

Jian J, et al. (Insights into the role of progranulin in immunity, infection, and inflammation. J Leukoc Biol.2012).

Jiao J, et al. (MicroRNA-29b regulates the expression level of human progranulin, a secreted glycoprotein implicated in frontotemporal dementia. PLoS ONE 5:e10551.2010).

Kao AW, et al. (A neurodegenerative disease mutation that accelerates the clearance of apoptotic cells. Proc Natl Acad Sci USA.2011).

Kayasuga Y, et al. (Alteration of behavioural phenotype in mice by targeted disruption of the progranulin gene. Behav Brain Res 185:110-118.2007).

Kessenbrock K, et al. (Proteinase 3 and neutrophil elastase enhance inflammation in mice by inactivating antiinflammatory progranulin. J Clin Invest 118:2438-2447.2008).

Kipps CM, et al. (Understanding social dysfunction in the behavioural variant of frontotemporal dementia: the role of emotion and sarcasm processing. Brain 132:592-603.2009).

Kleinberger G, et al. (Increased caspase activation and decreased TDP-43 solubility in progranulin knockout cortical cultures. J Neurochem.2010).

Kohlschutter A, Schulz A (Towards understanding the neuronal ceroid lipofuscinoses. Brain Dev 31:499-502.2009).

Kril JJ, Halliday GM (Pathological staging of frontotemporal lobar degeneration. J Mol Neurosci 45:379-383.2011).

LeDoux J (The emotional brain, fear, and the amygdala. Cell Mol Neurobiol 23:727-738.2003).

LeDoux J (The amygdala. Curr Biol 17:R868-874.2007).

Lee R, Kermani P, Teng KK, Hempstead BL (Regulation of cell survival by secreted proneurotrophins. Science 294:1945-1948.2001).

Levenson JM,et al. (Regulation of histone acetylation during memory formation in the hippocampus. J Biol Chem 279:40545-40559.2004).

Lewandoski M, et al. (Fgf8 signalling from the AER is essential for normal limb development. Nat Genet 26:460-463.2000).

Liau LM, et al. (Identification of a human glioma-associated growth factor gene, granulin, using differential immuno-absorption. Cancer Res 60:1353-1360.2000).

Lim H-Y, et al. (Progranulin contributes to endogenous mechanisms of pain defense after nerve injury in mice. J Cell Mol Med.2011).

Lindzey G, et al. (Social dominance in inbred mouse strains. Nature 191:474-476.1961).

Lister KJ, Hickey MJ (Immune complexes alter cerebral microvessel permeability: roles of complement and leukocyte adhesion. Am J Physiol Heart Circ Physiol 291:H694-704.2006).

Liu W, et al. (Behavioral disorders in the frontal and temporal variants of frontotemporal dementia. Neurology 62:742-748.2004).

Logue SF, et al. (Hippocampal lesions cause learning deficits in inbred mice in the Morris water maze and conditioned-fear task. Behav Neurosci 111:104-113.1997).

Lu R, Serrero G (Inhibition of PC cell-derived growth factor (PCDGF, epithelin/granulin precursor) expression by antisense PCDGF cDNA transfection inhibits tumorigenicity of the human breast carcinoma cell line MDA-MB-468. Proc Natl Acad Sci USA 97:3993-3998.2000).

Mackenzie IRA (The neuropathology and clinical phenotype of FTD with progranulin mutations. Acta Neuropathol 114:49-54.2007).

Mackenzie IRA, et al. (The neuropathology of frontotemporal lobar degeneration caused by mutations in the progranulin gene. Brain 129:3081-3090.2006).

Mackenzie IRA, Rademakers R (The molecular genetics and neuropathology of frontotemporal lobar degeneration: recent developments. Neurogenetics 8:237-248.2007).

Malaspina A, et al. (Differential expression of 14 genes in amyotrophic lateral sclerosis spinal cord detected using gridded cDNA arrays. J Neurochem 77:132-145.2001).

Maren S, et al. (Retrograde abolition of conditional fear after excitotoxic lesions in the basolateral amygdala of rats: absence of a temporal gradient. Behav Neurosci 110:718-726.1996).

Martens LH, et al. (Progranulin deficiency promotes neuroinflammation and neuron loss following toxin-induced injury. J Clin Invest 122:3955-3959.2012).

Matsubara T, et al. (PGRN is a key adipokine mediating high fat diet-induced insulin resistance and obesity through IL-6 in adipose tissue. Cell Metab 15:38-50.2012).

Matsumura N, et al. (Oncogenic property of acrogranin in human uterine leiomyosarcoma: direct evidence of genetic contribution in in vivo tumorigenesis. Clin Cancer Res 12:1402-1411.2006).

McCoy MK, Tansey MG (TNF signaling inhibition in the CNS: implications for normal brain function and neurodegenerative disease. Journal of neuroinflammation 5:45.2008).

McGuire SO, et al. (Tumor necrosis factor alpha is toxic to embryonic mesencephalic dopamine neurons. Exp Neurol 169:219-230.2001).

McIsaac SM, et al. (Toll-like receptors in the host defense against Pseudomonas aeruginosa respiratory infection and cystic fibrosis. J Leukoc Biol 92:977-985.2012).

Meiner VL, et al. (Disruption of the acyl-CoA:cholesterol acyltransferase gene in mice: evidence suggesting multiple cholesterol esterification enzymes in mammals. Proc Natl Acad Sci U S A 93:14041-14046.1996).

Miller J, et al. (Quantitative relationships between huntingtin levels, polyglutamine length, inclusion body formation, and neuronal death provide novel insight into huntington's disease molecular pathogenesis. Journal of Neuroscience 30:10541-10550.2010).

Moisse K, et al. (Cytosolic TDP-43 expression following axotomy is associated with caspase 3 activation in NFL-/- mice: support for a role for TDP-43 in the physiological response to neuronal injury. Brain Res 1296:176-186.2009a).

Moisse K, et al. (Divergent patterns of cytosolic TDP-43 and neuronal progranulin expression following axotomy: implications for TDP-43 in the physiological response to neuronal injury. Brain Res 1249:202-211.2009b).

Monami G, Gonzalez EM, Hellman M, Gomella LG, Baffa R, Iozzo RV, Morrione A (Proepithelin promotes migration and invasion of 5637 bladder cancer cells through the activation of ERK1/2 and the formation of a paxillin/FAK/ERK complex. Cancer Res 66:7103-7110.2006).

Moy SS, et al. (Sociability and preference for social novelty in five inbred strains: an approach to assess autistic-like behavior in mice. Genes Brain Behav 3:287-302.2004).

Moya PR, et al. (Altered 5-HT2C receptor agonist-induced responses and 5-HT2C receptor RNA editing in the amygdala of serotonin transporter knockout mice. BMC Pharmacol 11:3.2011).

Mukherjee O, et al. (Molecular characterization of novel progranulin (GRN) mutations in frontotemporal dementia. Hum Mutat 29:512-521.2008).

Musunuru K, et al. (From noncoding variant to phenotype via SORT1 at the 1p13 cholesterol locus. Nature 466:714-719.2010).

Naphade SB, et al. (Progranulin expression is upregulated after spinal contusion in mice. Acta Neuropathol 119:123-133.2010).

Neumann M, et al. (Ubiquitinated TDP-43 in frontotemporal lobar degeneration and amyotrophic lateral sclerosis. Science 314:130-133.2006).

Okura H, et al. (HDL/Apolipoprotein A-I Binds to Macrophage-Derived Progranulin and Suppresses its Conversion into Proinflammatory Granulins. Journal of atherosclerosis and thrombosis.2010).

Ong CHP, Bateman A (Progranulin (granulin-epithelin precursor, PC-cell derived growth factor, acrogranin) in proliferation and tumorigenesis. Histol Histopathol 18:1275-1288.2003).

Ong CHP, et al. (Regulation of progranulin expression in myeloid cells. Am J Physiol Regul Integr Comp Physiol 291:R1602-1612.2006).

Palop JJ, et al. (Quantifying biomarkers of cognitive dysfunction and neuronal network hyperexcitability in mouse models of Alzheimer's disease: depletion of calcium-dependent proteins and inhibitory hippocampal remodeling. Methods Mol Biol 670:245-262.2011).

Park B, et al. (Granulin is a soluble cofactor for toll-like receptor 9 signaling. Immunity 34:505-513.2011).

Pereson S, et al. (Progranulin expression correlates with dense-core amyloid plaque burden in Alzheimer disease mouse models. J Pathol 219:173-181.2009).

Petkau TL, et al. (Synaptic dysfunction in progranulin-deficient mice. Neurobiology of disease.2011).

Petkau TL, et al. (Progranulin expression in the developing and adult murine brain. J Comp Neurol 518:3931-3947.2010).

Philips T, et al. (Microglial Upregulation of Progranulin as a Marker of Motor Neuron Degeneration. J Neuropathol Exp Neurol 69:1191-1200.2010).

Pickford F, et al. (Progranulin is a chemoattractant for microglia and stimulates their endocytic activity. Am J Pathol 178:284-295.2011).

Plowman GD, et al. (The epithelin precursor encodes two proteins with opposing activities on epithelial cell growth. J Biol Chem 267:13073-13078.1992).

Polymenidou M, et al. (Long pre-mRNA depletion and RNA missplicing contribute to neuronal vulnerability from loss of TDP-43. Nat Neurosci.2011).

Rabinovici GD, Miller BL (Frontotemporal lobar degeneration: epidemiology, pathophysiology, diagnosis and management. CNS Drugs 24:375-398.2010).

Rademakers R, et al. (Phenotypic variability associated with progranulin haploinsufficiency in patients with the common 1477C-->T (Arg493X) mutation: an international initiative. Lancet neurology 6:857-868.2007).

Rascovsky K, et al. (Sensitivity of revised diagnostic criteria for the behavioural variant of frontotemporal dementia. Brain 134:2456-2477.2011).

Ratnavalli E, et al. (The prevalence of frontotemporal dementia. Neurology 58:1615-1621.2002).

Renton AE, et al. (A hexanucleotide repeat expansion in C9ORF72 is the cause of chromosome 9p21-linked ALS-FTD. Neuron 72:257-268.2011).

Roberson ED (Frontotemporal dementia. Current neurology and neuroscience reports 6:481-489.2006).

Rosen EY, et al. (Functional genomic analyses identify pathways dysregulated by progranulin deficiency, implicating Wnt signaling. Neuron 71:1030-1042.2011).

Rosen HJ, et al. (Patterns of brain atrophy in frontotemporal dementia and semantic dementia. Neurology 58:198-208.2002).

Rosen HJ, et al. (Recognition of emotion in the frontal and temporal variants of frontotemporal dementia. Dement Geriatr Cogn Disord 17:277-281.2004).

Ryan C, et al. (Progranulin is expressed within motor neurons and promotes neuronal cell survival. BMC neuroscience 10:130.2009).

Santacruz K, et al. (Tau suppression in a neurodegenerative mouse model improves memory function. Science 309:476-481.2005).

Saudou F, et al. (Huntingtin acts in the nucleus to induce apoptosis but death does not correlate with the formation of intranuclear inclusions. Cell 95:55-66.1998).

Scearce-Levie K, et al. (Abnormal social behaviors in mice lacking Fgf17. Genes Brain Behav 7:344-354.2008).

Seeley WW, et al. (Early frontotemporal dementia targets neurons unique to apes and humans. Ann Neurol 60:660-667.2006).

Seeley WW, et al. (Neurodegenerative Diseases Target Large-Scale Human Brain Networks. Neuron 62:42-52.2009).

Sephton CF, et al. (Identification of neuronal RNA targets of TDP-43-containing Ribonucleoprotein complexes. J Biol Chem.2010).

Serrero G (Autocrine growth factor revisited: PC-cell-derived growth factor (progranulin), a critical player in breast cancer tumorigenesis. Biochem Biophys Res Commun 308:409-413.2003).

Shankaran SS, et al. (Missense mutations in the progranulin gene linked to frontotemporal lobar degeneration with ubiquitin-immunoreactive inclusions reduce progranulin production and secretion. J Biol Chem 283:1744-1753.2008).

Shmelkov SV, et al. (Slitrk5 deficiency impairs corticostriatal circuitry and leads to obsessive-compulsive-like behaviors in mice. Nat Med 16:598-602, 591p following 602.2010).

Skibinski G, et al. (Mutations in the endosomal ESCRTIII-complex subunit CHMP2B in frontotemporal dementia. Nat Genet 37:806-808.2005).

Smith KR, et al. (Strikingly different clinicopathological phenotypes determined by progranulin-mutation dosage. Am J Hum Genet 90:1102-1107.2012).

Sriram K, et al. (Deficiency of TNF receptors suppresses microglial activation and alters the susceptibility of brain regions to MPTP-induced neurotoxicity: role of TNF-alpha. FASEB J 20:670-682.2006).

Suh HS, et al. (Regulation of progranulin expression in human microglia and proteolysis of progranulin by matrix metalloproteinase-12 (MMP-12). PLoS One 7:e35115.2012).

Tang W, et al. (The Growth Factor Progranulin Binds to TNF Receptors and Is Therapeutic Against Inflammatory Arthritis in Mice. Science.2011).

Tangkeangsirisin W, Serrero G (PC cell-derived growth factor (PCDGF/GP88, progranulin) stimulates migration, invasiveness and VEGF expression in breast cancer cells. Carcinogenesis 25:1587-1592.2004).

Tapia L, et al. (Progranulin deficiency decreases gross neural connectivity but enhances transmission at individual synapses. J Neurosci 31:11126-11132.2011).

Tolkatchev D, et al. (Structure dissection of human progranulin identifies well-folded granulin/epithelin modules with unique functional activities. Protein Sci 17:711-724.2008).

Tronche F, et al. (Disruption of the glucocorticoid receptor gene in the nervous system results in reduced anxiety. Nat Genet 23:99-103.1999).

Tsien JZ, et al. (Subregion- and cell type-restricted gene knockout in mouse brain. Cell 87:1317-1326.1996).

Van Damme P, et al. (Progranulin functions as a neurotrophic factor to regulate neurite outgrowth and enhance neuronal survival. J Cell Biol 181:37-41.2008).

Van Deerlin VM, et al. (Common variants at 7p21 are associated with frontotemporal lobar degeneration with TDP-43 inclusions. Nat Genet.2010).

Vossel KA, Miller BL (New approaches to the treatment of frontotemporal lobar degeneration. Curr Opin Neurol 21:708-716.2008).

Wang W-X, et al. (MiR-107 Regulates Granulin/Progranulin with Implications for Traumatic Brain Injury and Neurodegenerative Disease. Am J Pathol.2010).

Watts GDJ, et al. (Inclusion body myopathy associated with Paget disease of bone and frontotemporal dementia is caused by mutant valosin-containing protein. Nat Genet 36:377-381.2004).

Welch JM, et al. (Cortico-striatal synaptic defects and OCD-like behaviours in Sapap3-mutant mice. Nature 448:894-900.2007).

Werner KH, et al. (Emotional reactivity and emotion recognition in frontotemporal lobar degeneration. Neurology 69:148-155.2007).

Wex T, et al. (Mucosal Progranulin expression is induced by H. pylori, but independent of Secretory Leukocyte Protease Inhibitor (SLPI) expression. BMC gastroenterology 11:63.2011).

Wils H, et al. (Cellular ageing, increased mortality and FTLD-TDP-associated neuropathology in progranulin knockout mice. J Pathol.2012).

Xu J, et al. (Extracellular progranulin protects cortical neurons from toxic insults by activating survival signaling. Neurobiology of aging.2011).

Xu SQ, et al. (The granulin/epithelin precursor abrogates the requirement for the insulin-like growth factor 1 receptor for growth in vitro. J Biol Chem 273:20078-20083.1998).

Yasui K, et al. (Increased progranulin in the skin of amyotrophic lateral sclerosis: an immunohistochemical study. J Neurol Sci 309:110-114.2011).

Yin F, et al. (Exaggerated inflammation, impaired host defense, and neuropathology in progranulin-deficient mice. The Journal of experimental medicine.2009).

Yin F, et al. (Behavioral deficits and progressive neuropathology in progranulin-deficient mice: a mouse model of frontotemporal dementia. FASEB J.2010).

Youn BS, et al. (Serum progranulin concentrations may be associated with macrophage infiltration into omental adipose tissue. Diabetes 58:627-636.2009).

Zanocco-Marani T, et al. (Biological activities and signaling pathways of the granulin/epithelin precursor. Cancer Res 59:5331-5340.1999).

Zhang B, Horvath S (A general framework for weighted gene co-expression network analysis. Stat Appl Genet Mol Biol 4:Article17.2005).

Zhang H, Serrero G (Inhibition of tumorigenicity of the teratoma PC cell line by transfection with antisense cDNA for PC cell-derived growth factor (PCDGF, epithelin/granulin precursor). Proc Natl Acad Sci USA 95:14202-14207.1998).

Zhang J, et al. (Essential function of HIPK2 in TGFbeta-dependent survival of midbrain dopamine neurons. Nat Neurosci 10:77-86.2007).

Zhou H, et al. (transgenic rat model of neurodegeneration caused by mutation in the TDP gene. PLoS Genet 6:e1000887.2010a).

Zhou J, et al. (Divergent network connectivity changes in behavioural variant frontotemporal dementia and Alzheimer's disease. Brain 133:1352-1367.2010b).

Zhu J, et al. (Conversion of proepithelin to epithelins: roles of SLPI and elastase in host defense and wound repair. Cell 111:867-878.2002).

APPENDIX I

Supplemental Material for Chapter 2

Supplemental Methods

Generation of PGRN-deficient mice. A targeting vector for the *Grn* locus was created with loxP sites flanking the entire *Grn* coding region, including the 3'UTR. Neomycin resistance and thymidine kinase (TK) genes were used for positive and negative selection, respectively. The vector was electroporated into RF8 (Meiner et al., 1996) 129SC/Jae ESCs and positive clones were selected at a frequency of approximately 1 in 15. The positive clones were injected into C57BL/6J blastocysts to create chimeras. The chimeras were then bred with C57BL/6J females to confirm germline transmission of the Grn^{flox} allele. The $Grn^{flox/+}$ mice were bred with mice expressing Cre recombinase under the β-actin promoter (Lewandoski et al., 2000) to create mice that globally lack progranulin. These mice were then backcrossed with C57BL/6J mice to remove the Cre transgene. The $Grn^{+/-}$; Cre– mice were then bred to homozygosity to generate a *Grn*-null allele. The genotyping for the *Grn*-deficient mice includes the following primers: S1 (5'-agtggggctggccacttct-3'). S2 (5'-aagattcctcgctgggacatg-3') and AS1 (5'-gaatgctggtgtcagagggcc-3'). The $Grn^{flox/flox}$ mice were bred with mice expressing Cre recombinase under the Cd11b promoter (Boillée et al., 2006) to create mice that lack progranulin in myeloid cells. All mice utilized in the paper exist on a mixed background consisting of 62.5% C57BL/6J, 12.5% 129Sv/Jae, and 25% FVB. All procedures were approved by UCSF Animal Research and followed NIH guidelines.

Needlestick. Three-month-old wild-type mice were anesthetized and placed on a stereotactic injection platform. A hole was drilled in the skull and a 33-gauge needle was inserted three times sequentially into the hippocampus. Following trauma, the scalp was

closed and the mice were allowed to recover. A day later the mice were sacrificed and the brains were collected for analysis. Mice were monitored according to IACUC protocol and received proper analgesics as needed.

Acute MPTP treatement. 1-methyl-4-(2'-methylphenyl)-1,2,3,6-tetrahydrophine (MPTP, 4μg/g) or equivalent volume of PBS was injected intrperitoneally inot three-month-old female mice (littermates) by four injections per day for two days. The mice were monitored according to the approved IACUC protocol and their health was scored prior to each injection. The mice were sacrificed the day after final injection and perfused with 4% PFA prior to brain extraction. The brains were post-fixed in 4% PFA overnight, followed by cryoprotection in 15% sucrose for 24 hours and then 30% sucrose for 24 hours. The brains were embedded for cryosectioing and cut into 40μm coronal sections. The sections containing the SNpc were stained using anti-TH (Millipore) and Iba1 (Wako) using a DAB technique (Zhang et al., 2007). Stereological counting of Bregma -2.8 to -4.04 mm (6 serial sections) at 100X magnification was utilized to quantify the number of TH-, IBA1-, and Nissl-positive cells in the SNpc (single hemisphere) using the StereoInvestigator Software, version 9 (MBF Bioscience) (Zhang et al., 2007).

Primary Cultures. All cultures were grown in humidified incubators at 37°C, supplemented with 5% CO_2. The ventral midbrain was harvested from E13.5 embryos as previously described (Hynes et al., 1994, Farkas et al., 2003, Zhang et al., 2007). Cells from wild-type (*n*=5) and PGRN-deficeint (*n*=4) embryos were plated on six coverslips each. On day in vitro (DIV) 4, the cells were treated with vehicle, 0.2μM or 0.5μM

MPP+ (in duplicate) for 3 days and then fixed in 4% PFA. Following staining, the coverslips were imaged using a Zeiss LSM confocal (40X magnification). Images were stitched together and the number of cells was quantified using ImageJ software.

Mixed cortical cultures were prepared as previously described (Chen et al., 2005). Briefly, the cortices from postnatal day 1 (P1) pups were harvested and plated on poly-L-lysine coated 12mm coverslips (BIOCOAT) in DMEM (high glucose) supplemented with 10% FBS and penicillin/streptomycin (P/S) for eight days. On DIV5, the cultures were infected with lentivirus. On DIV8, the media was changed to Neurobasal media (Invitrogen) supplemented with N2 (Invitrogen), L-glutamine, and P/S. Four days later the conditioned media was collected and the cultures were fixed with 4% PFA. The coverslips were then stained with anti-MAP2 (Millipore), IBA1, and GFAP (Dako). ~15 images per coverslip were taken using a Leica epifluorescent microscope (40X magnification). The number of MAP2-positive cells was counted per image in order to determine the number of surviving neurons. This experiment was repeated three times.

Primary microglial cultures were obtained from cerebral cortices harvested from P2-P4 pups. Then meninges were removed and the hemispheres were chopped with a razor blade and then triturated in DMEM, 20% FBS, P/S, and supplemented with 20ng/ml GM-CSF (Peprotech). The cells were grown in poly-L-lysine coated flasks. The media was replenished three days after the initial harvest. The microglia were harvested from the astrocyte layer 6-10 days later by shaking the flasks at 200rpm for two hours at 37°C. The media was removed and cells were pelleted. The microglia were resuspended in Neurobasal media supplemented with N2 supplement, L-glutamine, and P/S for 24 hours prior to experimentation.

Cortical neuron cultures were prepared as previously described (Saudou et al., 1998, Barmada et al., 2010). Briefly, E16-E18 embryo cortices were dissected and the meninges were removed. The brains were digested with papain (Sigma). The cells were plated on 96 well plates at a density of $0.6x10^6$ cells/ml in Neurobasal media supplemented with B27 supplement (Invitrogen), L-glutamine, and P/S.

Cytokine Analysis. Primary microglia were harvested and cultured in Neurobasal media supplemented with L-glutamine, N2 supplement, and P/S 24 hours prior to experiments. For mRNA analysis, the cells were plated at $1x10^6$ cells/ml on 6-well plates. For secreted cytokine time course measurements, the cells were plated at $2.5x10^5$ cells/ml on 24-well plates. After 24 hours in the N2-media, control or muPGRN lentivirus was added to the cultures for 24 hours. The microglia were stimulated with PBS or 100 ng/ml LPS (Sigma) plus 100 U/ml IFNγ (Sigma) with or without 200 ng/ml Etanercept (gift M.G. Tansey) for up to 24 hours. Conditioned media was collected for use in neuronal survival assays (6-well plates) or for ELISA (24-well plates) and the cells were lysed in Trizol (Invitrogen) for RNA extraction. Secreted cytokine levels were quantitated using the Mouse Pro-inflammatory 7-plex cytokine ELISA by Meso Scale Discovery.

Neuron Survival Analysis. To fluorescently label neurons, pure cortical cultures were transfected with EGFP on DIV4 using Lipofectamine2000 (Invitrogen). Following transfection, microglial conditioned media was added to the cultures. The plates were imaged every 24 hours using an automated microscopy system described by Arrasate and Finkbeiner and others (Arrasate et al., 2004, Arrasate and Finkbeiner, 2005, Barmada et

al., 2010, Miller et al., 2010). Neuronal death was determined by loss of GFP fluorescence, blebbing of the soma, or neurite retraction. Kaplan-Meier and cumulative risk of death curves were generated and statistical significance was determined using the log-rank test in R. Hazard ratios between groups and conditions were calculated using Cox proportional hazards analysis in R (Barmada et al., 2010).

Real-time PCR. RNA was harvested using Trizol according to the manufacturer's protocol from tissue (liver, kidney, brain) or cultured primary neurons and microglia. RNA (1-2μg) was reverse-transcribed using random hexamers to generate cDNA using the SuperScript III First-Strand Synthesis System (Invitrogen). The primers used for the qPCR were as follows, *Cylco* (F 5'-tggaagagcaccaagacaaca-3', R 5'-tgccggagtcgacaatgat-3'), *Grn* (F 5'-tggttcacacacgatgcgtttcac-3', R 5'-aaaggcaaagacactgccctgttg-3'), *Tnfa* (F 5'-acggcatggatctcaaagac-3', R 5'-agatagcaaatcggctgacg-3') *Il1b* (F 5'-gcttcaggcaggcagtatc-3', R 5'-aggatgggctcttcttcaaag-3'), *Il10* (F 5'-agaccctcaggatgcggc-3', R 5'-ccactgccttgctcttattttca-3'). The reaction was run using the SYBR green Master Mix (QIAGEN) on an ABI Prism 7770 (Applied Biosystems). The data is normalized to the internal standard, cyclophilin, and subsequently normalized to an experimental control (ΔΔCT method, Invitrogen).

Murine Progranulin ELISA. Plasma was collected using a lithium heparin column (BD Biosciences) from 6-week-old mice. PGRN levels were quantified using an ELISA kit (Adipogen). Conditioned media was centrifuged to remove cellular debris. Secreted

PGRN was quantified using an in-house ELISA system, using PGRN-deficient media as an internal control.

Immunoblotting. Frozen hemibrains were dissected into cortex, hippocampus, and cerebellum. The tissue was homogenized in RIPA buffer (Sigma) and sonicated. Conditioned media was centrifuged to remove cellular debris. Proteins were separated using the NuPage system (Invitrogen) and murine progranulin was detected using a polyclonal antibody (AF2557) (R&D Systems, Inc). Loading accuracy was determined either by detecting tissue actin (Sigm) or Ponceau S (Sigma) to detect total protein in conditioned media.

Immunohistochemistry/Immunocytochemistry. Free-floating tissue sections were stained as previously described for both the DAB and fluorescent techniques (Zhang et al., 2007). The following primary antibodies were incubated overnight at room temperature: TH (1:1000, Millipore), IBA1 (1:5000, Wako), GFAP (1:5000, Dako), PGRN (1:100, R&D Systems). Secondary antibodies (Vector Labs, 1:300) were incubated for 1.5 hrs at room temperature. For DAB, sections were washed with 0.1M Tris, pH 8.0 and exposed to DAB solution (Vector Labs). The sections were mounted onto slides and coverslipped using Permount (Thermo Fisher Scientific) or Vectashield (Vector Labs). Images were taken at 4X magnification. Confocal images were taken using the Zeiss LSM10 (63X magnification). Cells were permeabilized with 0.1% Triton and blocked with 10% normal goat serum. The following primary antibodies were incubated overnight at 4°C: TH (1:1000, Millipore), TUJ1 (1:1000, Cell Signaling, MAP2 (1:500, Millipore). Secondary

antibodies (Invitrogen) were incubated for one hour at room temperature and the slides were coverslipped with Vectashield for imaging.

Supplemental Results

Progranulin is expressed in neurons and activated microglia in the CNS

To investigate PGRN expression and function in the CNS, we generated PGRN-deficient mice. The murine *Grn* locus was targeted to introduce loxP sites flanking exons 2-13 (Figure A1.1A,B). Homozygous ($Grn^{-/-}$) mice were generated by crossing the *Grn*-floxed mice with β-actin–Cre mice (Lewandoski et al., 2000). Deletion of *Grn* was verified using quantitative PCR and immunoblotting (Figure A1.1C,D). Plasma levels of PGRN in $Grn^{+/-}$ mice were reduced by ~60% (Figure A1.1E), similar to what is seen in humans with *GRN* haploinsufficiency (Coppola et al., 2008, Ghidoni et al., 2008, Finch et al., 2009).

We examined PGRN expression in the adult murine brain. Immunoblotting revealed expression in the cortex, hippocampus, and cerebellum (Figure A1.1D). Immunohistochemical staining using a PGRN-specific antibody showed that PGRN was present mostly in neurons in various regions of the CNS, including cerebral cortex, CA1 and CA3 regions of the hippocampus, the substantia nigra pars compacta (SNpc) and ventral tegmental area (VTA). (Figure A.2A). PGRN binds the scavenger receptor, *Sortilin1*, on neurons and is subsequently endocytosed (Hu et al., 2010). Therefore, immunohistochemial detection is not sufficient to determine endogenous expression versus uptake of the PGRN protein. In addition, PGRN could also be detected in non-neuronal cells, which morphologically resemble glia (Figure A1.2A, arrow heads).

Indeed, double immunofluorescent confocal microscopy showed that PGRN co-localized with markers for microglia, but not with astrocytes (Figure A1.2B). We observed no PGRN staining in *Grn*$^{-/-}$ animals (Figure A1.2A).

Progranulin expression is upregulated in activated macrophages in vitro (Ong et al., 2006), in microglia following injury to the peripheral nervous system (Moisse et al., 2009, Naphade et al., 2010), and in patients with neurodegenerative disease (Malaspina et al., 2001, Baker et al., 2006, Mackenzie et al., 2006, Philips et al., 2010). To determine whether acute expression of PGRN increases in activated CNS microglia in vivo, we induced direct traumatic injury to the cerebral cortex and hippocampus by needlestick. After 24 hours, there were increased numbers of microglia expressing increased PGRN at the injury site (Figure A1.2C). Thus, PGRN expression in microglia is upregulated in response to acute injury in the CNS.

Supplemental Figures

Neuron Genotype	Media	N	HR	P
Grn$^{+/+}$	Neurobasal + B27	744	Ref	
Grn$^{-/-}$	Neurobasal + B27	1137	1.17	0.008
Grn$^{+/+}$	Neurobasal + N2	513	Ref	
Grn$^{-/-}$	Neurobasal + N2	426	1.21	0.007

Table A1.1. Progranulin-deficiency affets cortical neuron survival in vitro.

Hazard ratios (HR) were determined for populations of neurons over time to indicate alterations in survival. Progranulin-deficient primary cortical neurons cultured in the absence of glia have decreased survival. HR, hazard ratio.

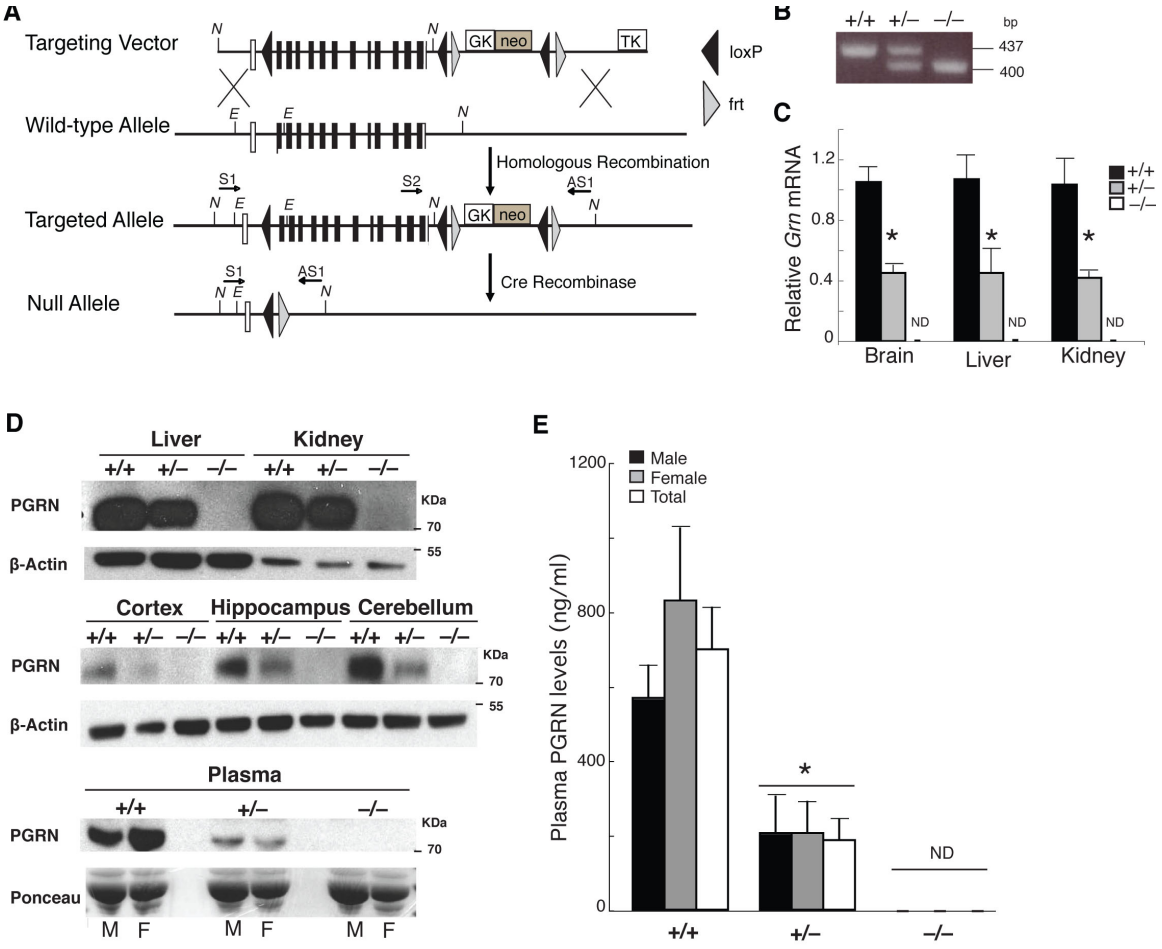

Figure A1.1. Generation of progranulin-deficient mice.

(A) Generation of the targeting vector with loxP sequences flanking the entire *Grn* coding regio (black boxes represent coding exons). Black triangles, loxP sites; grey triangles, FRT sites; grey box, neomycin-resistance cassette (neo); white box, thymadine kinase (TK). Primers for the genotyping reaction are denoted with black arrows. Key restriction enzyme sites are indicated (N, *Not1*; E, *EcoRI*). **(B)** PCR genotyping results for *Grn*-deficient mice after crossing with mice expressing Cre under the β-actin promoter. **(C)** Relative *Grn* mRNA expression in brain, liver, and kidney of 6-week-old PGRN-deficient mice. (ND, not detected). *p < 0.001. **(D)** PGRN protein levels evaluated with immunoblotting of liver, kidney, brain, and plasma samples taken from 6-week-old PGRN-deficient mice. **(E)** PGRN protein levels found in the plasma of 6-week-ole PGRN-deficient mice detected using ELISA. (ND, not detected). Total refers to data from both sexes combined (M, male; F, female). *p < 0.001.

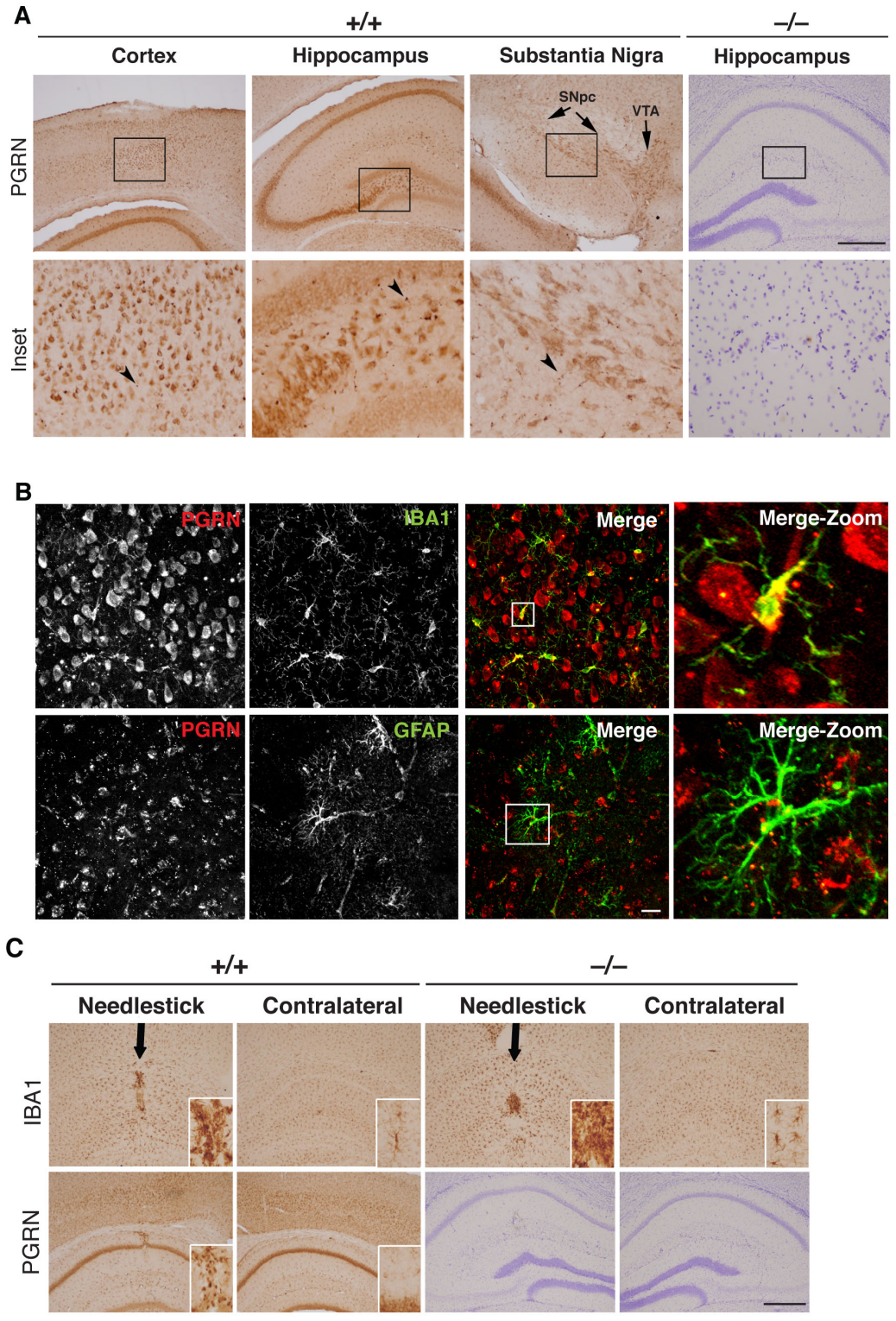

Figure A1.2. Progranulin expression in the CNS.

(A) Immunohistochemistry showing the presence of PGRN in neurons of the frontal cortex, hippocampus, and substantia nigra pars compacta (SNpc). Boxes indicate area imaged at higher magnification shown in the inset images. Arrow heads highlight detection of PGRN in non-neuronal cells. VTA, ventral tegmental area. Bar = 1200 μm. **(B)** Confocal images showing that in addition to neurons, PGRN protein can be detected in microglia, but not astrocytes. The inset box in the merged image depicts the cell imaged at higher magnification to demonstrate co-localization of PGRN expression. Bar = 20 μm. **(C)** PGRN expression is upregulated in microglia 24 hours following a needlestick trauma to the hippocampus. Activated microglia (morphology-inset) are present in the area of the needle track in both wild type and PGRN-deficient mice compared with the contralateral, uninjured hemisphere. These activated microglia have upregulated PGRN expression (inset) that is not present in the PGRN-deficient brains. Bar = 1200 μm.

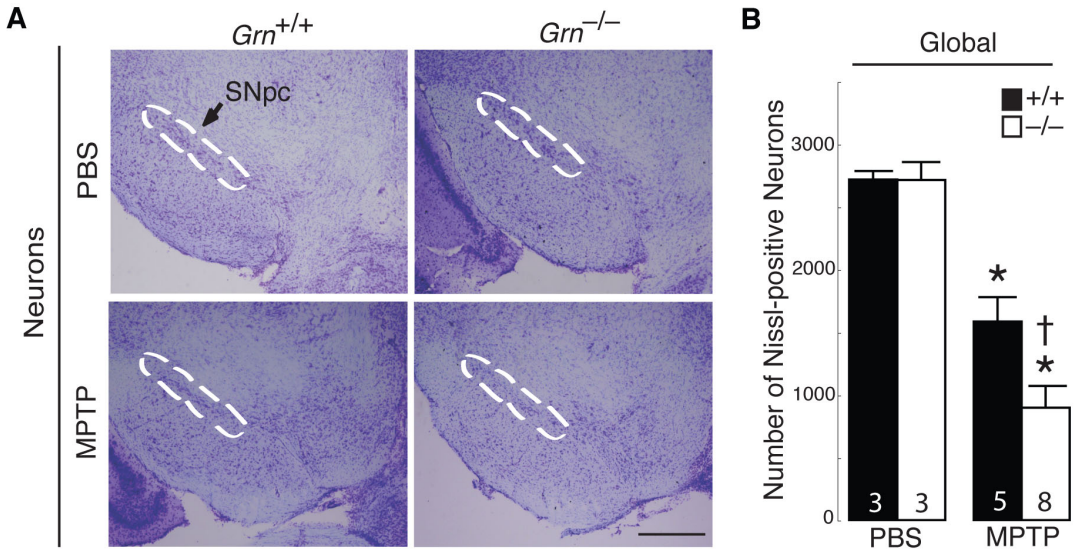

Figure A1.3. Death of all neuronal populations in the SNpc following MPTP treatment.

(A) Representative SNpc sections showing decreased numbers of Nissl-positive neurons following MPTP exposure in PGRN-deficient mice compared to control. Dashed lines denote the SNpc. Bar = 500 μm. **(B)** Quantification of Nissl-positive neurons in the SNpc. Numbers indicate the *n* per group. *p < 0.05 PBS compared with MPTP. †p < 0.05 $Grn^{+/+}$ MPTP compared with $Grn^{-/-}$ MPTP.

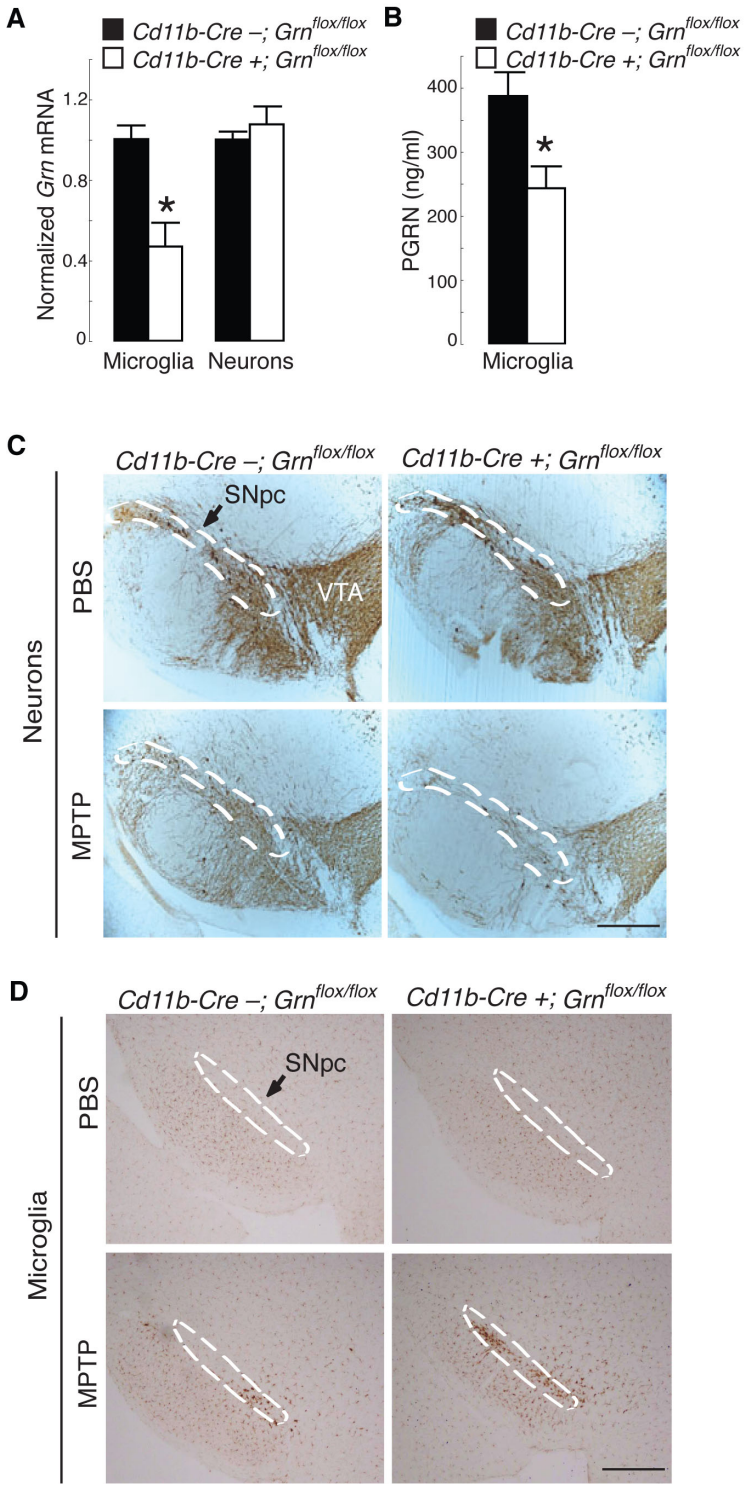

Figure A1.4. Efficiency and phenotype of *Cd11b-Cre* mice following MPTP treatment.

(A) Graph showing *Grn* mRNA levels in microglia and cortical neurons *in vitro.* *p < 0.001 *Cd11b-Cre–;Grn*$^{flox/flox}$ compared with *Cd11b-Cre+;Grn*$^{flox/flox}$ cells. **(B)** Quantification of secreted PGRN levels in microglial cultures. *p < 0.01 *Cd11b-Cre–;Grn*$^{flox/flox}$ compared with *Cd11b-Cre+;Grn*$^{flox/flox}$ microglia. **(C)** Representative SNpc sections showing decreased numbers of TH-positive neurons following MPTP treatment in *Cd11b-Cre+;Grn*$^{flox/flox}$ mice. VTA, ventral tegmental area; dashed lines denote the SNpc. Bar = 500 μm. **(D)** Representative images showing increased microgliosis in *Cd11b-Cre+;Grn*$^{flox/flox}$ mice treated with MPTP demonstrated by IBA1 staining. Dashed circle and arrow denote the SNpc. Bar = 500 μm.

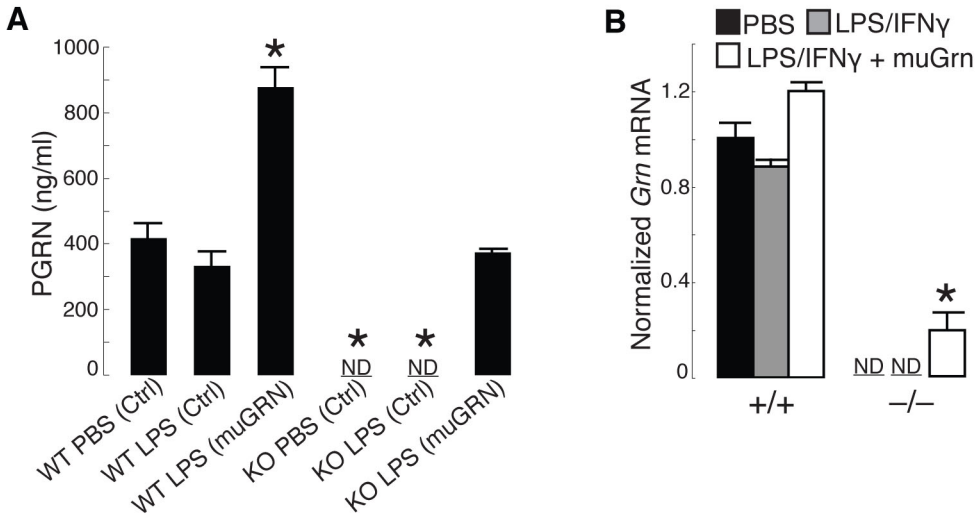

Figure A1.5. Murine PGRN lentiviral infection restores PGRN expression in microglia.

(A) Quantification of secreted PGRN from microglia infected with either murine PGRN or control lentivirus and LPS/IFNγ stimulation. *$p < 0.001$ compared with WT PBS control infected microglia. **(B)** Graph showing *Grn* mRNA levels following infection with either a murine PGRN or control lentivirus and LPS/IFNγ stimulation. *$p < 0.05$ compared with KO PBS.

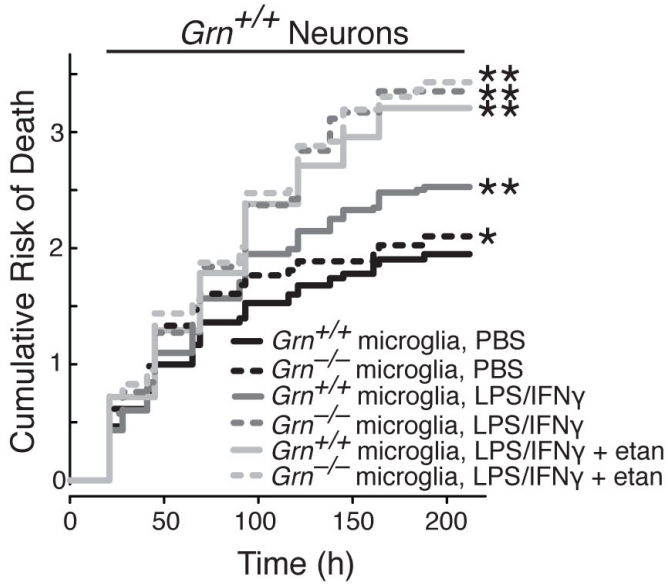

Figure A1.6. Depletion of TNFα using Etanercept is not sufficient to rescue cytotoxic neuronal death *in vitro.*

Wild type neurons exposed to conditioned media from LPS/IFNγ-treated PGRN-deficient microglia had an increased risk of death that is not attenuated by depletion of TNFα by co-treatment with Etanercept. *$p < 0.01$(log-rank test), WT PBS compared with KO PBS. **$p < 0.0001$ (log-rank test), LPS/IFNγ-treated microglial conditioned media compared with PBS treated conditioned media.

APPENDIX II

Supplemental Material for Chapter 3

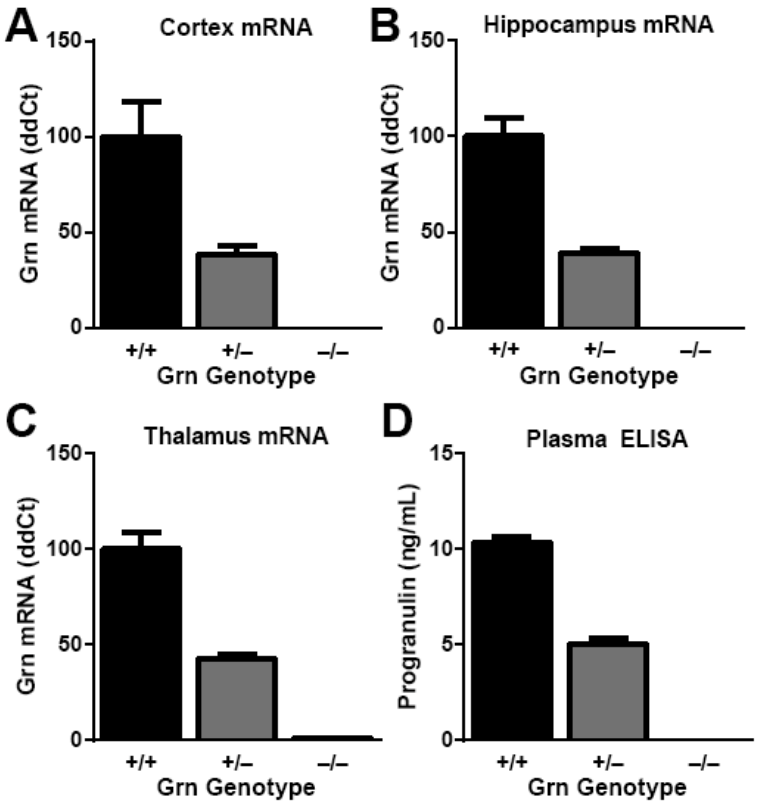

Figure A2.1 Progranulin levels are reduced by approximately 50% in *Grn*$^{+/-}$ mice.

Brain *Grn* mRNA levels were reduced by slightly more than 50% in the (A) cortex, (B) hippocampus, and (C) thalamus in *Grn*$^{+/-}$ mice compared with *Grn*$^{+/+}$ mice. (D) *Grn*$^{+/-}$ plasma PGRN levels were reduced by 50% compared to *Grn*$^{+/+}$ mice. In all cases, progranulin levels were undetectable in the *Grn*$^{-/-}$ mice.

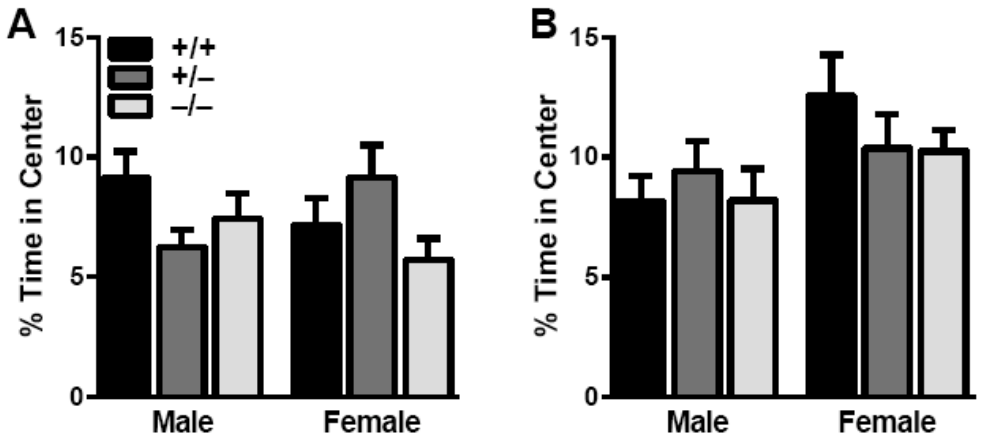

Figure A2.2. Progranulin deficient mice do not have age-related anxiety.

Anxiety levels were determined using an open field test. There were no differences in the amount of time the PGRN-deficient mice spent in the center of the field compared to wild-type mice at (A) 4 months or (B) 12 months of age.

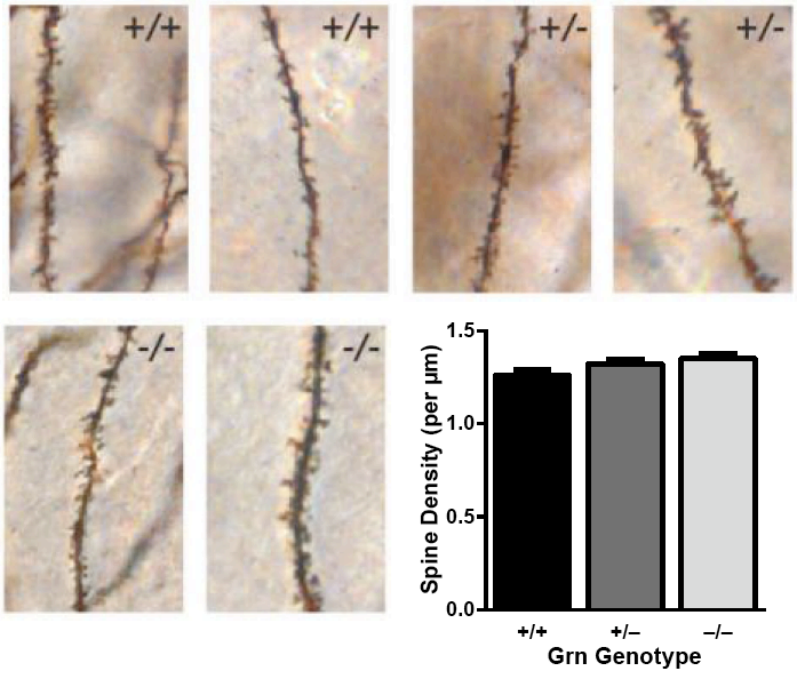

Figure A2.3. Progranulin deficiency does not alter hippocampal spine density in a separate *Grn* mouse model.

Representative images of pyramidal cell spine density in the CA1 region for $Grn^{+/+}$, $Grn^{+/-}$, and $Grn^{-/-}$ mice following Golgi staining. When the spine number is quantified, there are no differences between the three genotypes.

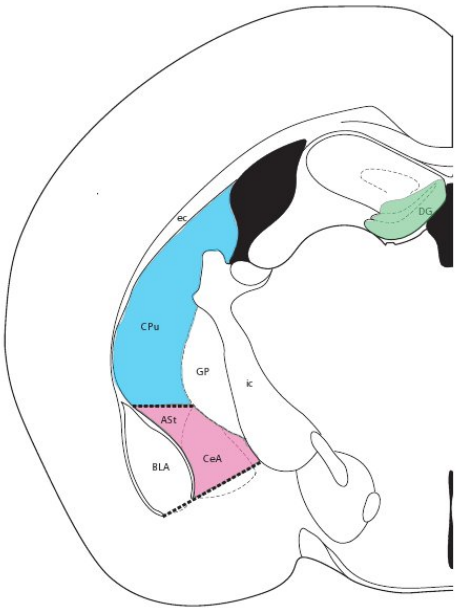

Figure A2.4. Map indicating areas for c-fos quantification.

Landmarks used by a blinded observer to quantify the number of c-fos positive cells in the amygdala, caudate putamen, and dentate gyrus following novel environment exposure.

Publishing Agreement

It is the policy of the University to encourage the distribution of all theses, dissertations, and manuscripts. Copies of all UCSF theses, dissertations, and manuscripts will be routed to the library via the Graduate Division. The library will make all theses, dissertations, and manuscripts accessible to the public and will preserve these to the best of their abilities, in perpetuity.

Please sign the following statement:

I hereby grant permission to the Graduate Division of the University of California, San Francisco to release copies of my thesis, dissertation, or manuscript to the Campus Library to provide access and preservation, in whole or in part, in perpetuity.

Lauren H. Martens
Author Signature

1/5/13
Date